Background Functional Connectivity Reveals Neural Mechanisms of Top-Down Attentional Control

by

Yichen Li

A dissertation accepted and approved in partial fulfillment of the

requirements for the degree of

Doctor of Philosophy

in Psychology

Dissertation Committee:

Dr. Ben Hutchinson, Chair

Dr. Brice Kuhl, Core Member

Dr. Dasa Zeithamova, Core Member

Dr. James Murray, Institutional Representative

University of Oregon

Spring 2024

DISSERTATION ABSTRACT

Yichen Li

Doctor of Philosophy in Psychology

Title: Background Functional Connectivity Reveals Neural Mechanisms of Top-Down Attentional Control

Top-down attentional control is essential for efficiently allocating our limited attentional resources to process complex natural environments, focusing on information relevant to our goals. The neural mechanism underlying this pervasive cognitive ability can be dichotomized into externally-oriented, which allocates attention to perceptual details, and internally-oriented, which direct attention to mnemonic episodes. Extensive research has investigated these neural mechanisms by focusing on the *operations* of attentional control, executed in response to a stimulus, by examining the evoked activity patterns in the brain. However, growing evidence indicates the importance of exploring these neural mechanisms supporting the *states* of attentional control that persist over time, by scrutinizing the intrinsic functional interaction patterns among brain regions. The present dissertation follows along the latter perspective to extend our current knowledge of the neural mechanism of top-down attentional control. In a series of two experiments, background functional connectivity (BGFC) analyses were applied to isolate intrinsic functional organizations of the brain from stimulus-evoked signals. Utilizing a whole-brain, data-driven approach combined with machine learning, important neural interaction circuits and pathways were revealed in response to switching between externally and internally oriented attentional control states (Chapter 2) and concurrently representing multiple states requiring either external or internal attention (Chapter 3). Moreover, evidence was provided suggesting the systematic distinctions between stimulus-related signals (captured by evoked activity) and state-

related signals (captured by BGFC) in reflecting the process of top-down attentional control. Finally, in Chapter 4, a self-developed open-source Python library (BGFC-kit) was introduced for streamlining the preprocessing steps of BGFC analyses. Together, the works in this dissertation provide important insights and facilitate future investigations of the general neural mechanisms underlying top-down attentional control.

This dissertation includes previously published and unpublished co-authored material.

ACKNOWLEDGMENTS

The completion of this dissertation owes immeasurable gratitude to the unwavering support, guidance, and encouragement I have received over the past five years. My heartfelt thanks extend to all those who generously contributed to my journey. While I cannot possibly name everyone, their impact remains deeply cherished.

Foremost, I express my profound appreciation to my advisor, Dr. Ben Hutchinson. His expertise, patience, and dedication have been instrumental in nurturing my growth as an independent researcher. I am particularly grateful for Dr. Hutchinson's encouragement to explore new avenues, experiment with the unknown, and pursue my passions. His unwavering support has been invaluable to me. I extend my gratitude to the esteemed members of my dissertation committee: Dr. Brice Kuhl, Dr. Dasa Zeithamova, and Dr. James Murray. Their guidance, valuable insights, and encouragement have been pivotal in shaping the trajectory of this work. I am also deeply appreciative of all current and former members of the Hulabrow and the Kuhl lab. Your camaraderie, engaging conversations, and constructive feedback have enriched my academic journey in countless ways.

Most importantly, to my parents, and my wife, thank you for your unwavering love and support, thank you for not giving me up, and thank you for being my rock during my hardest time.

TABLE OF CONTENTS

LIST OF FIGURES

Figure Page

LIST OF TABLES

Table Page

CHAPTER I

GENERAL INTRODUCTION

This chapter contains an edited section of unpublished co-authored material. I am the primary author of this material, and I incorporated editing advice from Dr. Ben Hutchinson.

Overview

Attention is a core property of all human cognitive operations. Given limited cognitive capacity to process competing options, attention allows one to select, modulate, and sustain focus on information most relevant for behavioral goals. One of the central problems in attention research is to unravel the top-down attentional control mechanism in the brain and to understand how such a mechanism manages all information-processing in the brain to achieve efficient behavioral performance (Desimone & Duncan, 1995; Hopfinger et al., 2000; Parasuraman, 2000; Petersen & Posner, 2012; Posner & Petersen, 1990). The pervasive influence of top-down attentional control in our daily lives makes its examination challenging, often leading to multiple interconnected yet seemingly distinct research paths. The central challenge that this dissertation addresses is to study top-down attentional control as a multi-module configuration of neural measures (e.g., evoked activity and intrinsic functional structures of the brain; Cole et al., 2019; Turk-Browne, 2013) and cognitive abilities (e.g., perception and memory retrieval; Chun et al., 2011; Chun & Johnson, 2011).

One aspect of top-down attentional control research aims to comprehend how the brain selectively attends to goal-relevant information within perceptual domains. For instance, in a hypothetical scenario where an individual converses in a noisy bar, attention must be directed to the conversation while filtering out irrelevant auditory and visual stimuli. This prompts inquiries into the neural processes underlying the registration of behavioral goals within the brain and the

subsequent control of perceptual information processing within the visual and auditory cortices. In the context of human fMRI, research in this area tends to reveal different attentional control mechanisms depending on the specific fMRI neural measure utilized. A commonly accepted perspective on this mechanism suggests that the behavioral objective is encoded through the *evoked activity patterns* of blood oxygen level-dependent (BOLD) signals in the frontal brain regions (Corbetta & Shulman, 2002; Hopfinger et al., 2000). Attentional control, in turn, entails the information captured by these activity patterns serving as directives transmitted along neuronal pathways between brain regions to influence the activities elsewhere in the brain. (e.g., Cole et al., 2016; Dosenbach et al., 2008; Miller & Cohen, 2001). Additionally, alongside evoked neural activity, the neural pathways themselves were also actively modulated in accordance with behavioral goals (Al-Aidroos et al., 2012). This modulation is reflected by changes in *functional connectivity (FC) patterns* of the brain, quantified through statistical dependence, such as correlation, between the timeseries of BOLD signals among brain regions (Friston, 1994). Consequently, the brain inherently optimizes the processing pathways for goal-pertinent information, even when there is no elicited brain activity, to align with the behavioral goal (e.g., Al-Aidroos et al., 2012; Turk-Browne, 2013).

Moreover, top-down attentional control is not limited to externally allocation toward perceptual information but can also be internally directed for mnemonic or reflective purposes (Chun et al., 2011; Chun & Johnson, 2011). In the context of engaging conversations, individuals may need to attend externally to the perceptual details of what the other person is saying (i.e., perception), but also need to attend internally for recollecting the context or past events (i.e., memory retrieval). This prompts inquiries into the neural processes underlying top-down attentional control regarding the allocation to or switching between external and internal

processing domains. Research in this area seeks to bridge the seemingly unrelated topics such as memory and perception, aiming to understand the similarities and differences between these cognitive abilities (Lepsien & Nobre, 2006; Li et al., 2023; Long & Kuhl, 2021; Poskanzer & Aly, 2023; Verschooren et al., 2019).

This dissertation aims to integrate and advance these aspects of attentional control research. Specifically, the focus is on understanding the mechanisms underlying the flexible allocation of attention between external and internal information processing, taking into account modulations in both FC patterns and evoked activity patterns. The dissertation begins by examining how top-down attentional control efficiently switches between prioritizing external and internal information processing streams (Chapter 2). I proceed to investigate the top-down attentional control mechanism capable of concurrently representing multiple behavioral goals, particularly emphasizing those involving both perceptually and mnemonically driven factors. (Chapter 3). I then present and introduce a self-developed open-source python package that aims to facilitate and streamline the investigation of intrinsic FC patterns (Chapter 4). I conclude with a discussion of what has been learned as well as potential future applications (Chapter 5).

The remainder of this introductory chapter provides essential background information. In the following section, I outline two complementary and intertwined theories concerning the neural mechanisms governing top-down attentional control: the guided activation account and the switching train tracks account (Miller & Cohen, 2001; Turk-Browne, 2013). Following this, I review the two commonly used neural measures in human fMRI data analyses: evoked activity patterns and intrinsic functional connectivity (FC) patterns (Friston, 1994; Norman et al., 2006). I highlight their quantitative independence and stress that both previously discussed theories suggest the study of top-down attentional control neural mechanisms should involve examining

and combining both neural measures. Finally, I introduce the taxonomy distinguishing between external and internal attention (Chun et al., 2011) and illustrate how this taxonomy guides our exploration of the attentional control mechanisms using the aforementioned neural measures.

Mechanisms of top-down attentional control system

As our understanding of the world expands and our behavioral capabilities grow, our evolved systems coordinate mental, perceptual, and motor processes toward common behavioral goals. Maintaining sustained behavioral goals is crucial for navigating the daily influx of information and reducing ambiguity. Specifically, the attentional control system can operate in a "top-down" manner, voluntarily biasing attention and information processing toward goal-driven outcomes, enabling the early selection and processing of goal-relevant information (Corbetta & Shulman, 2002; Posner & Petersen, 1990). A substantial body of work has investigated the underlying neural mechanisms responsible for top-down attentional control, reaching consensus on two key components of this system. First, understanding the properties and functions of specific brain regions is essential, as they play a crucial role in guiding and coordinating attentional resources, such as the prefrontal cortex (PFC), or more broadly, the frontal-parietal control network (Corbetta & Shulman, 2002; Dosenbach et al., 2008; Miller & Cohen, 2001). Second, understanding how different brain regions communicate is vital, as efficient top-down attentional control would require the interplay of multiple brain regions and networks (Al-Aidroos et al., 2012; Felleman & Van Essen, 1991; Mesulam, 1990; Turk-Browne, 2013). In this section, we review two complementary accounts of top-down attentional control, shedding light on how important brain networks coordinate information processing throughout the brain in a goal-directed way (**Figure 1.1**).

Guided activation account of attentional control

Originally proposed by Miller and Cohen (2001), the guided activation account emphasizes the crucial role of the prefrontal cortex (PFC) in maintaining behavioral goals and "guiding" activity throughout the brain. According to this account, when forming behavioral goals, the PFC evokes patterns of neuronal activations to actively sustain these goals in a multivariate manner. These activation patterns in the PFC represent subtle combinations of events and contingencies which are learned over time. Importantly, these activation patterns in the PFC don't directly execute input-output mappings required for task performance; instead, they guide the activation of other brain regions, such as visual areas, which are responsible for executing these mappings and providing the necessary outputs for task completion (Miller & Cohen, 2001). For instance, PFC neurons might produce a specific activation pattern to prioritize attending to an ongoing conversation while ignoring ambient sounds. This activation pattern in the PFC then influences the auditory cortex through neural pathways, thus biasing and modulating the auditory cortex activation patterns to facilitate behavioral goals (**Figure 1.1A)**.

Recent research on functional brain organization has broadened the focus from the prefrontal cortex (PFC) to include a wider network known as the frontal-parietal control network (Dosenbach et al., 2006; Yeo et al., 2011). Functional connectivity (FC) is assessed between brain regions at rest to identify functionally homogeneous regions that may be anatomically separated (Biswal et al., 1995; Friston, 1994). Numerous studies have provided consistent evidence that the FC pattern in the human brain at rest demonstrates a meaningful network structure of functionally coupled regions, rather than being random (Damoiseaux et al., 2006; Fox & Raichle, 2007; Van Dijk et al., 2010; Yeo et al., 2011). The PFC is consistently grouped into the frontal-parietal control network, which plays a key role in coordinating and controlling

goal-guided information processing (Gordon et al., 2016; Power et al., 2011; Schaefer et al., 2018; Shen et al., 2013). For example, research has demonstrated that the control network as a whole, not just the PFC, can reflect and maintain sustained behavioral goals throughout a task (e.g., Dosenbach et al., 2006). Additionally, works on activity flow mapping have provided substantial evidence demonstrating how the evoked activation pattern in the control network can efficiently influence and guide the activation patterns in other brain regions. Specifically, Cole et al. (2016) demonstrated that the evoked activation pattern of any region can be accurately predicted by estimating the FC-weighted sums of the activations at other locations, referred to as the sum of activity-flow estimates. Importantly, the control network has been identified as a hub densely functionally coupled with all other brain networks (Cole, Laurent, et al., 2013; Gordon et al., 2018; Gratton, Sun, et al., 2018), exhibiting the most flexible and rapid shifts in functional coupling patterns with other networks in response to changes in attentional control demands (Cole, Reynolds, et al., 2013). This research highlights the validity of having the activation patterns of the control network to guide the activation pattern of other networks during the top-down attentional control processes.

Collectively, the guided activation theory of top-down attentional control suggests that the PFC (and the control network in general) gradually learns the mapping between different scenarios and the corresponding actions needed. When a behavioral goal is set, the control network produces activation patterns that precisely mirror the ongoing behavioral goal. These patterns then direct other brain networks via functional connectivity pathways, allowing them to engage and synchronize their behavior with the defined goal. Consequently, the brain operates harmoniously to accomplish efficient top-down attentional control.

Switching train tracks account of attentional control

As previously indicated, functional connectivity (FC) among brain regions serves as conduits through which evoked activities propagate. A major line of research following the guided activation account focuses on examining the information conveyed by evoked activities transmitted through FC pathways, while comparatively less attention has been paid to exploring whether the FC pathways themselves offer valuable insights. Yet it's crucial to acknowledge that the guided activation account also anticipates changes in these pathways, as the evoked activity patterns in the prefrontal cortex (PFC) contain the appropriate representations that can select the pathways required for the task (Miller & Cohen, 2001). Highlighting this aspect of the guided activation process, the switching train tracks model of attentional control was proposed to focus on understanding how attentional control operates through modulations of FC pathways (Turk-Browne, 2013). Specifically, this account proposes that in the presence of a behavioral goal, FC pathways undergo significant modulation to strengthen connections between areas of the human cortex relevant to the goal (akin to switching train tracks), thereby prioritizing the processing of goal-relevant information (Al-Aidroos et al., 2012). Importantly, extending beyond the guided activation account, the switching train tracks account emphasizes that the FC pathway modulations happen intrinsically, independent of evoked activity in the brain, and persist without external stimulation (**Figure 1.1B)**.

Recent research has provided empirical evidence suggesting that top-down attentional control does indeed modulate the FC pathways. Several investigations have compared the functional network organization of the human brain during “resting-state” and various cognitive “task-states” where top-down attentional control is required. These studies have consistently shown that while the resting-state network organization remains highly stable and persistent

across tasks (Fox & Raichle, 2007; Gratton, Laumann, et al., 2018; Shehzad et al., 2009), different behavioral objectives subtly influence functional network organization as a mechanism of top-down attentional control (Braun et al., 2015; Cole et al., 2014; Finc et al., 2020). In particular, early research has established that the functional network organization of the human brain during “resting-state” can predict individual traits and behavioral performance differences across various cognitive tasks, such as fluid intelligence and attention capacity (Finn et al., 2015; Rosenberg et al., 2016). However, recent evidence suggests that the "task-state" functional network organization structure, due to the subtle yet significant FC modulations induced by goals of cognitive tasks, can notably enhance the accuracy of predicting individual differences across a broad spectrum of cognitive tasks, including working memory, sustained attention, and cognitive control (Cole et al., 2021; Fong et al., 2019; Greene et al., 2018; McCormick et al., 2022). Moreover, recent works have also supported the switching train tracks account by providing evidence that the modulation of brain network organization is independent from task-evoked activations. A series of works demonstrated that FC pathways undergo goal-relevant modulations both before the initiation of tasks (Ploner et al., 2010; Preti et al., 2017; Sadaghiani et al., 2015) and even after task completion (LaBar & Cabeza, 2006; Tambini et al., 2017). Additionally, other studies have successfully identified significant changes in FC pathways even after quantitatively removing evoked activities from the recorded brain BOLD signals, which will be further discussed in the following section (Al-Aidroos et al., 2012; Córdova et al., 2016; K. Duncan et al., 2014; Norman-Haignere et al., 2012; Tompary et al., 2018).

Notably, the switching train tracks account highlights that top-down attentional control can manifest in FC pathway modulations among brain regions beyond just the PFC. Indeed, the subtle yet significant modulations of functional network structure often encompass changes in

coupling strengths among regions throughout the entire brain. For example, Cohen and D'Esposito (2016) illustrated across the entire brain that tasks with simple motor response-centered goals amplified coupling among regions within the same network, while the FC pathways between distinct networks remained restricted, resulting in a more "segregated" functional organization. Conversely, tasks involving complex goals like working memory fostered a more "integrated" functional organization, promoting enhanced FC pathways among regions associated with disparate brain networks across the entire brain.

Together, the switching train tracks model of attentional control proposes that the network architecture of the human brain, as assessed by functional connectivity (FC) patterns, resembles a map of train tracks that typically remains stable over time. Top-down attentional control acts like a lever, altering the connections between brain regions, thus prioritizing the processing of goal-relevant information needed to accomplish behavioral objectives. Importantly, this mechanism was proposed to occur concurrently yet independently from evoked activities in the brain.

Measuring state-related neural processes with background functional connectivity

Stimulus- and state-related neural processes

Previous research has posited that engaging in goal-directed cognitive tasks elicits two distinct sets of neural processes. Firstly, tasks prompt stimulus-related neural processes, which denote transient neural signal changes within relevant brain regions in response to information processing for the cognitive task. Secondly, tasks also induce state-related neural processes, characterized by goal-specific neural pathway that persist in the background of external stimulus processing to optimize task performance (Otten et al., 2002; Summerfield et al., 2006; Turk-Browne, 2013). Both the guided activation and switching train tracks theories reviewed

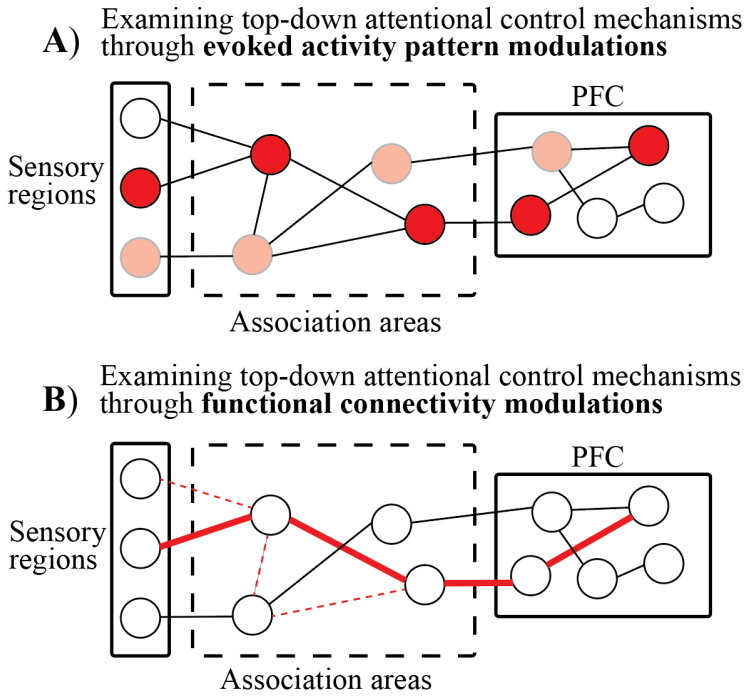

Figure 1.1. Exploring top-down attentional control by focusing on either evoked activity patterns or functional connectivity (FC) patterns.
A) The line of work that investigates top-down attentional control mechanisms by focusing on examining evoked activity patterns. The guided activation account posits that the top-down behavioral goal is represented by the evoked activity patterns in the PFC, which influence the evoked activation pattern at other brain locations, allowing the sensory regions to process stimuli in a goal-relevant manner. Thus a major line of research based on this account primarily focuses on understanding evoked activity responses, revealing regions involved in top-down attentional control processes (solid red dots) and those relevant to processing the nuisances of behavioral tasks (e.g., task difficulties, features of the stimulus etc.; light red dots). **B**) The line of work that investigates top-down attentional control mechanisms by focusing on examining modulations of functional connectivity patterns. The switching train tracks account stresses that top-down attentional control induces modulations of FC pathways between brain regions. The FC modulations enhance pathways for goal-relevant information processing (thick red lines) while weakening those for irrelevant information (dotted red lines). Crucially, FC pathway modulations are independent of evoked activities, persist even without external stimulations, and reveal FC pathways relevant solely for top-down attentional control (solid red dots), excluding those related to processing behavioral task nuances (light red dots).

previously suggest that a complete understanding of both stimulus-related and state-related neural processes is crucial for a thorough examination of top-down attentional control (Miller & Cohen, 2001; Turk-Browne, 2013). As such, the two different types of neural processes correspond precisely to the two lines of research into top-down attentional control mechanisms:

studies that focus on evoked activity patterns aim to investigate stimulus-related neural processes, while research on functional connectivity (FC) modulations seeks to understand state-related neural processes.

In human fMRI research, investigating evoked activity patterns means analyzing how changes in the BOLD signal in brain voxels respond to external stimuli during different cognitive tasks, thus capturing stimulus-related neural process. In particular, task-based functional magnetic resonance imaging (fMRI) studies have long been used to investigate how and where regional, stimulus-evoked responses emerge in the brain during various cognitive processes. Examining stimulus-evoked responses has been an extremely fruitful approach to understanding which brain regions support the component processes of task-driven cognition and the representational capabilities of the human brain (Kanwisher, 2010; Norman et al., 2006). On the other hand, FC examines the strength of coupling strengths between different brain regions over time. The idea is that while specific brain regions tend to be specialized at one or a few cognitive operations (e.g., the medial temporal lobe plays a critical role in forming and retrieving long-term memories; Nyberg et al., 1996), unique cognitive states engage unique combinations of component interactive processes (Turk-Browne, 2013). Therefore, instead of being captured by univariate activity or multivariate patterns in a single brain region, state-related neural processes are best captured by FC, which quantifies distributed neural interactions induced by cognitive tasks (Friston, 1994). It's important to acknowledge that FC measurements can be exaggerated or even inaccurate because of the impact of stimulus-evoked activities, presenting a significant methodological challenge in distinguishing these signals from one another in human fMRI data. In the following sections, we delve into the challenge of measuring FC with the presence of tasks, and the utilization of background functional connectivity (BGFC) as a variant of FC

measure to disentangle intrinsic neural pathway modulations from stimulus-evoked activities in brain signals.

Co-activation confounds in task-state functional connectivity

Task-state FC refers to the neural interaction patterns of the brain during various cognitive tasks. Note that here we refer to task-state FC as the FC-based neural measure computed based on preprocessed BOLD timeseries, *without* removing the stimulus-evoked response. One major challenge in investigating state-specific neural processes using functional connectivity is so-called "co-activation confounds" introduced by stimulus-related activity in multiple regions (Cole et al., 2019). Specifically, task-state FC measures consist of two additional sources of variance compared to resting-state, one being the actual state-related neural processes for optimal task performances, but another being two or more brain regions "co-activating" in response to external stimuli at the same time, without being in communication with one another per se. As shown in **Figure 1.2**, two brain regions can demonstrate spurious FC modulations by both responding to the presence of an external stimulus when, in fact, no state-related modulations exist. Empirical evidence suggests that without removing stimulus-evoked responses, around 7% of brain connections increased during tasks compared to rest, but only 2% remained after accounting for the coactivation confounds, suggesting that more than half of the task-state FC connections are inflated (Cole et al., 2019). As a result, the explanatory power of task-state FC is potentially significantly limited by this issue. For example, a previous study attempted to identify "state-related" FC templates for multiple tasks (e.g., memory retrieval) and yielded a set of connections that are predictive of a cognitive task (Shirer et al., 2012). However, due to the problem of coactivation confounds and the differences in the type and timing of

external stimuli across tasks, it is hard to conclude that any connections revealed by the templates are necessarily attributed to the task state (e.g., the state of memory retrieval).

Introducing background functional Connectivity

Background functional connectivity (BGFC) is a variant of FC measurement designed to solve the co-activation problem. In the preprocessing phase, stimulus-evoked responses are removed, using various techniques, leaving only the residual (thus background) timeseries for subsequent connectivity analyses (Cole et al., 2019; Frank & Zeithamova, 2023). Specifically, the stimulus-evoked response can be modeled and then removed or accounted for using a general linear model. There are several different existing approaches that fit into this family of techniques. Some existing approaches model the evoked response (using either a 'canonical' HRF, or preferably, through estimation using a finite impulse response model which does not make assumptions about the shape of the underlying response) and then statistically regress it out of the timeseries data, leaving only the residuals for subsequent analyses (Cole et al., 2019; Fair et al., 2007). Thus, BGFC is argued to capture task-modulated, state-specific neural processes in human fMRI, that are free from any extrinsic factors.

Previous studies have demonstrated the use of BGFC, showing that even with the absence of stimulus-evoked activity signals, the remaining state-related FC pathways still demonstrate important and meaningful differences in response to cognitive states. A series of studies involved participants being presented with composite images containing both faces and scenes as stimuli, with instructions to focus attention either on the face or the scene component, depending on the task at hand (Al-Aidroos et al., 2012; Córdova et al., 2016; Norman-Haignere et al., 2012; Tompary et al., 2018). The underlying hypothesis was that top-down attentional control regarding the visual processing of either face or scene components would induce modulation in

the FC pathways of the ventral visual stream, aligning with the respective attentional objective. As anticipated, the findings revealed that when attention was directed towards visualizing the face component, FC pathways between the visual cortex and face-specialized regions such as the fusiform area, perirhinal cortex, and superior temporal sulcus were strengthened. Conversely, when the focus was on visualizing the scene component, FC pathways between visual regions and scene-specialized areas like the parahippocampal cortex exhibited enhancement. Furthermore, recent research has presented compelling evidence indicating that alterations in BGFC pathways across the brain are closely linked to the efficiency of top-down attentional control. For instance, past research has suggested that modifications in BGFC patterns within the medial temporal lobe can accurately forecast an individual's level of internal attentional focus: this level of internal attentional focus is assessed by their capacity to effectively encode, retrieve, and generalize information (Cooper & Ritchey, 2019; Frank et al., 2019; Gruber & Otten, 2010).

The taxonomy of internal vs. external attention

An inherent aspect of top-down attentional control is its pervasive presence in our daily lives across a vast repertoire of cognitive tasks. This emphasizes its importance as a central focus in human cognitive neuroscience research, yet it also makes studying this area somewhat complex and difficult to handle: even minor changes in behavioral goals or cognitive demands can lead to modulations in both stimulus-evoked and state-related neural processes. Consequently, it is imperative to devise a systematic approach to classify and investigate top-down attentional control without becoming entangled in the nuanced intricacies of micro-level variations. In this regard, the development of a taxonomy that organizes top-down attentional control at a broader level proves beneficial. One such taxonomy distinguishes top-down attentional control between external and internal attention, based on the nature of the target

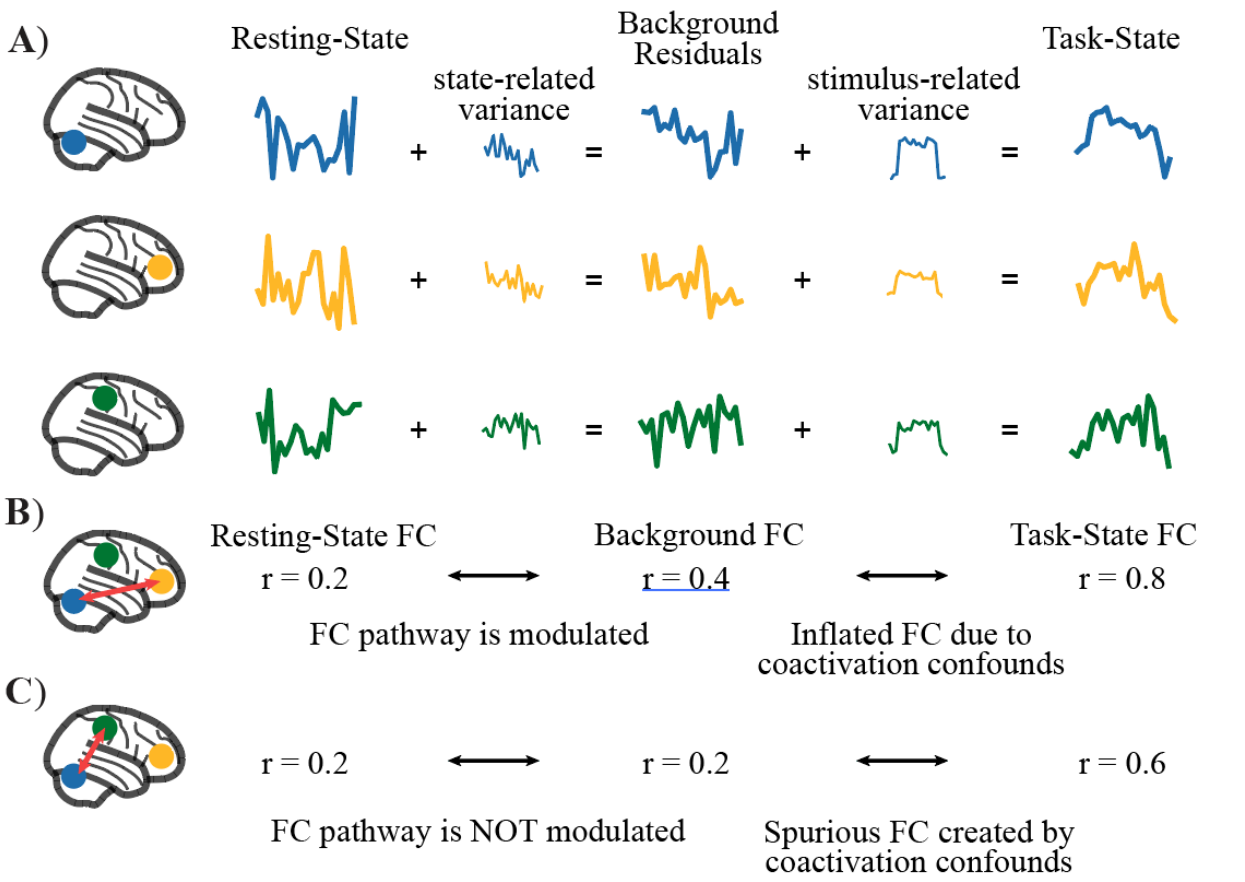

Figure 1.2. Coactivations among brain regions in response to stimulus onset inflate task-state functional connectivity.
A) When engaging in a cognitive task, resting state functional connectivity is complicated by two additional sources of variance: one is the state-related neural reconfiguration modulated by the cognitive task; another is the stimulus-related coactivation confounds, unrelated to the task per se. The background functional connectivity method aims to isolate the state-related neural modulations from stimulus-related coactivation. **B**) When the task indeed modulates FC strength between two regions, stimulus-related variance can inflate such measure. Specifically, as the FC measure between the yellow and blue regions increased from 0.2 during rest to 0.8 during the task, one would make the conclusion that the neural interaction between these two regions is task-specific. Although this conclusion is correct, the task-specific modulation on FC measure can be exaggerated by stimulus-evoked activity. **C**) When the task does not modulate FC strength between two regions, stimulus-related variance is enough to create spurious FC strength changes. Specifically, as the FC measure between the green and blue regions increased from 0.2 during rest to 0.6 during the task, one would make the conclusion that the neural interaction between these two regions is task-specific. However, this modulation in FC is solely due to the fact that the two brain regions co-activate external stimuli, and the neural interaction between the two regions has nothing to do with maintaining the state of the task.

information upon which attention operates (Chun et al., 2011). In accordance with this taxonomy, the top-down attentional control mechanism for external attention entails the voluntary selection, modulation, and integration of perceptual information across various modalities. Conversely, the top-down attentional control mechanism for internal attention facilitates the management of internally generated information, encompassing processes such as introspection and the retrieval of episodic memory.

This taxonomy of external and internal attention mirrors real-life dichotomies. In everyday situations, the same external stimulus can serve as both the target of perception and the cue for memory retrieval. When attention is directed externally, perceptual details are processed, whereas internal attention allocation leads to the processing of mnemonic episodes. It thus become a central question to understand the neural mechanisms enabling the brain to selectively represent perceptual details when behavioral goals emphasize perception, and memory details when goals require recollection. Previous research has suggested that the brain employs two distinct modes for external and internal processing (Hasselmo et al., 1996; Honey et al., 2017; Long & Kuhl, 2019). Yet, the precise neural mechanisms facilitating efficient attention allocation and switching between external and internal processing are still unclear.

In the human fMRI literature, previous studies comparing externally- and internally-oriented top-down attentional control typically align with the two sets of neural processes: one emphasizing the localization and interpretation of evoked activity, and the other examining intrinsic changes in functional connectivity pathways during attentional processing (Miller & Cohen, 2001; Summerfield et al., 2006; Turk-Browne, 2013). Investigations focusing on evoked activity have identified two complementary systems: a "task-positive" system that is more active during external-oriented processing, involving auditory, visual, and somatosensory areas, as well

as the lateral prefrontal cortex (lPFC) and superior parietal lobule (SPL); and a "task-negative" or default system that is more active during internal-oriented processing, encompassing the posterior cingulate (PCC), precuneus (PCUN), lateral inferior parietal cortex (IPC), inferior temporal cortex, and medial prefrontal cortex (mPFC; Corbetta & Shulman, 2002; Golland et al., 2007, 2008). Furthermore, prior studies suggest that external (perceptual) and internal (mnemonic) processing of the same information result in distinct differences. For instance, the representation of information shifts the location from the visual cortex during externally oriented processing to the ventral parietal cortex during internally oriented processing (Long & Kuhl, 2021). Additionally, the neural presentation of information also undergoes meaningful goal-relevant changes during internal compared to external processing (Chanales et al., 2019; Favila et al., 2018, 2022; Zhao et al., 2021).

Alternatively, studies focusing on intrinsic FC pathway modulations have indicated that external and internal-oriented attentional control enhance distinct sets of intrinsic pathways throughout the brain that are *unrelated* to evoked activities. For instance, a body of research has delved into understanding intrinsic FC modulations centered on the hippocampus, a region long recognized as crucial for both externally allocating attention for encoding information and internally allocating attention for retrieving information (Hasselmo et al., 1996; Norman, 2010). It has been found that subregions of the hippocampus alter their interaction patterns as attentional control shifts from external to internal. Specifically, intrinsic FC between area CA1 and the ventral tegmental area strengthens when the goal is to encode perceptual information, whereas intrinsic FC between area CA1 and DG/CA3 strengthens when the goal is to retrieve mnemonic information (K. Duncan et al., 2014). Moreover, recent studies suggest that intrinsic FC between the hippocampus and the basal ganglia is heightened when the behavioral goal involves orienting

attention externally (i.e., explicit instruction), while intrinsic FC between the hippocampus and the dorsal attention network (DAN) is heightened when the goal involves orienting attention internally (Poskanzer & Aly, 2023).

Goal and structure of the dissertation

This dissertation aims to delve deeper into the neural mechanisms underlying top-down attentional control in humans, particularly in externally and internally oriented information processing. Despite existing research in this area, two key questions remain unanswered. Firstly, previous studies have predominantly focused solely on either evoked activities or intrinsic functional connectivity (FC) to uncover the neural underpinnings of top-down attentional control. However, each approach alone only offers limited perspectives, leaving it unclear whether the two neural measures tap into distinct or overlapping aspects of the cognitive process. Secondly, prior research investigating intrinsic FC modulations in externally versus internally oriented attentional control has typically adopted a seed-based approach, focusing on the FC pathway modulations of specific regions (e.g., hippocampus) or networks (e.g., default network). However, this method may overlook crucial FC dynamics elsewhere in the brain that characterize the dichotomy of the two top-down attentional control processing streams. To address these gaps, this dissertation presents a set of two human fMRI studies employing a whole-brain, exploratory approach to systematically examine intrinsic FC pathway modulations through BGFC as top-down attentional control transitions from external to internal. Furthermore, these studies compare the findings obtained through both activity- and connectivity-based analyses to elucidate the extent to which, and in which brain regions, the two neural measures diverge.

Chapter 2 endeavors to comprehend the intrinsic FC pathway modulations as top-down attentional control transitions from external to internal information processing. This is achieved by comparing the FC dynamics between states of perception and memory retrieval, with each state being the sole top-down goal at a given time. Background functional connectivity (BGFC) and an intensive exploratory method, full correlation matrix analyses (FCMA), are employed to scrutinize the intrinsic FC pathway changes for every voxel in the brain during these states. Furthermore, Chapter 2 investigates whether connectivity-based and activity-based neural measures capture distinct aspects of cognitive processes, and which cognitive aspects each neural measure is most sensitive to. In Chapter 3, the focus shifts to understanding the intrinsic FC pathway modulations underlying the transition from externally to internally oriented information processing in multitasking conditions. Specifically, the brain's ability to simultaneously attend to perceptual and mnemonic information is examined using BGFC. This includes exploring multitasking scenarios involving two externally oriented tasks as well as scenarios involving one externally and one internally oriented task. Additionally, Chapter 3 explores how BGFC complements conventional evoked activity patterns in representing multiple states simultaneously. In Chapter 4, a self-developed open-source Python library (BGFC-kit) is introduced to streamline future BGFC analyses. This library aims to simplify and standardize the implementation of BGFC analyses. Lastly, chapter 5 concludes with a summary of the results and a discussion on the broader implications of the findings.

CHAPTER II

PERCEPTION AND MEMORY RETRIEVAL STATES ARE REFLECTED IN DISTRIBUTED PATTERNS OF BACKGROUND FUNCTIONAL CONNECTIVITY

From Li, Y. P., Wang, Y., Turk-Browne, N. B., Kuhl, B. A., & Hutchinson, J. B. (2023). Perception and Memory Retrieval States are Reflected in Distributed Patterns of Background Functional Connectivity. *NeuroImage*, 120221.

Introduction

When a familiar visual stimulus (e.g., a colleague) is encountered, it might serve as the target of perceptual scrutiny (e.g., their current facial expression) or the trigger for episodic memory retrieval (e.g., something they said in the past). Numerous cognitive theories and neuroimaging studies have contrasted the cognitive processes and brain regions engaged during perception versus retrieval (Bosch et al., 2014; Chun & Johnson, 2011; Kosslyn et al., 1995; McClelland et al., 1995; O'Reilly & McClelland, 1994; Polyn et al., 2005; Wheeler et al., 2000). The majority of this work has focused on investigating the operations performed upon the *stimulus*, such as how the stimulus is encoded into long-term memory or how the stimulus is used to drive memory recollection (Favila et al., 2020; Fernandez et al., 2022; H. Kim, 2013). However, evidence also suggests that perception and memory retrieval are characterized by distinct 'states' that are sustained over time and independent from external stimuli . Characterizing how perception and retrieval states are implemented in the brain represents an important challenge, but one that is complicated by methodological and analytical factors.

One potentially powerful way to characterize distinct cognitive states is by measuring patterns of functional connectivity within the brain (Cohen & D'Esposito, 2016; Fritch et al., 2021; Shirer et al., 2012; Song & Rosenberg, 2021). Functional connectivity is typically

computed over extended windows of time and is therefore well-suited to measure states that putatively persist across, or in the absence of, external stimuli. However, a critical issue in applying functional connectivity during cognitive tasks is that any observed correlations in neural activity may be largely or entirely driven by stimulus-evoked neural responses. That is, if two brain regions consistently respond to external stimuli, this will induce apparent "connectivity" between these regions. Several fMRI studies have addressed this concern by using "background" connectivity—an approach in which stimulus-evoked responses are explicitly modeled and removed, with connectivity then computed using the residual (background) activity (Al-Aidroos et al., 2012; Cole et al., 2019; K. Duncan et al., 2014; Norman-Haignere et al., 2012; Turk-Browne, 2013). Conceptually, this approach can isolate interactions between brain regions that reflect sustained, endogenous processing as opposed to transient, exogenous responses to stimuli (Summerfield et al., 2006; Turk-Browne, 2013).

To date, only a limited number of fMRI studies have used background connectivity to test for differences between perception and memory retrieval states (Cooper & Ritchey, 2019; K. Duncan et al., 2014). Moreover, these studies have only considered potential interactions (connectivity) between a relatively limited number of brain regions. For example, Cooper and Ritchey (2019) examined background FC patterns exclusively between *a priori*, memory-related brain regions in the posterior-medial (PM) and anterior-temporal (AT) networks. They found that regions in these networks exhibited stronger background connectivity during retrieval compared to perception, providing important evidence that perception versus retrieval states can be linked to stimulus-independent processes. While this type of targeted, seed-based analysis is highly valuable for testing specific hypotheses about regions of a priori interest, it is inherently blind to interactions involving non-seed regions (Turk-Browne, 2013). In other words, discoveries are

systematically biased to come from the regions that are tested (Wang et al., 2015). Thus, there is value to unbiased approaches that allow for background FC to be more comprehensively measured—ideally, across the whole brain. That said, while conducting whole-brain functional connectivity may be theoretically appealing, it can be computationally intractable, particularly if applied without down-sampling data. For example, brain volumes consisting of 50,000 voxels would yield 1.25B voxel pairs ('connections') to analyze. For this reason, previous attempts to measure whole-brain functional connectivity have tended to substantially reduce the dimensionality of data by grouping voxels into regions or parcels (e.g., Pantazatos et al., 2012; Shirer et al., 2012; Watanabe et al., 2012).

Here, we sought to identify patterns of background connectivity associated with perception versus retrieval states using full correlation matrix analysis (FCMA) applied to human fMRI data. In contrast, to typical seed-based connectivity measures, FCMA comprehensively considers connectivity between every possible pair of voxels in the brain using sophisticated approaches to overcome historical computational limitations (Kumar et al., 2022; Turk-Browne, 2013; Wang et al., 2015). Specifically, FCMA uses a combination of machine learning (support vector machine; SVM) and parallel computing to efficiently map patterns of connectivity to stimulus or task information (Turk-Browne, 2013; Wang et al., 2015). The computational efficiency afforded by this approach is substantial in that it can reduce computation time from weeks to hours and has the potential to reveal information in fine-grained connectivity patterns that would be missed by conventional seed-based functional connectivity (Wang et al., 2015). We applied FCMA using an experiment that manipulated perception versus retrieval states while carefully controlling for three potentially confounding variables: (1) subjects performed the same judgments on the same images across both perception and retrieval tasks, minimizing differences

in task demands and sensory content; (2) subjects were familiarized with the images in all conditions, minimizing differences in novelty/encoding across perception and retrieval; and (3) behavioral accuracy was matched across key conditions in an attempt to minimize differences in task difficulty.

To preview, we report four main findings: (1) background connectivity, which is orthogonal to evoked responses, allowed for classification of perception versus retrieval states with remarkably high accuracy; (2) perception and retrieval states can be discriminated parsimoniously based on background connectivity patterns in a relatively small number of clusters that span three functional communities: the control network, default mode network (DMN), and retrosplenial cortices (RSC); (3) connections within the control network were relatively stronger during perception states whereas connections within the DMN were relatively stronger during retrieval states; and (4) RSC shifted its coupling with the control network and DMN as a function of cognitive state, suggesting that it acts as a hub for transitioning between perception and retrieval.

Methods

Subjects

Twenty-seven adults with normal or corrected-to-normal vision were recruited to participate for monetary compensation at Princeton University. Three subjects were excluded due to excessive head motion for a total of 24 subjects in the current sample (eleven reported male, mean age = 23.3 years). The Princeton University Institutional Review Board approved the study protocol, and all subjects provided informed consent. The sample size is on par with previous studies that examined functional connectivity changes with memory (Cooper & Ritchey, 2019) and used FC patterns to differentiate task states (Shirer et al., 2012).

Materials

Stimuli consisted of 64 scene and 64 face images. The scene images were collected from the "Massive Memory" dataset (Konkle et al., 2010; http://konklab.fas.harvard.edu/#). The face images were obtained from the FEI face database (Thomaz & Giraldi, 2010; https://fei.edu.br/~cet/facedatabase.html) and contained emotionally neural expressions. Scrambled images were generated as the weighted average between the actual image and its phase-scrambled version (Oppenheim & Lim, 1981; Stojanoski & Cusack, 2014). The script for creating the phase-scrambled images was adopted from code by Nicolaas Prins (e.g., as described here: https://github.com/rordenlab/spmScripts/blob/master/bmp_scramble.m).

Experimental Design and Procedure

During the pre-scan training phase (~20-30 minutes prior to scanning), subjects viewed randomly assigned pairs of images (always consisting of one face and one scene) and indicated how successfully they were in forming a mental association between the images. After viewing all stimuli pairs, they were given a 2-alternative force choice task (AFC) in which a face would be presented above two scenes (or vice versa) and the subjects had to indicate which of the bottom images had been paired with the top image before. The cycle of association-forming and 2-AFC task continued until subjects got each association correct two times in a row (**Figure 2.1A left**).

During the scanning session, subjects completed 3 task conditions across 6 functional runs (2 runs for each condition) using a block design. In the *Perceive* task condition, subjects were asked to identify the visual features of each cue on the screen. That is, if a face cue was presented, subjects were instructed to make a male/female judgment of the face via a button box, whereas if a scene cue was shown, subjects were instructed to make natural/man-made judgment of the scene. On the other hand, during the *Retrieve* task condition, subjects were asked to judge the gender or

naturalness of the cue-associated image (i.e., the pair mate of the cue from the training phase). For example, if a face cue was shown, subjects needed to retrieve the specific associated scene image (not presented) and make a natural/man-made decision on that remembered information. Likewise, if a scene cue was shown, subjects were supposed to retrieve the specific associated face image and make a male/female decision on that remembered information. To minimize the probability that the neural correlates we later identified were not driven solely by differences in task difficulty between *Perceive* and *Retrieve* task conditions, we included a *Scramble* condition. During the *Scramble* condition, subjects completed the same task as they did in the *Perceive* condition, but the visual cues were scrambled using a weighted average of the original image and its phase-scrambled version. The weight of this average was established based on a behavioral pilot study using the same design which sought to vary the weight until accuracy between the *Scramble* and *Retrieve* task conditions was matched (**Figure 2.1 right**). Note that although these two conditions were equated in terms of accuracy, they did differ in terms of reaction time (see Results and Discussion sections). Each run started with a 6-s blank lead-in period, followed by 8 task epochs and ended with a 6-s lead-out period. Each epoch consisted of a 4-s presentation of instructions, followed by 8 2-s presentations of single images presented at central fixation separated by a 1-s interstimulus interval. Each sequence of stimuli was followed by a 12-s inter-block-interval. Together, the duration of each trial, epoch, and run was 3 s, 40 s and 332 s, respectively. Note that all epochs within a functional run are of the same condition, and that all visual stimuli of an epoch are of the same category (i.e., either all faces or all scenes). The order of the runs was randomized across all subjects and presented in different orders. The order of the three conditions was randomized across the first three runs for each subject and then the same order was repeated for the last three runs of that subject.

Image Acquisition and Preprocessing

The fMRI data were acquired with a 3T scanner (Siemens Prisma) at the Princeton Neuroscience Institute. Functional data were acquired using a T2*-weighted multiband EPI sequence (repetition time = 1 s, echo time = 26 ms, flip angle = 50°, FOV = 260 x 260, resolution = 2.5 x 2.5 x 2.5 mm, multiband acceleration factor = 4) with 44 axial slices aligned to the anterior commissure/posterior commissure. A whole-brain T1-weighted MPRAGE 3D anatomical volume (1 x 1 x 1 mm voxels) was collected to improve registration. One phase and two magnitude field maps were collected to correct field inhomogeneities.

The first 6 lead-in volumes of each functional run were manually discarded before entering the preprocessing pipeline. Image preprocessing was performed using fMRIPrep 20.1.0rc1 (Esteban et al., 2019). All functional images were corrected for slice-acquisition time, head motion, and susceptibility distortion, and were normalized to a standard template, yielding preprocessed BOLD runs in MNI152NLin2009cAsym space. Following use of fMRIPrep, the minimally preprocessed functional runs were further processed using FSL (Woolrich et al., 2001) with a Nipype implementation (Gorgolewski et al., 2011). All functional images were smoothed with a 5.0 mm FWHM Gaussian kernel and high-pass filtered at 0.01 Hz. For each subject, the intensity values in each voxel in each of the 6 functional runs were then normalized using the mean and standard deviation of the resting period. The resting period for each functional run was defined as the 6 lead-out volumes plus all 12-s inter-block intervals of that run, which were shifted for 4 TRs to account for the hemodynamic delay. This normalization is intended to remove the BOLD signal differences across runs and thus all 6 runs were then concatenated to one time series and used for further modeling.

Stimulus-Evoked and Residual (i.e., background) Activity

We computed residual activity by modeling and then regressing out the stimulus-evoked component from the preprocessed data in order mitigate stimulus-evoked coactivation confounds (Al-Aidroos et al., 2012; Cole et al., 2019). First, we constructed a confound regression model using FSL (implemented in NiPype) in order to minimize the effect of the following confound variables (obtained from fMRIPrep): six head motion parameters and the mean time series from white matter and cerebrospinal fluid. The resulting timeseries from regressing out the confound regressors are referred to as the stimulus-evoked activity timeseries in all subsequent analyses, as they are fully preprocessed, yet contain the stimulus-evoked components. Second, we estimated and removed the stimulus-driven components from the stimulus-evoked timeseries using a finite impulse response (FIR) model, which modeled the first 36 TRs for every epoch separately for face and scene epochs, resulting in 36 (TR) x 2 (epoch category) x 3 (condition) = 216 regressors. FIR is believed to be the optimal GLM for removing stimulus-evoked response because it does not assume the shape of the hemodynamic response function (Cole et al., 2019; Norman-Haignere et al., 2012). The residual timeseries data are referred to as the residual activity and used for computing background functional connectivity for all subsequent analyses.

Full Correlation Matrix Analysis on Residual Activity

We utilized full correlation matrix analysis (FCMA) as implemented in the Brain Imaging Analysis Kit (BrainIAK; version 0.11; http://brainiak.org) to conduct an unbiased, whole-brain voxel-wise FC analysis that systematically considers all pairwise correlations in the brain to explore the differences in connectivity configurations between perception and retrieval states. All FCMA jobs were executed on Talapas, the HPC cluster at University of Oregon (https://racs.uoregon.edu/talapas). Each FCMA inner loop job was spread across 4 nodes, with each node supporting 28 threads and a job took around 4 hours to complete. Each node was

equipped with two Intel E5-2690v4 processors, with 128 GB of memory. FCMA took in the residual activity and computed a full correlation matrix (i.e., whole-brain voxel-wise correlation matrix; 92745 voxels x 92745 voxels) for each task epoch. Therefore, for each subject, 8 (epoch) x 2 (run) = 16 full correlation matrices were computed per task condition (i.e., *Perceive*, *Retrieve* and *Scramble*; **Figure 2.1 c-e**). Using these full correlation matrices, FCMA aimed to (i) examine whether perception (*Perceive* and *Scramble*) versus retrieval (*Retrieve*) states can be successfully decoded from background connectivity patterns, and (ii) identify the connectivity configuration that characterizes each cognitive task state. Notably, the whole-brain correlation matrix is not easily interpretable by humans given its high dimensionality, and FCMA solves this problem by identifying of the most important/diagnostic regions of the brain involved in discriminating cognitive states (**Figure 2.1F**). Specifically, FCMA implements a nested leave-one-subject-out cross-validation (LOOCV) framework: the outer loop contains 23 training subjects (23 x 48 epochs/subject = 1104 epochs) and 1 left-out test subject (1 x 48 epochs/subject = 48 epochs) for each outer-loop iteration; and the inner-loop uses 22 training subjects (22 x 48 epochs/subject = 1056 epochs) and 1 left-out test subject (1 x 48 epochs/subject = 48 epochs) within the outer training set for each inner-loop iteration. Importantly, the inner-loop intends to select the top *k* most useful voxels (based on their connectivity patterns) from the training data (**Figure S2.1**) and the outer loop aims to train classifiers on connectivity patterns of the selected voxels and test their ability to predict left-out data (**Figure 2.1G, H**). Note that we also performed parcel-level analysis to demonstrate the sensitivity advantage of our more fine-grained approach. We utilized the MNI version of the Schaefer parcellation scheme (https://github.com/ThomasYeoLab/CBIG/tree/master/stable_projects/brain_parcellation/Schaefer2018_LocalGlobal/Parcellations/MNI; Schaefer et al., 2018), and performed analyses on

parcellations of different granularity (400 and 1000 parcels), which yielded comparable patterns of results as one another.

For each iteration of the outer loop, the inner-loop worked with the training data from 23 subjects (N-1 subjects) and performed a separate, nested LOOCV. Specifically, the inner-loop tested the accuracy of using each voxel's seed maps (i.e., how much the voxel is connected to all other voxels in the brain) to differentiate perception (i.e., *Perceive* and *Scramble*) from retrieval (i.e., *Retrieve*) state (**Figure S2.1**). Each voxel would get an accuracy score for separating *Retrieve* and *Perceive* FC patterns, and another score for separating *Retrieve* and *Scramble* FC patterns. The minimum score of the two was assigned to the voxel and all assigned scores were averaged across the 23 inner-loop LOOCV iterations (i.e., training using 22 subjects and testing on a left out subject). The minimum score was used to make sure one of the two comparisons did not drive the overall effect and thus voxel selection prioritized discovery of regions which were sensitive to both comparisons. For example, a voxel's seed map might be able to separate *Retrieve* from *Scramble* well by picking up the visual content information (i.e., scramble vs. intact), but not separate *Retrieve* from *Perceive* well when the visual content difference was absent. Computing the minimum accuracy scores allowed us to measure how well more comprehensively each voxel's seed map encoded cognitive task state differences.

The resulting scores indicated the ability of each voxel to differentiate perception from retrieval states independent of the test data (i.e., the left out subject in the outer loop). Based on these scores, masks of the top k most useful voxels were created from each inner-loop and the whole-brain full correlation matrices were reduced to k x k correlation matrices. The current study tested all results with k = 100, 1000, 3000, 5000, 7000, 10000 and 15000 voxels, and subsequently focused on results using k = 3000. this was done for two reasons. First, model

performances dramatically improved as the voxel masks were enlarged from k = 100 to k = 3000. However, model performance seemed to plateau when the top 3000 voxels were selected. Second, our information mapping pipeline (See **Methods: *Information Mapping***) identified a shared mask that included about 3500 voxels. The results from k = 3000 therefore provides the most direct comparison and is the most representative for subsequent analyses. Using these k x k connectivity matrices, the FCMA outer-loop trained 3 classifiers (one for each pair of task conditions, e.g., *Perceive* vs. *Retrieve*) and tested the model performance using the left-out testing data.

Regular Cross-Validation and Generalization Tests

Classifiers built during FCMA were first trained and tested on the same task condition comparison (regular cross-validation). To quantify and compare model performance for each task comparison, we computed the area under the receiver operating characteristic curve (AUC) for each classifier. One way ANOVA was used to compare the AUCs for the three classifiers. The goals of the regular cross-validation tests were to examine (i) whether task conditions could be successfully decoded from background connectivity patterns and (ii) whether task condition comparisons that involve cognitive task state differences (e.g., *Retrieve* vs. *Perceive*) could be decoded with higher accuracies relative to the comparison that did not involve such differences (e.g., *Scramble* vs. *Perceive*).

During the generalization test, a classifier was trained on one task condition comparison (e.g., *Perceive* vs. *Retrieve*) but tested on a different comparison (e.g., *Perceive* vs. *Scramble*). The generalization test can be conducted between each pair of task condition comparisons; we argue that the bidirectionally averaged generalization AUCs should indicate the classifiers' sensitivity to a certain dimension of task differences (**Figure 2.2D**). For example, both the

Retrieve vs. *Perceive* and *Retrieve* vs. *Scramble* comparisons involve cognitive task state differences. As a result, high bidirectionally averaged AUC scores across classifiers trained on *Retrieve* vs. *Perceive* and tested on *Retrieve* vs. *Scramble* and vice versa would indicate that the classifiers were indeed trained to pick up on cognitive task state information. On the other hand, high bidirectionally averaged AUC score across *Retrieve* vs. *Perceive* and *Scramble* vs. *Perceive* comparisons would suggest that the classifiers were trained to pick up on task difficulty (as reflected by decreased reaction times and increased accuracy in the *Perceive* condition compared to the others) differences. Likewise, high bidirectionally averaged AUC scores across *Scramble* vs. *Perceive* and *Scramble* vs. *Retrieve* comparisons would suggest that the classifiers were trained to detect scrambled versus intact visual features. Thus, the averaged bidirectional generalization accuracies served to measure the degree to which differences in cognitive task states, task accuracies, and visual content drove classifier performance. The primary goal of the generalization test, then, was to examine whether classifiers were able to preferentially detect connectivity patterns underlying perception versus retrieval task state differences.

Multivoxel Pattern Classification Analyses

We trained activity pattern-based classifiers to test 1) whether FCMA classifier performances were driven by any coactivation confounds left in the residual activity and 2) whether simple MVPA and background FC patterns rely on the same type of cognitive processes. The evoked activity for each voxel was calculated as the average across the 24 TRs thought to capture the peak evoked BOLD response (shifted 4s to account for hemodynamic delay), resulting in a single value for each voxel per epoch. As such, the number of features used for MVPA classification was equal to the number of voxels in the brain mask. Per the first goal, using the *k* voxel masks generated by FCMA inner-loop (See section: ***Full Correlation Matrix***

Analysis on Residual Activity), we trained pattern classifiers using residual activity to perform the regular cross-validation tests (**Figure S2.2**). Per the second goal, with each set of *k* voxel masks, we trained pattern classifiers using stimulus-evoked activity to perform the regular cross-validation test (**Figure 2.3B middle**). Pattern classification analyses were performed using a support vector classifier (C = 1) implemented in the Scikit-learn module in Python (Pedregosa et al., 2011).

Information Mapping

Due to the leave-one-out cross-validation scheme, each fold of the outer-loop produced non-identical sets of top voxels. To obtain a common mask, we combined the FCMA inner-loop with non-parametric permutation tests to generate a group-level mask that included the top voxels differentiating perception from retrieval states better than chance. We obtained this group-level mask in three steps. First, using a LOOCV scheme across all 24 subjects, we averaged the classification accuracy composite score (i.e., the minimum of the accuracy scores for separating *Retrieve* vs. *Perceive* and *Retrieve* vs. *Scramble* FC patterns) for each voxel (**Figure S2.1**) and used this as the "observed" score for each voxel. Second, we shuffled the labels of all three task conditions for each subject and repeated the outer-loop training-testing pipeline using the shuffled labels for 100 iterations. As a result, we generated a null distribution of the classification accuracy composite scores for each voxel. Using the mean and standard deviation of the classification accuracy score null distribution for each voxel, we z-transformed the observed feature selection score computed above (i.e., the group-averaged composite accuracy score). We chose a relatively stringent voxel-wise primary threshold ($P < 0.0001$) to reduce the likelihood of false positives and to avoid finding large voxel clusters that span the brain (Woo et al., 2014). Voxels that passed the threshold were divided into clusters using

3dClusterize and the corresponding cluster-extent threshold was computed using 3dClustSim with AFNI (whole-volume alpha-values: -athr < 0.01). In total, 62 clusters passed the cluster-extent threshold, with size ranging from 620 to 2 voxels. In the last phase of the information mapping, we selected clusters according to their size and whether they improved model performance when combined with all larger clusters. Specifically, we began with the largest cluster (620 voxels), then we sequentially added voxels from the next largest cluster to our mask and used the FCMA outer loop to test how well this set of voxels differentiated perception from retrieval states. In other words, we iteratively ran a set of FCMA outer loop tests, and measured the change in classification performance as the mask accumulated each new cluster of voxels (**Figure S2.3A**). The rationale for performing cluster selection is to identify the smallest number of "sufficient" nodes whose network dynamics capture the differences between perception and retrieval states and ultimately reduce the full correlation matrix of the brain to a tractable set of representative ROIs.

Community Detection

We applied community detection algorithms on the clusters identified by information mapping, aiming to understand the network level differences between perception and retrieval states. Specifically, we averaged across all voxels within each cluster to obtain cluster-level time series data for each epoch. Cluster-level background functional connectivity (FC) matrices were then computed for each epoch for every subject, and then averaged within each task condition, resulting in one group-averaged connectivity matrix for the *Perceive*, *Scramble,* and *Retrieve* conditions respectively. Community detection on weighted graphs (i.e., the connectivity matrices calculated above) was performed using the Louvain algorithm via NetworkX in Python. Following the approach used in prior work (Barnett et al., 2021; Ji et al., 2019), we ran the

algorithm 1000 times on the weighted graphs to tune the resolution parameter in order to maximize modularity, which in turn captures how well a network can be subdivided into non-overlapping groups (Rubinov & Sporns, 2011). The tuned resolution parameters (gamma) were 1.10, 1.13, 1.19, for Perceive, Retrieve and Scramble task conditions, respectively. To visualize intra- and intramodular connectivity, we used the Fruchterman-Reingold force-directed projection implemented in NetworkX to project the graphs onto 2D spaces.

Within- and Between-Communities Connectivity

To further understand network-level differences within and between the communities identified using the steps above (DMN, Control, and RSC; see **Results**), we computed a cluster-wise subject-level FC matrix for each task condition. We averaged the FC matrices for *Perceive* and *Scramble* conditions to create composite matrices that reflect FC dynamics underlying the perception state. To examine the coupling pattern across communities, we averaged across the connectivity strength between clusters (nodes) within the same functional community using both perception and retrieval state FC matrices. A paired sample t-test was used to examine whether DMN-Control connectivity strength differed between perception and retrieval states; and a two-way repeated measures ANOVA was then used to examine whether RSC nodes changed their coupling pattern with respect to the DMN and Control network nodes. To examine within-community connectivity strength, we averaged the connectivity strength between all nodes within the DMN, Control, and RSC regions for both perception and retrieval states. Similarly, a two-way repeated measures ANOVA was used to assess whether a functional community was biased toward a certain cognitive task state. All statistical analyses were performed using Pingouin 0.5.1 with Python3.

Pattern Similarity Analyses on Stimulus-Evoked Activity

The goal of this set of analyses was to identify any potential differences between the three functional communities in their roles in performing cognitive tasks. We focused on three different cognitive aspects and tested the degree to which each functional community was sensitive to (i) the current visual category (i.e., face vs. scene), (ii) the current behavioral task (i.e., gender vs. naturalness judgement), and/or (iii) the current cognitive state (i.e., perception or retrieval). To do that, we performed pattern similarity analyses using both stimulus-evoked activity patterns and background connectivity patterns.

To obtain the stimulus-evoked activity patterns, we extracted the 24 task TRs for each epoch (after being shifted 4 s to account for hemodynamic delay) from the post-confound regression time-series. These stimulus-evoked estimates were then averaged along the time dimension and reshaped into a vector for each cluster (length of the vector is the number of voxels in that cluster). Background connectivity patterns for each cluster were computed as the correlation over time between the cluster and the other 15 clusters, reshaped into a 15-dimensional vector for each ROI (**Figure 2.6B**). To compute pattern similarity measures, the Fisher's Z transformed correlations between each pair of vectors from different functional runs were calculated (Kriegeskorte et al., 2009; **Figure 2.6A**). Sensitivity was quantified as the difference between within-state epoch pattern similarity and between-state epoch pattern similarity. For example, when examining sensitivities for the current task judgement, pattern similarities were computed among all epochs with the same judgement (i.e., gender to gender and naturalness to naturalness) and compared to those with different judgments (i.e., gender to naturalness). Sensitivity was calculated by using the average within-state pattern similarity score minus the average between-states pattern similarity score. Thus, a significantly positive sensitivity index would suggest that the given ROI produced relatively distinct activity and/or

connectivity patterns for the two aspects of the task (state, content, or judgement). We averaged the sensitivity scores across ROIs within the same functional communities. A one-way ANOVA was used to compare sensitivity scores of each cognitive process across the three functional communities.

Results

Behavioral Results

We designed an fMRI task that required subjects to perform judgments on information that was either available in the perceptual environment (perception) or had to be retrieved from memory (retrieval), in both cases matched in terms of visual content and task accuracy (**Figure 2.1A**). Overall, subjects demonstrated greater accuracy in the *Perceive* compared to *Retrieve* condition, but comparable accuracy between *Scramble* and *Retrieve* conditions (**Figure 2.1B**).

Figure 2.1. Task paradigm and analysis flowchart.
(**A**) Behavioral training and in-scanner tasks. Subjects formed mental associations between face and scene images outside of the scanner and then made judgments on either perceptual or mnemonic information in the scanner. (**B**) In-scanner behavioral performance, with the orange bar indicating the sample mean and asterisks indicating $p < 0.001$. (**C**) Each condition had 16 epochs per subject, with each epoch lasting 40 s. (**D**) The residual activity for each task epoch was computed by regressing out the stimulus-evoked component using a finite impulse response general linear model. **(E**) Whole-brain voxel-wise background FC matrices were computed for each task epoch. These matrices were *n*-by-*n* shape, where *n* is the total number of voxels in the brain (n = 92,745). (**F**) Background FC matrices of FCMA-selected voxels. FCMA was implemented to select a certain number of voxels whose connectivity patterns were most accurate for separating perception and retrieval states based on two-way classifications of epochs from different conditions. The details of the feature selection process are shown in **Figure S2.1**. In essence, FCMA reduced the whole-brain correlation matrix to a *k*-by-*k* correlation matrix for each epoch, where *k* is the number of voxels selected by FCMA. The current study tested multiple values of *k*, ranging from 100 to 15,000. (**G**) Model training. Using a cross-validation framework, SVM classifiers with precomputed linear kernel were trained to separate all task condition comparisons. (**H**) Model testing. Trained models were tested using the left-out subject for each fold. During the regular cross-validation test, the model was tested on the same task condition comparison as it was trained on. During the generalization test, the model was tested on a different task condition comparison than it was trained on.

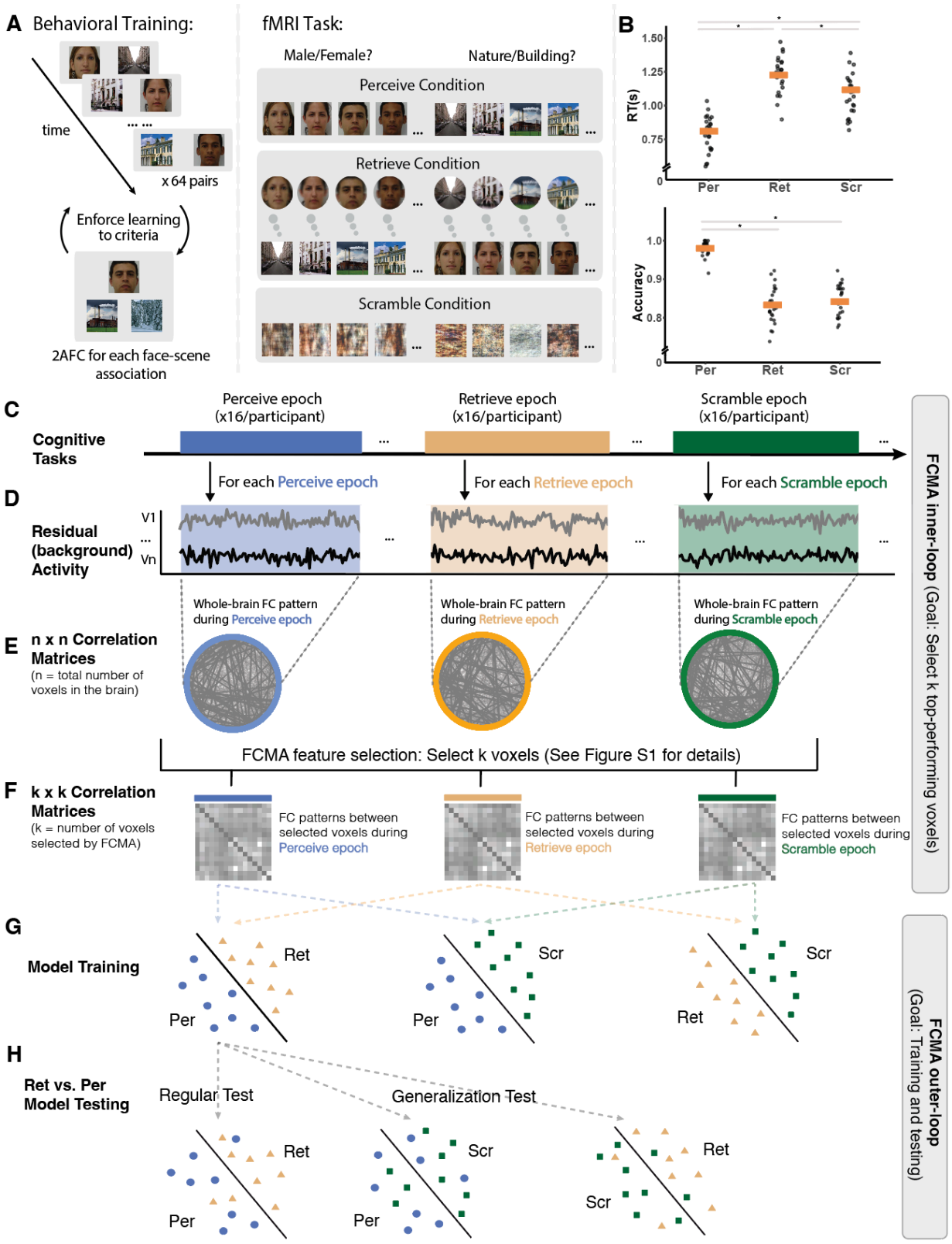
A Behavioral Training:
time
x 64 pairs
Enforce learning to criteria
2AFC for each face-scene association
fMRI Task:
Male/Female?
Nature/Building?
Perceive Condition
Retrieve Condition
Scramble Condition
B
RT(s)
Per
Ret
Scr
Accuracy
C
Cognitive Tasks
Perceive epoch (x16/participant)
Retrieve epoch (x16/participant)
Scramble epoch (x16/participant)
D
Residual (background) Activity
V1
Vn
For each Perceive epoch
For each Retrieve epoch
For each Scramble epoch
E
n x n Correlation Matrices
(n = total number of voxels in the brain)
Whole-brain FC pattern during Perceive epoch
Whole-brain FC pattern during Retrieve epoch
Whole-brain FC pattern during Scramble epoch
FCMA feature selection: Select k voxels (See Figure S1 for details)
F
k x k Correlation Matrices
(k = number of voxels selected by FCMA)
FC patterns between selected voxels during Perceive epoch
FC patterns between selected voxels during Retrieve epoch
FC patterns between selected voxels during Scramble epoch
FCMA inner-loop (Goal: Select k top-performing voxels)
G
Model Training
Ret
Per
Scr
Per
Scr
Ret
H
Ret vs. Per Model Testing
Regular Test
Generalization Test
Ret
Per
Scr
Per
Ret
Scr
FCMA outer-loop (Goal: Training and testing)

Specifically, one-way (condition) repeated measures ANOVAs revealed a main effect of condition for both reaction time ($F_{(2, 46)} = 288.8$, $p < 0.001$, $\eta^2 = 0.97$) and accuracy ($F_{(2, 46)} = 91.21$, $p < 0.001$, $\eta^2 = 0.90$). Although accuracy in the *Perceive* condition was significantly greater than that in the *Retrieve* condition ($t_{(23)} = 13.4$, $p < 0.001$, 95% CI = [0.16, 0.22], Cohen's d = 3.55), the *Retrieve* and *Scramble* conditions did not significantly differ, serving as a useful point of comparison ($t_{(23)} = -1.65$, $p = 0.11$, 95% CI = [-0.07, 0.01], Cohen's d = 0.45). The process (see Methods) used to match accuracy across Retrieve and Scramble conditions was not designed to match reaction time between Retrieve and Scramble conditions, which significantly differed from one another. Specifically, subjects differed across the three conditions in terms of reaction time ($F_{(2,46)} = 230.9$, $p < 0.001$, $\eta^2 = 0.91$) and had a significantly slower reaction time in the Retrieve condition compared to Perceive and Scramble conditions and slower reaction times for Scramble compared to Perceive (Retrieve vs. Perceive: $t_{(23)} = 18.8$, $p < 0.001$, 95% CI = [0.39, 0.0.49], Cohen's d = 3.63; Retrieve vs. Scramble: $t_{(23)} = 6.94$, $p < 0.001$, 95% CI = [0.10, 0.19], Cohen's d = 1.11; Scramble vs. Perceive: $t_{(23)} = 16.44$, $p < 0.001$, 95% CI = [0.26, 0.33], Cohen's d = 2.37).

Perception and Retrieval Involve Distinct Background Connectivity Patterns

We first examined whether perception and retrieval states involve different "state-related" whole-brain FC patterns. Using background connectivity analysis, voxel-wise whole-brain correlation matrix was computed for each epoch (**Figure 2.1E**; for details see **Methods**: ***Stimulus-Evoked and Residual Activity***). We then applied full correlation matrix analysis (FCMA) to test whether a trained support vector machine (SVM) could successfully separate perception epochs (*Perceive* and *Scramble*) from retrieval epochs (*Retrieve*; **Figure 2.1G-H**). To evaluate binary classifier performance within the top-performing voxels, we computed the

receiver operating characteristic (ROC) curves and area under the ROC curve (AUC) for each classifier per subject, with larger AUC indicating better model performance (Hanley & McNeil, 1982). We started by having FCMA select $k = 100$ best performed voxels to train the classifier and gradually increased k until classifier performance asymptoted (for details see **Methods**: ***Full Correlation Matrix Analysis on Residual Activity***). As seen in **Figure 2.2A,** accuracy plateaued when the mask reached roughly 3,000 voxels, and the overall pattern of results across conditions did not dramatically change as a function of the mask size used. Accordingly, we performed follow-up analyses on the top $k = 3{,}000$ voxel masks. These analyses suggested that classifiers trained on background FC patterns successfully differentiated epochs of perception from retrieval states (*Perceive* vs. *Retrieve*: $M_{AUC} = 0.87 \pm 0.06$, $t_{(23)} = 28.62$, $p < .001$, 95% CI = [0.84, 0.89], Cohen's d = 5.84; *Retrieve* vs. *Scramble*: $M_{AUC} = 0.83 \pm 0.08$; $t_{(23)}$ 19.39, $p < .001$, 95% CI = [0.79, 0.86], Cohen's d = 3.96; one-sample t-test against chance-level performance of $\bar{\mu} = 0.5$; see also **Figure S2.2A** for results in terms of proportion correct). Control analyses showed that state-related differences were selectively captured by background FC measures and not by left-over differences in the stimuli-evoked component of the signal. In particular, pattern analysis using residual activity patterns (i.e., simple MVPA on residual timeseries) in the same voxel masks failed to discriminate any task condition comparisons (all model performances ≈ 50% correct; **Figure S2.2B**).

One potential concern with the connectivity results above is that the above-chance classification performance was not strictly related to differences in perception versus retrieval states *per se* and might reflect the contribution of several potential confounding factors. For example, in addition to capturing differences in perception and retrieval, the *Perceive* vs. *Retrieve* comparison also varied in terms of task difficulty (as measured by accuracy and reaction

time) and the *Scramble vs. Retrieve* comparison also varied in terms of sensory input (i.e., partially scrambled vs. intact stimuli). To ensure that the variations in background FC patterns (among FCMA-selected voxels) were most strongly induced by state-related differences, we performed two extra sets of analyses to rule out these potential confounds. First, we tested the background FC pattern separability of *Perceive* vs. *Scramble* conditions—a task condition comparison that differed in terms of both task difficulty and visual content *but not* in perception/retrieval cognitive states. If the background FC patterns contain mostly state-related information, having equated perception state for both *Perceive* and *Scramble* should worsen classifier performance. Consistent with this hypothesis, AUC significantly differed between the non-state-related and state-related background FC classifiers ($F_{(2,46)} = 20.30$, $p < 0.001$, $\eta^2 = 0.47$), with post-hoc tests revealing that *Perceive-Scramble* AUC was significantly lower than *Retrieve-Perceive* ($t_{(23)} = -5.62$, $p < 0.001$, 95% CI = [-0.19, -0.09], Cohen's d = 1.45; **Figure 2.2A**) and *Retrieve-Scramble* ($t_{(23)} = -4.10$, $p < 0.001$, 95% CI = [-0.15, -0.05], Cohen's d = 0.97). No significant difference was observed in the comparison of *Retrieve-Perceive* to *Retrieve-Scramble*, although there was a trend for higher AUC for *Retrieve-Perceive* ($t_{(23)} = 1.82$, $p = 0.08$, 95% CI = [-0.01, 0.08], Cohen's d = 0.52).

In the second set of analyses, we leveraged classification generalization to assess the degree to which background FC patterns capture differences within each of three dimensions: (1) cognitive state (i.e., perception vs. retrieval); (2) task difficulty; and (3) visual content (for details see **Methods**: ***Regular Cross-Validation and Generalization Tests***). This was operationalized as how well a classifier trained on one pair of conditions generalized to another pair of conditions that differed on the same putative dimension (**Figure 2.1H**). We predicted that generalizability as measured by averaged bidirectional AUC should be greatest for task condition comparisons

that involve state-related differences (i.e., *Perceive* vs. *Retrieve* to/from *Scramble* vs. *Retrieve***;** **Figure 2.2B**) compared to task difficulty or visual content. Indeed, we found that background FC classifiers differed in their sensitivities to the three dimensions (cognitive task state: M_{AUC} = 0.78 $\pm$ 0.07; task difficulty: M_{AUC} = 0.68 $\pm$ 0.07; visual content: M_{AUC} = 0.53 $\pm$ 0.11; $F_{(2,69)}$ = 52.80, $p < 0.001$, η^2 = 0.60, **Figure 2.2C**). Follow-up t-tests suggested that generalization of background FC classification was highest when state-related differences were aligned compared to other dimensions of generalization (*ts* > 5.78, *p*s < 0.001). Together, these two analyses provide additional support to the finding above that the pattern of background FC contains information about perception and retrieval states above and beyond other differences between conditions.

Background Connectivity and Evoked Activity Patterns Capture Distinct Cognitive Processes

Previous research has shown that stimulus-evoked, multi-voxel activity patterns reflect ongoing cognitive processes and can be used to train classifiers for separating task conditions (Norman et al., 2006). How such measures relate to background FC is less well understood. Accordingly, we investigated whether patterns of stimulus-evoked activity reflect similar or distinct aspects of perception and retrieval states compared with patterns of background FC. Specifically, we trained MVPA classifiers on stimulus-evoked activity patterns for each pair of task conditions and compared the performance to classifiers trained using background FC patterns (**Figure 2.3 left and middle**; for details see **Methods**: ***Pattern Similarity Analyses on Stimulus-Evoked Activity***). Stimulus-evoked activity patterns led to reliable classification of task conditions (*Retrieve* vs. *Perceive*: M_{auc} = 0.86 $\pm$ 0.06; *Scramble* vs. *Perceive*: M_{auc}= 0.90 $\pm$ 0.12; *Scramble* vs. *Retrieve*: M_{auc}= 0.90 $\pm$ 0.12; *ts* > 37.62, *p*s < 0.001). Interestingly, however,

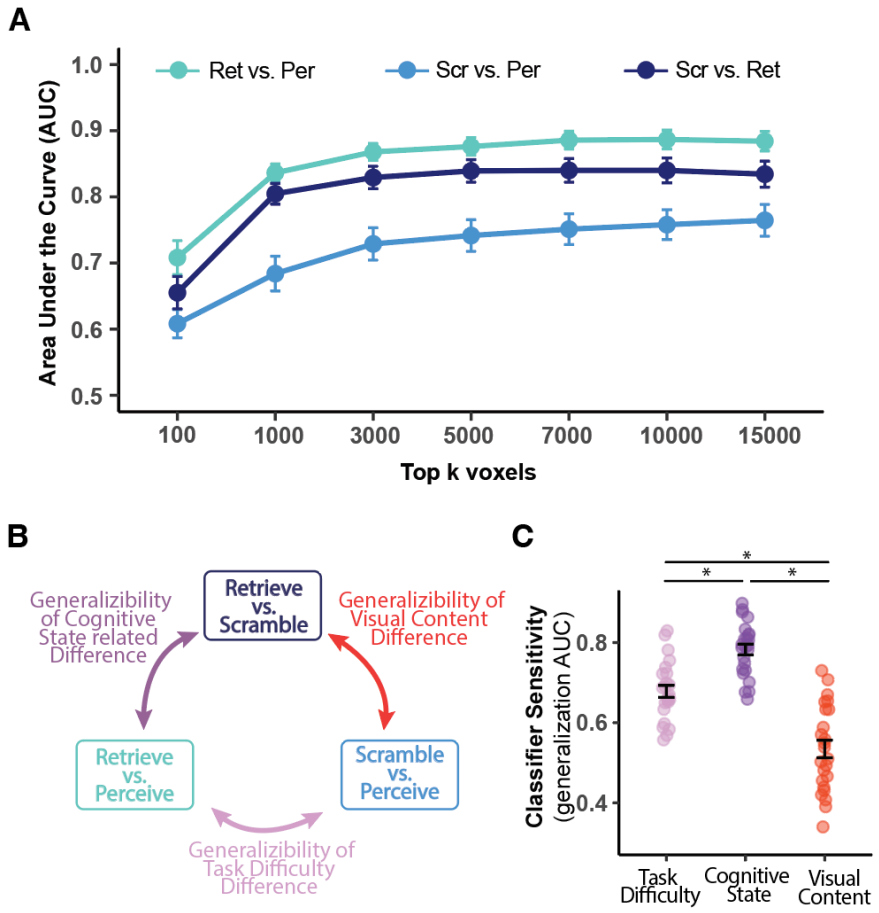

Figure 2.2. Classification of task conditions based on different features.
A) Performance of background FC classifiers as a function of the number of voxels selected by FCMA. Area under the receiver operating characteristic curve (AUC) was computed for each leave-one-subject-out testing fold to examine the performance of the binary classifiers. The error bars indicate the standard error of the mean AUC across all subjects being tested. The results suggest that the top 3,000 voxels were able to differentiate task conditions as well as larger sets of voxels and so were used for follow-up analyses. **B)** Schematic diagram for measuring sensitivity to different aspects of cognitive processes using generalization tests. For example, given that both *Retrieve* vs. *Scramble* and *Retrieve* vs. *Perceive* comparisons involve state-related differences, success in classifying *Retrieve* vs. *Perceive* with the background FC classifier trained on *Retrieve* vs. *Scramble* (and vice versa) would provide strong evidence that the classifier is sensitive to state-related differences. **C)** Sensitivity of background FC classifiers to three distinctions: cognitive state (i.e., perception vs. retrieval), visual content (i.e., scrambled vs. intact), and task difficulty (i.e., low vs. high accuracy). Sensitivity was quantified as the average AUC from classifiers trained on one set of conditions and tested on another set along the same task-related dimension (generalization test). Error bars indicate the standard error of the mean across all testing folds. Asterisks indicate $p < 0.05$.

activity-based classification results demonstrated systematically different pattern compared to those of background FC-based classification. Specifically, a two-way repeated measures ANOVA with comparisons (*Retrieve* vs. *Perceive*, *Scramble* vs. *Perceive, Scramble* vs. *Retrieve*) and neural measure (stimulus-evoked activity, background FC) revealed a main effect of neural measure ($F_{(1,23)} = 58.60$, $p < 0.001$, $\eta^2 = 0.72$), highlighting the overall impact of using evoked-responses for classification. There was also a main effect of comparison ($F_{(2,46)} = 16.19$, $p < 0.001$, $\eta^2 = 0.41$). Strikingly, the ANOVA also revealed differential sensitivity across comparisons as a function of neural measure ($F_{(2,46)} = 9.70$, $p < 0.001$, $\eta^2 = 0.30$). Based on post-hoc t-tests (see **Figure 2.3**), this interaction appeared to be driven by relatively greater classification performance for comparisons involving cognitive state differences (i.e., *Retrieve* vs. *Perceive* and *Scramble* vs. *Retrieve*) than those both involving perceptual decisions (i.e., *Scramble* vs *Perceive*), but only for background FC as the neural measure. Activity-based classification, on the other hand did not show a similar relationship.

The above findings are suggestive that stimulus-evoked activity and background FC may capture distinct aspects of the underlying cognitive state. To test this hypothesis more directly, we trained hybrid classifiers that combined both stimulus-evoked activity and background FC. The decision confidences of the hybrid classifier were computed as the averaged decision function outputs from both FC and MVPA classifiers. The rationale is that the hybrid classifiers should achieve better performance than either classifier on its own if the two neural measures capture distinct state-related processes (Manning et al., 2018). In line with the above results, a two-way repeated measures ANOVA revealed a significant main effect of classifier types (i.e., FC vs. MVPA vs. hybrid; $F_{(2,46)} = 68.32$, $p < 0.001$, $\eta^2 = 0.75$; **Figure 2.3**). Follow-up analyses showed that the average AUC of hybrid classifiers was significantly greater than background FC

classifiers ($t_{(23)}$ = 9.95, p < 0.001, 95% CI = [0.11, 0.17], Cohen's d = 2.58) and evoked-activity MVPA classifiers ($t_{(23)}$ = 3.06, p = 0.006, 95% CI = [0.01, 0.04], Cohen's d = 0.88). Together, these results suggest that evoked activity and background FC reflect distinct, possibly complementary, neural signatures of cognitive processes, with the latter displaying more relative sensitivity to state-related differences across retrieval and perception.

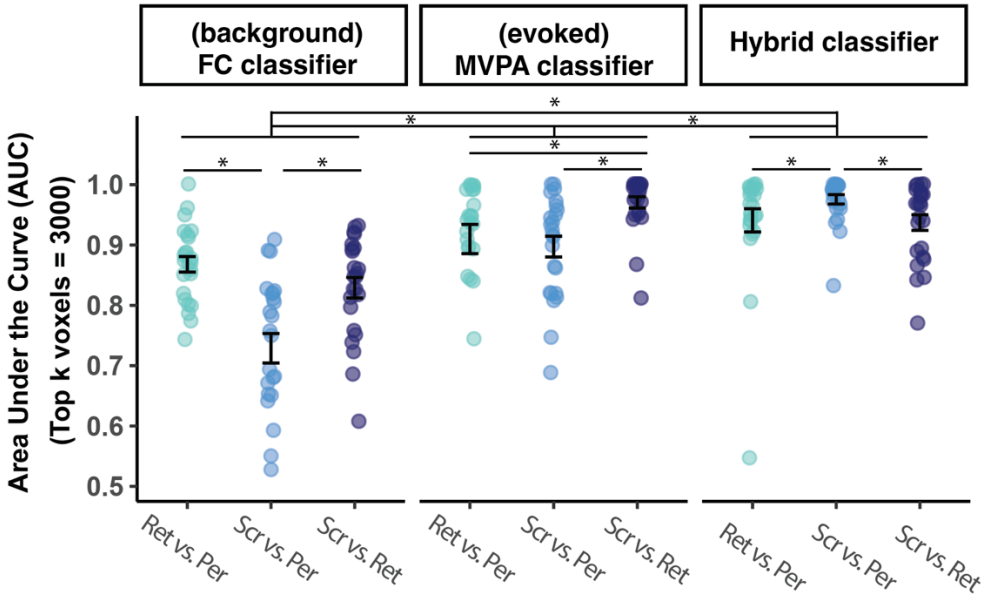

Figure 2.3. Classification of task conditions based on different neural measures. Comparing performance of binary classifiers trained with different neural measures: background FC (left), evoked activity (middle), hybrid FC + activity (right). Each dot represents a subject. The error bars indicate the standard error of the mean AUC across all subjects being tested.

Regions and Functional Communities Underlying Perception and Retrieval States

The results so far suggest that background FC patterns of FCMA selected voxels capture differences between perception and retrieval states. However, the interpretation of these results in terms of brain regions is complicated by two key issues: 1) the top voxels were not necessarily identical across cross-validation folds and 2) the number of connections between voxels remains quite large. We sought to address each of these issues in turn. Per the first issue, because of leave-one-subject-out cross-validation, different sets of voxels were selected by FCMA for each

left-out testing subject/fold. Accordingly, to allow further characterization and interpretation of state-related background FC patterns, we combined the FCMA inner-loop (**Figure S2.1**) with permutation-based statistical inference tests to obtain a shared set of voxels across all testing folds (yielding roughly 3500 voxels) whose background FC patterns captured state-related differences (for details see **Methods**: ***Information Mapping***). Per the second issue, even with a shared voxel mask, it may still be intractable to interpret FC patterns consisting of millions of connections (i.e., $\sim 8 \times 10^6$ unique connections among 3500 voxels). For this reason, we further reduced the dimensions of FC patterns using clustering. We first identified spatially contiguous clusters of voxels in the shared mask using a novel FCMA-then-clustering pipeline (see **Methods** and **Figure S2.3**). This process revealed 16 clusters of interests, whose cluster-level background FC patterns provided a parsimonious summary of the neural sources distinguishing between perception and retrieval states (**Figure 2.4A**; **Table S2.1**).

Notably, in addition to its greater interpretability, this FCMA-then-clustering approach also produced superior classification accuracy to the use of *a priori* parcellation-based clusters (Feilong et al., 2021; Schaefer et al., 2018). That is, by repeating the analysis pipeline with predefined brain parcels (instead of fine-grained voxel-wise analysis), the 16 clusters derived from voxel-level analyses had significantly greater discrimination performance compared to the best performing 16 predefined parcels in the parcel-level analysis ($F_{(1,23)} = 96.71$, $p < 0.001$, $\eta^2 = 0.81$; **Figure S2.3B right**). This result held across different parcellation granularities (400 and 1000 parcels; Schaefer et al., 2018). Moreover, cluster-level background FC patterns retained their preference for state-related vs. non-state-related differences (**Figure S2.3**; $F_{(2,46)} = 24.09$, $p < 0.001$, $\eta^2 = 0.23$).

Although the analyses above inform *which* brain regions might be most involved in differentiating perception and retrieval cognitive states, they do not provide information about *how* the regions are differentially connected. Indeed, previous research has suggested that functionally coupled brain regions form large-scale functional communities (Yeo et al., 2011) and that a cluster may be associated with different functional communities across different cognitive states (Braun et al., 2015). With this in mind, we next examined the functional community structures of the 16 clusters of interest during each task condition (i.e., *Perceive*, *Retrieve*, and *Scramble*). Specifically, we applied the Louvain community detection algorithm (Blondel et al., 2008) to the group-averaged background FC matrices for each condition (see **Methods:** ***Community Detection*** for details). Interestingly, the community structures underlying all three task conditions were consistent in that the 16 clusters were consistently partitioned into 3 functional communities (**Figure 2.4A**). The first functional community consisted of regions from the conventional default mode network (Buckner et al., 2008), including the bilateral inferior parietal lobule, precuneus, medial prefrontal cortex, posterior cingulate cortex, and the middle temporal gyrus, which hereafter we refer to as the DMN. The second functional community consisted of the bilateral prefrontal cortex, bilateral intraparietal sulcus, superior frontal gyrus, and temporal gyrus, most of which are part of the frontoparietal control network (Marek & Dosenbach, 2018); we refer to this as the Control network[1]. The last community consisted of bilateral retrosplenial cortices (RSC; Gilmore et al., 2016).

[1] Note that some of the clusters (right intraparietal sulcus and the inferior temporal gyrus) had peak coordinates in the dorsal-attention network (according to Schaefer et al., 2018). Given that the remainder of the clusters (5 out of 7 clusters) fell into the Control Network we use that as the shorthand label.

As an initial step to characterize the contribution of these different functional communities, we examined their evoked activation profiles during each task condition, using the averaged beta values estimated by an FIR model (**Figure S2.4**; see **Method: *Stimulus-Evoked and Residual Activity***). Consistent with network-level activity reported in past work, we found that DMN clusters deactivated (task-negative) during both perception and retrieval states, whereas Control network clusters activated (task-positive; Kim et al., 2015). Interestingly, only the activation profile of RSC clusters differed between perception and retrieval states: task-positive during the retrieval state but task-negative during the two conditions in the perception state.

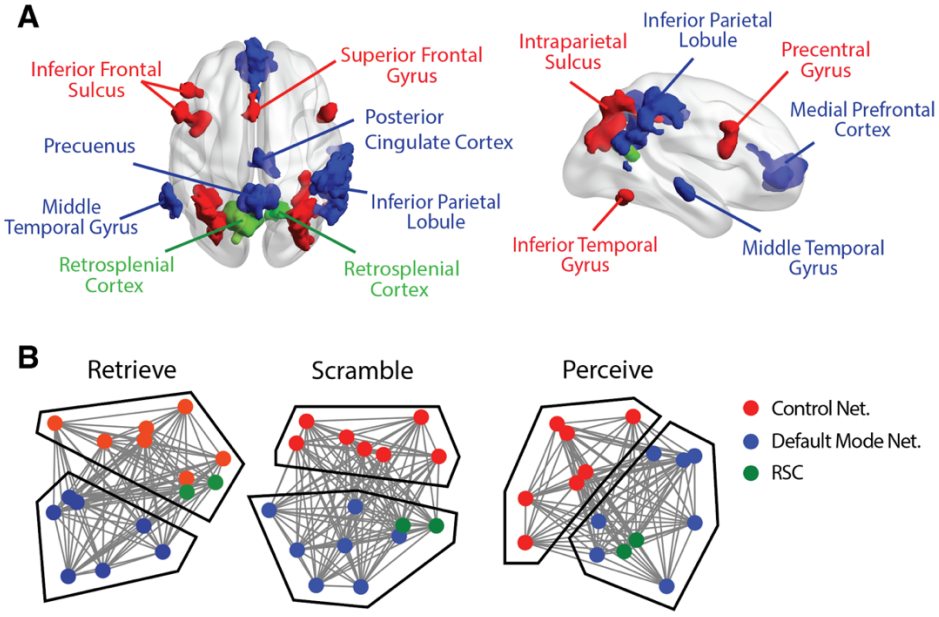

Figure 2.4. The regions of interest identified by the pipeline and their network structure. **A**) The 16 clusters of interest identified through the information mapping pipeline, partitioned into 3 functional communities. The color indicates the functional community assignment of each cluster. **B**) Force-directed graphs generated using the Fruchterman-Reingold algorithm implemented in NetworkX (V2.7.1; Fruchterman & Reingold, 1991). The projected physical distance in the graph indicates the degree to which nodes are being functionally connected. The color indicates the functional community allegiance of each cluster. Solid black lines represent manual delineations of the coupling pattern of RSC nodes.

Within- and Between-Community Background FC Discriminates Perception from Retrieval States

Our FCMA-then-clustering pipeline successfully identified a tractable number of connections among selected brain clusters that robustly differentiated perception from retrieval states. In the next set of analyses, we aimed to characterize the nature of the difference in background FC by comparing within- and between-community FC strength across the two cognitive states. For each subject, we averaged across background FC matrices within each cognitive state (i.e., perception and retrieval). FC matrices from *Perceive* and *Scramble* conditions were thus averaged together in order to obtain a single measure of background FC for perception state for each subject. Note that we expected to observe background FC differences because the clusters were selected because of their sensitivity to state-related changes; the goal of this analysis is to interpret this difference. First, we sought to visualize the within- and between-community structure using force-directed plots which allow a concise representation of connectivity between all the regions. As can be seen in **Figure 2.4B,** connectivity between Control and DMN communities appeared to be stable across conditions, RSC was more closely connected with the Control network during retrieval (*Retrieve* condition) and with the DMN during perception (*Perceive* and *Scramble* conditions).

Next, in order to quantify within-community dynamics, we examined background FC for all cluster pairs within the same functional community during perception and retrieval states. **Figure 2.5A** shows the group-level differences in cluster-to-cluster background FC strength across the two states (perception minus retrieval). Visual inspection revealed that most intra-Control network connections (17 out of 21 connections) were stronger during the perception state, whereas the majority of intra-DMN connections (17 out of 21 connections) were stronger

during the retrieval state. Quantitively, a repeated-measures ANOVA with factors of cognitive state (perception vs. retrieval state) and functional community (DMN, Control network, and RSC) revealed a significant interaction ($F_{(2, 46)} = 19.05$, $p < 0.001$, $\eta^2 = 0.45$; **Figure 2.5B**). This interaction was driven by the fact that the averaged background FC strength among RSC clusters ($t_{(23)} = 2.94$, $p = 0.007$, 95% CI = [0.02, 0.1], Cohen's d = 0.49) and cluster pairs within the Control network ($t_{(23)} = 2.26$, $p = 0.03$, 95% CI = [0.01, 0.06], Cohen's d = 0.42) was stronger during perception compared to retrieval state (**Figure 2.5A left**), whereas it was numerically stronger among clusters in DMN during retrieval than perception state ($t_{(23)} = 1.87$, $p = 0.07$, 95% CI = [-0.06, 0.01], Cohen's d = 0.32; **Figure 2.5A right**). Additionally, the ANOVA revealed a significant main effect of functional community ($F_{(2, 46)} = 228.56$, $p < 0.001$, $\eta^2 = 0.91$). Clusters within the Control network had overall stronger connectivity density compared to those within in the DMN ($t_{(23)} = 5.54$, $p < 0.001$, 95% CI = [0.05, 0.1], Cohen's d = 0.93). Note that this result holds even after accounting for the anatomical distances between clusters (**Figure S2.5**). Greater coupling between RSC regions may have possibly been driven by the fact that the two RSC clusters were close to each other anatomically. Lastly, the ANOVA did not show a significant main effect of cognitive state ($F_{(1, 23)} = 2.06$, $p = 0.16$, $\eta^2 = 0.08$), suggesting that the overall background FC densities were comparable across perception and retrieval.

Finally, to better understand across network connectivity, we examined background FC for cluster pairs in different functional communities across perception and retrieval states. Specifically, as a function of the two states, we assessed each set of between-network connections separately, both in an individual, cluster-wise manner as well as averaged across all between-network connections. Based on the relative stability across conditions of Control/DMN communities compared to RSC seen in **Figure 2.4B**, we will present the results from

Control/DMN connectivity and then connectivity with the RSC in turn. First, in terms of the Control/DMN communities, there were only hints of condition-dependent connectivity changes (**Figure 2.5C**). For example, the right precentral gyrus (rPreCG; Control) tended to couple with DMN clusters more strongly during the retrieval state, whereas the superior frontal gyrus (SFG; Control) had stronger coupling with DMN clusters during the perception state (**Figure 2.5D**). However, in aggregate, the averaged background FC strength of cluster pairs in Control network and DMN were comparable across the two cognitive states ($t_{(23)} = 1.38$, $p = 0.18$, 95% CI = [-0.1, -0.02], Cohen's d = 0.39). In contrast, RSC shifted from coupling with the Control network to DMN, as cognitive states shifted from retrieval to perception respectively (**Figure 2.5E**).

Figure 2.5. Connectivity configurations during perception and retrieval cognitive states. **A**) Group-level differences in background FC strength between each pair of clusters (within the same functional community) across perception and retrieval. The color of each cell represents the sign and magnitude of the *t* values, with a positive value indicating stronger coupling during perception state and a negative value indicating stronger coupling during retrieval state. Asterisks indicate $p < 0.05$ after FDR correction. Note that we did not depict the background FC matrix for the retrosplenial cortex (RSC) due to the small number of clusters. The background FC strength between the two RSC regions is 0.88 during the perception state and 0.82 during the retrieval state. **B**) Background FC averaged across all pairwise connections within the same functional community across perception and retrieval states. The error bars indicate the standard error of the mean across all subjects. Asterisks indicate $p<0.05$ **C**) Group-level differences in background FC between pairs of clusters in different functional communities (DMN and Control network) across perception and retrieval states. The color of each cell represents the sign and magnitude of the *t* values and asterisks indicate $p < 0.05$ after FDR correction. **D**) Background FC patterns of superior frontal gyrus (SFG) and right precentral gyrus (PreCG) during perception and retrieval states. Asterisks imply $p < 0.05$ after FDR correction. **E**) Group-level differences in background FC between RSC clusters and DMN/Control clusters across perception and retrieval states. The color of each line represents the sign of the *t* values, with purple indicating stronger coupling during the perception state and green suggesting stronger coupling during the retrieval state. Solid lines indicate $p < 0.05$ after FDR correction. **F**) Background FC strength averaged across all pairwise connections between RSC clusters and DMN/Control clusters. The error bars indicate the standard error of the mean across all subjects. Asterisks indicate $p<0.05$. ITG: inferior temporal gyrus; IPS: Intraparietal sulcus; PreCG: precentral gyrus; IFS: inferior frontal sulcus; SFG: superior frontal gyrus; RSC: retrosplenial cortex; mPFC: medial prefrontal cortex; IPL: inferior parietal lobule; PCUN: precuneus; MTG: middle temporal gyrus; PCC: posterior cingulate cortex.

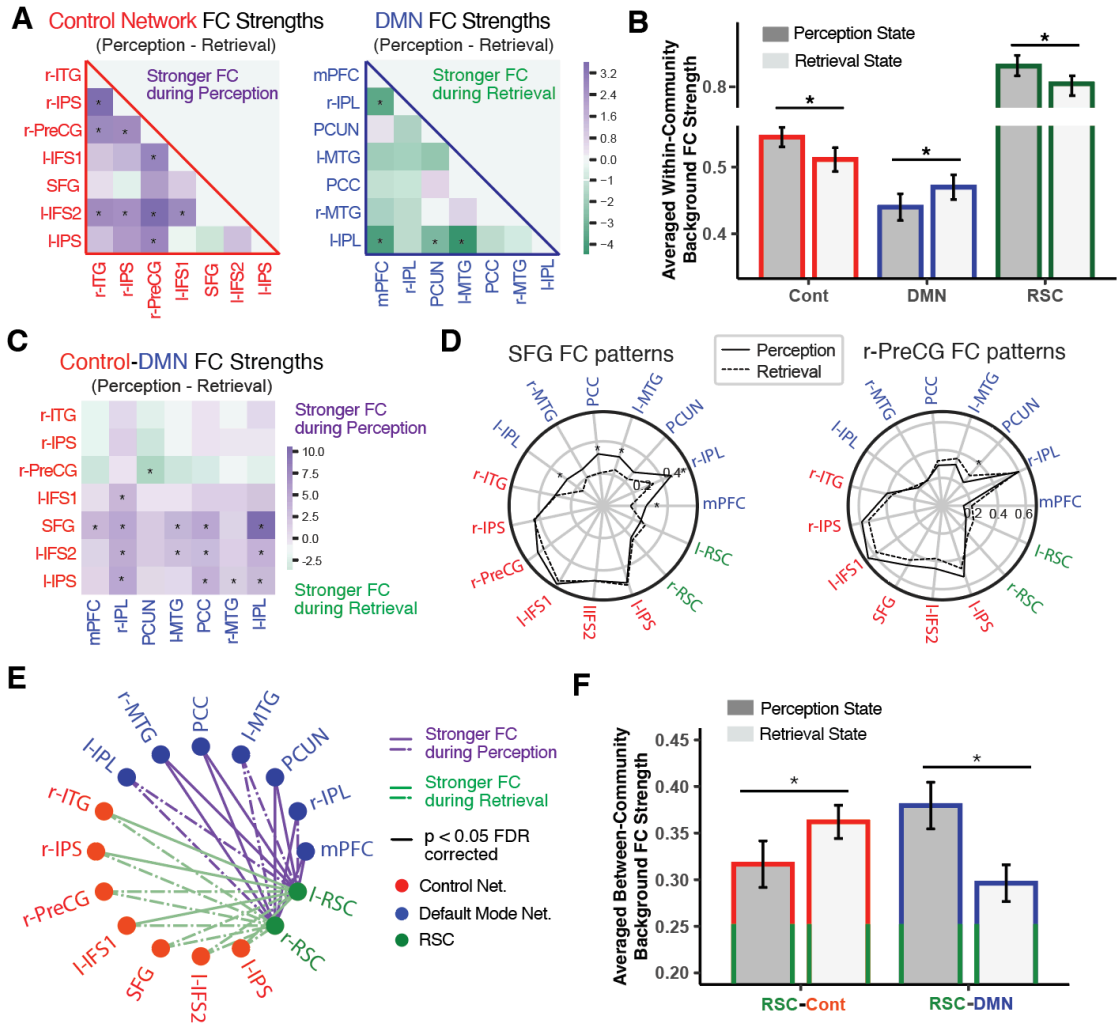

A repeated-measures ANOVA with factors of cognitive state (perception and retrieval) and functional community pair (i.e., the averaged connectivity measure between RSC nodes and regions in either Control or DMN regions) revealed a significant interaction ($F_{(1, 23)} = 100.94$, $p < 0.0001$, $\eta^2 = 0.81$; **Figure 2.5F**). Specifically, RSC nodes had stronger averaged background connectivity with DMN nodes during the perception state ($t_{(23)} = 4.83$, $p < 0.001$, 95% CI = [0.05, 0.12], Cohen's d = 0.76), but stronger background connectivity with Control nodes during the retrieval state. ($t_{(23)} = 2.35$, $p = 0.03$, 95% CI = [0.01, 0.09], Cohen's d = 0.43). The ANOVA

did not show a main effect of cognitive state ($F_{(1, 23)}$ 1.22, $p = 0.28$, $\eta^2 = 0.05$) or network pair ($F_{(1, 23)} = 0.01$, $p = 0.91$, $\eta^2 < 0.01$).

Retrosplenial Cortex Plays Unique Role across Perception and Retrieval States

Although until now we have focused on differences between conditions related to cognitive state (i.e., perception vs. retrieval), performing the task required tracking two other forms of information: (1) the visual category[2] currently being presented (i.e., face vs. scene) and (2) the behavioral judgement to perform (i.e., male/female vs. natural/manmade). Here, we performed pattern similarity analyses to assess how strongly these task components were represented in each cluster and functional community (**Figure 2.6A**). Further, given the divergence in sensitivity between background FC and evoked activity patterns reported above, we performed these analyses using both neural metrics. For each cluster, we calculated pattern similarity between pairs of epochs (**Figure 2.6B**) and compared within-class similarity (e.g., for visual category: face-face/scene-scene) and between-class similarity (e.g., face-scene) to index the cluster's sensitivity to a given component. We then averaged across clusters within each functional community, yielding 3 sensitivity indices for each functional community per subject.

Pattern similarity measures of background FC suggested that clusters in different functional communities had different levels of sensitivity to cognitive state (**Figure 2.6C**; $F_{(2,46)} = 6.32$, $p = 0.003$, $\eta^2 = 0.22$). In particular, RSC sensitivity was significantly greater than the Control network ($t_{(23)} = 2.98$, $p = 0.006$, 95% CI = [0.01, 0.05], Cohen's d = 0.78) and numerically greater than the DMN ($t_{(23)} = 1.95$, $p = 0.06$, 95% CI = [-0.01, 0.04], Cohen's d =

[2] Here we mean "visual category" to refer to the underlying stimuli used regardless of how scrambled they were. Although images were slightly scrambled, they still afforded well-off-chance M/F N/M judgements, making them dissimilar to traditional completely "scrambled" stimuli. Notably, calculating visual-category sensitivity using only non-scrambled stimuli does not change the results.

0.49). One-way ANOVAs did not reveal significant differences across functional communities in their background FC-based sensitivity to visual category and behavioral task (ps > 0.43). Although clusters were initially selected because their background FC patterns differentiated between cognitive states, perhaps leading to biased sensitivity estimates, this bias should not necessarily extend to differences in sensitivity between communities. Next, motivated by the differences between BG connectivity and evoked responses found above, we characterized pattern similarity using stimulus-evoked activity as well. Pattern similarity of evoked activity indicated that clusters in different functional communities also showed different level of sensitivity to visual category (**Figure 2.6D**; $F_{(2,46)} = 48.35$, $p < 0.001$, $\eta^2 = 0.68$) and behavioral judgment (**Figure 2.6E**; $F_{(2,46)} = 26.92$, $p < 0.001$, $\eta^2 = 0.54$). Further, the evoked activity patterns of RSC were significantly more sensitive to these two components than the DMN (visual-category: $t_{(23)} = 9.02$, $p < 0.001$, 95% CI = [0.12, 0.19], Cohen's d = 2.26; behavioral-judgment: $t_{(23)} = 5.70$, $p < 0.001$, 95% CI = [0.04, 0.08], Cohen's d = 1.38) and the Control network (visual-category: $t_{(23)} = 4.52$, $p < 0.001$, 95% CI = [0.05, 0.13], Cohen's d = 1.21; behavioral-judgment: $t_{(23)} = 5.00$, $p < 0.001$, 95% CI = [0.03, 0.07], Cohen's d = 1.25). One-way ANOVAs did not reveal significant differences across functional communities in their evoked activity-based sensitivity to cognitive states (ps > 0.25). Across metrics, these pattern similarity results highlight how RSC might be involved in many critical aspects of retrieving versus perceiving information (cognitive state, the visual content, and the behavioral judgment). However, interestingly, depending on whether the patterns are defined based on connectivity or activity, RSC can differentially capture the cognitive states of retrieval and perception relative to other regions.

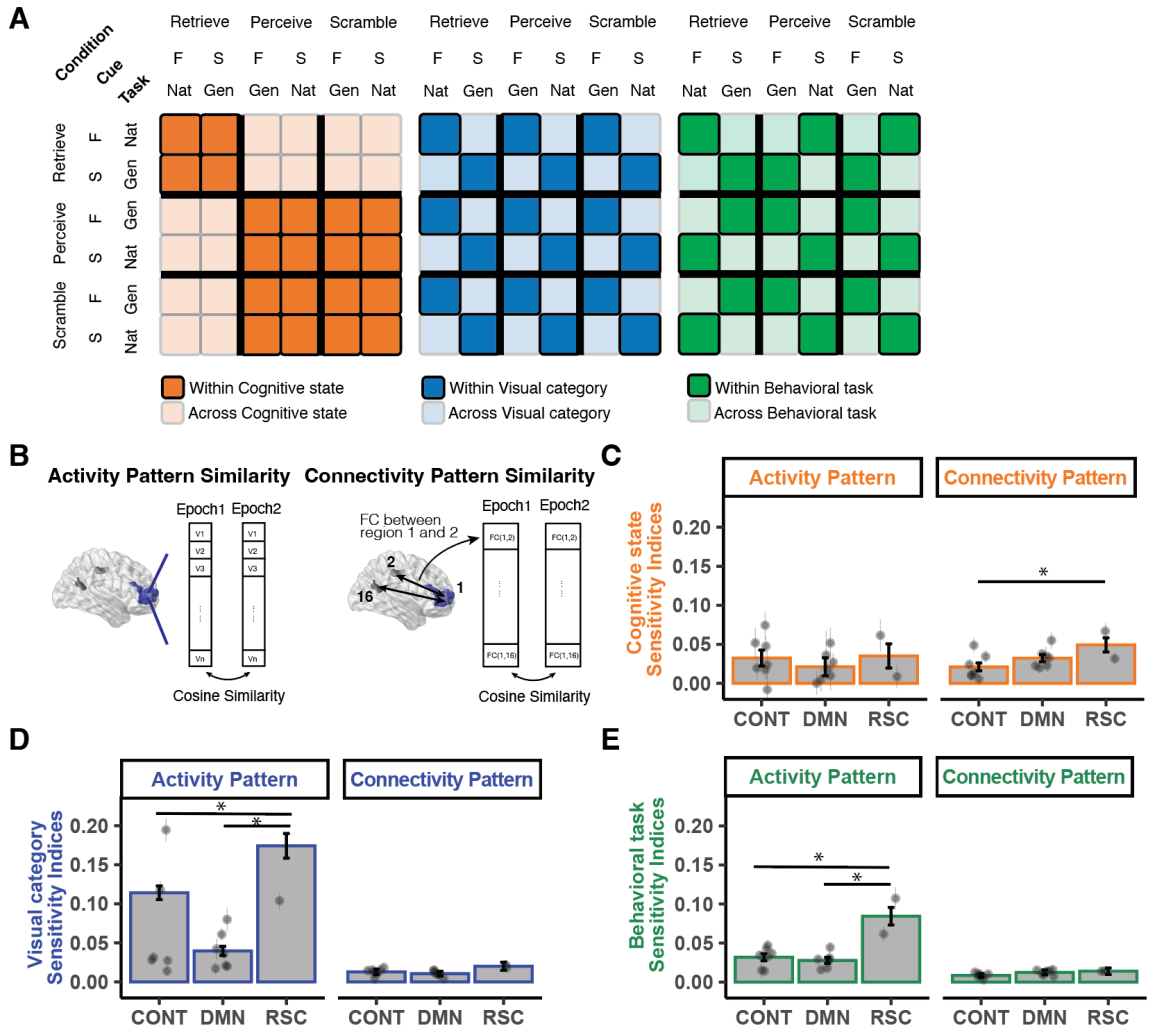

Figure 2.6. Pattern similarity analyses using both background FC patterns and stimulus-evoked activity patterns.

A) Diagram for computing pattern similarity measures between pairs of epochs for each of the three task components (cognitive state, visual category, behavioral task). Darker colors indicate epochs of the same class (e.g., visual categories being face-face) whereas light colors indicate epochs of different classes (e.g., visual categories being face-scene). **B**) Diagram for computing pattern similarity measures with both FC and activity patterns. When computing activity pattern similarity measures, each epoch is represented by a *n*-dimensional vector, where *n* is the total number of voxels in the respective cluster. When computing connectivity pattern similarity, each epoch is represented by a 15-dimensional vector, representing the background FC measure between this cluster and the other 15 clusters. **C**-**E**) Sensitivity indices of each functional community with regard to each of the three task component. Sensitivity indices were quantified as the average difference of within- vs. between-class epoch similarity. Each individual dot indicates the average across all subjects for a cluster and the error bars indicate the standard error of the mean across all subjects. Each bar represents the average across all subjects for a functional community and the error bars indicate the standard error of the mean across all clusters within the respective functional community. Asterisks indicate $p < 0.05$.

Discussion

The goal of the current study was to characterize and differentiate perception versus retrieval states in a way that captures the complexity of whole-brain functional connectivity (FC). First, we found that patterns of background FC across perception versus retrieval states were systematically different from one another (**Figure 2.2A**). Moreover, the differences were best captured by background FC patterns between 16 clusters across 3 hypothesized functional communities (**Figure 2.4; Table S2.1**). Our whole-brain analysis pipeline allowed us to extend findings from previous research (Cooper & Ritchey, 2019) by identifying important brain clusters and coupling patterns beyond memory-related brain regions (**Figure 2.5**). Second, our results showed that background FC and evoked activity tend to capture distinct component processes (**Figure 2.3**), with the former being more "state-related" and the latter being more "stimulus-related" (Summerfield et al., 2006). Third, we demonstrated the utility of full correlation matrix analysis (FCMA; Kumar et al., 2022; Wang et al., 2015) and showed how the feature selection process of FCMA, paired with cluster-based dimensionality reduction, can be used to improve the interpretability of high-dimensional FC results (**Figure S2.1, S2.3**). We conclude by highlighting how the above findings are consistent with a framework of selective attention where, given the same perceptual input, directing attention externally would promote perception of the input-related sensory features, whereas directing attention internally would promote retrieval of the input-associated episodes (Chun et al., 2011).

Background Functional Connectivity Configurations Underlying Perception and Retrieval States

The current study had subjects use the same visual input as either the target of a perceptual judgement or the trigger for episodic memory. Our results suggest that in order to

successfully perform tasks in these different conditions the brain produces distinct background FC configurations to maintain a sustained cognitive state for either perception or retrieval (**Figure 2.2A**). It is worth noting that, despite our efforts to isolate these two states across the three conditions, there are several other possible differences between critical conditions. First, because the image associations were well-learned by the subjects, it is possible that incidental memory retrieval could happen during the Perceive and Scramble conditions. Although past univariate work has suggested that incidental and directed memory retrieval might engage different neural processes, the brain regions implicated in those processes do not appear to be at play here. That is, the peak coordinates reported in a representative study (Kompus et al., 2011) do not fall into any of the 16 clusters used here. As such, we believe the background FC results are more likely to reflect perception/retrieval state-related differences rather than incidental/directed memory retrieval per se. Second, although we sought to equate task difficulty between the Retrieve and Scramble conditions, there was still a reaction time difference suggestive of a difference in task demands. While the generalization analyses showing higher sensitivity for state differences rather than difficulty differences (as measured by accuracy and reaction time) suggest that a non-specific difficulty difference alone does not drive our effect, it is likely that the differences in reaction time reflect a difference in some other unspecified demand that would need to be explored in future work. Despite these points, we believe that our results still provide strong evidence for retrieval and perceptual state-related processing in the brain.

Similar state-related shifts in background FC configurations have been reported in previous work. Cooper and Ritchey (2019) found that pre-defined regions of interest in memory-related brain systems (anterior temporal and posterior medial networks; Ranganath & Ritchey,

2012) showed stronger background FC during retrieval over perception. Using a purely data-driven approach, a subset of our findings are largely consistent with Cooper and Ritchey (2019), as we found that the retrieval (vs. perception) state is characterized by stronger background coupling between clusters in the default mode network (DMN), which is important for internal cognitive processes (Buckner et al., 2008; Yeshurun et al., 2021). Specifically, our pipeline highlighted seven clusters in the DMN (blue clusters in **Figure 2.4A**; **Figure 2.5A, B**), including the bilateral inferior parietal lobule (IPL), posterior cingulate cortex (PCC), precuneus (PCUN), medial prefrontal cortex (mPFC) and bilateral middle temporal gyrus (MTG). Note that IPL, PCUN, and PCC are considered parts of the posterior medial (PM) network for memory-guided behaviors (Ranganath & Ritchey, 2012), and IPL, PCC and mPFC have been shown to form a "core recollection network", supporting memory retrieval success (Rugg & Vilberg, 2013). Indeed, several studies have showed that functional interactions between these regions contribute to different aspects of episodic memory (Cooper & Ritchey, 2019; Geib et al., 2017; King et al., 2015). In particular, the interaction between the IPL and PCUN may connect episodic features to form an integrated neural representation, while conceptual knowledge and existing schemas are integrated by PCC and mPFC (Ranganath & Ritchey, 2012; Ritchey & Cooper, 2020).

Our findings further extend previous work by showing that the perception (vs. retrieval) state is characterized by increased background FC within a functional community with clusters in both the Control Network and the Dorsal Attention network (red clusters in **Figure 2.4A**; **Figure 2.5A, B**). Although there are situations where these networks might be engaged during memory-related processes (Hutchinson et al., 2014; Rosen et al., 2016, 2018), much evidence suggests their consistent involvement in processing the external world. That is, previous research has consistently implicated these regions as being a part of a larger task-positive network that is

typically engaged when the brain processes external stimuli (Fornito et al., 2012; Golland et al., 2008). Together with the results concerning the DMN, our findings are consistent with the idea that the brain has two anatomically separable systems that primarily correspond to "externally oriented" versus "internally oriented" processing (Golland et al., 2008).

Our whole-brain data-driven approach also revealed the importance of the background FC patterns in retrosplenial cortex (RSC; green clusters in **Figure 2.4A**) for accurately characterizing perception versus retrieval states. Specifically, we showed that RSC-DMN coupling was substantially greater during perception whereas RSC-Control coupling was greater during retrieval (**Figure 2.5E**, **F**). This connectivity pattern may seem counterintuitive at first, but interestingly it replicates findings of previous research. RSC is hypothesized to be part of the PM network , and its background FC patterns were also examined in Cooper and Ritchey (2019). Their results suggested that, although most ROIs in the PM network showed stronger coupling with each other during retrieval compared to perception, the background FC patterns of RSC did not demonstrate observable enhancement during retrieval state with any other regions in the PM network (c.f., Figure 3C right in Cooper & Ritchey, 2019). Instead of showing stronger coupling with PM regions during the retrieval state, they found that RSC had numerically stronger background FC with task-positive regions, such as the inferior temporal cortex, which is consistent with what we observed (**Figure 2.5E**). Benefiting from the whole-brain data-driven approach, the current study revealed a more complete picture of RSC background FC during perception and retrieval states, identifying regions in the DMN and Control networks beyond classical memory-related systems (Cooper & Ritchey, 2019). Moreover, the RSC clusters identified here also displayed a 'flip' in evoked activity across perception and retrieval tasks (see Figure S4), replicating past work showing decreased/below-baseline activity during encoding

and increased/above-baseline activity during retrieval in medial parietal regions (e.g., Daselaar et al., 2009; Huijbers et al., 2012, 2013). A number of conceptual accounts have been offered in terms of understanding this 'flip' (Huijbers et al., 2012), however, such accounts typically imply that RSC/DMN connectivity would be greater during retrieval, which differs from what we found here (also see Cooper & Ritchey, 2019). Interestingly, these task-evoked 'flip' effects often span multiple subregions and/or functional networks (Huijbers et al., 2012, 2013), and a fruitful direction for future research might be assessing the heterogeneity of background functional connectivity within the RSC and surrounding regions.

Although the findings in RSC are consistent with past observations, conceptual interpretation of its role here remains speculative. We do note that previous human fMRI and rodent studies suggest that RSC is involved in connecting external and internal states (Bicanski & Burgess, 2018; Yeshurun et al., 2021). For example, a study in mice found that RSC integrates both allocentric mapping (the animal's location in the external world) and egocentric frame (the animal's internal representation of the location) to navigate through a maze (Alexander & Nitz, 2015) by combining sensory inputs and mnemonic information from the medial temporal network (Bicanski & Burgess, 2018). Similarly, human RSC has been proposed to be a hub for connecting external and internal worlds (Yeshurun et al., 2021), such that it integrates external cues with self-generated information to guide behavior (Ranganath & Ritchey, 2012). In this respect, background FC in RSC during perception and retrieval may capture the role of RSC in bridging perceptual and mnemonic information; however, it is unclear why RSC would express higher coupling with the functional community putatively less involved with the task at hand (e.g., with DMN during the perception state). Accordingly, we believe an important direction of

future research will be to fully characterize how the RSC assists in establishing perception and retrieval states.

The current results provide information concerning the BOLD correlates of retrieval and perception states which might complement existing findings from other modalities. A large number of findings from intracranial and scalp EEG in humans have suggested a link between cognitive states and a host of oscillatory dynamics in the brain (for reviews see Kahana, 2006; Nyhus & Curran, 2010). Although the relationship between oscillatory dynamics in the cortex and states such as episodic memory retrieval is multi-faceted (Hanslmayr et al., 2016), a recent study employing a similar task as here found that retrieval and perceptual/encoding states could be differentiated based on scalp EEG with a speculative role of frequencies in the theta range (Long & Kuhl, 2019). Interestingly, this is consistent with past work showing a link between aspects of theta rhythms occurring before the onset of the stimulus and subsequent perception- (Hanslmayr et al., 2013) or retrieval-related processing (Addante et al., 2011). Future research is required, however, to fully understand if and how particular oscillatory EEG rhythms might relate to the background BOLD connectivity and the degree to which key subcortical regions implicated in oscillatory dynamics such as the hippocampus and thalamus might additionally influence the specific cortical connections observed here.

Background FC Captures "State-Related" Signals and Evoked Activity Reflect "Stimulus-Related" Signals

Different mental states can be reflected in distributed and overlapping patterns of evoked activity in the brain. An influential line of work has aimed to decode this information using the technique referred to as multivariate pattern analysis (MVPA; Norman et al., 2006). At the same time, another line of complementary work has investigated the inter-regional connectivity

structure of the brain by examining the patterns of BOLD correlations (functional connectivity; FC) between multiple brain regions (Smith, 2012). Both approaches have been fruitful, resulting in tremendous insights into our understandings of human cognitive processes (Haxby, 2012; Song & Rosenberg, 2021). Importantly, some previous research has suggested that these two neural measures are likely to capture and reflect distinct, or at least non-overlapping aspects of cognitive processes. For example, Song et al. (2021) found that when viewing or listening to narratives, ongoing attentional engagement can only be predicted by FC-based models, whereas models trained with regional activity patterns failed to capture this information. Additionally, Manning et al. (2018) showed that an ensemble model that relied on both FC- and activity-based neural measures outperformed models that utilized either measure on its own. This result suggests that FC and activity patterns can capture partially non-overlapping variance in cognitive processes.

Extending these findings, the current study suggests that background FC-based measures are more sensitive to differences in cognitive states whereas activity-based measures are more likely to reflect differences in stimulus-related features of the task. Specifically, we found that background FC-based classifiers better separated task conditions that involved state-related (i.e., perception vs. retrieval) than those that primarily involved stimulus-related differences (e.g., visual content). On the contrary, MVPA classifiers did not demonstrate a clear preference for state-related comparisons over stimulus-related distinctions (**Figure 2.3**). Our findings are in line with the theory that the fMRI data acquired at each voxel are composed of both state-related and stimulus-related activity, and that FC-based measures could be better suited to capture "state-related" signals whereas activity patterns better capture the "event-related" component (Summerfield et al., 2006). These findings are suggestive that background connectivity

measures, or similar, might be informative for investigating complex state-related neural dynamics beyond perception and retrieval. That is, this form of connectivity appears to show state-like dynamics in the brain: arising before task onset (e.g., preparatory state; Sadaghiani et al., 2015), maintained in the background during task performance (e.g., ongoing state; Cohen & D'Esposito, 2016), and carried over after the end of a task (e.g., lingering state; Tambini et al., 2017). We posit that FC-based measures which remove or account for evoked responses, have the potential to capture these aspects of cognitive states across a wide variety of domains. It is also worth noting that there are different types of FC-based measures; the current study primarily tested the background FC measures by regressing out the stimulus-evoked component using a general linear model (Al-Aidroos et al., 2012; Bejjanki et al., 2017; Norman-Haignere et al., 2012; Tompary et al., 2018). However, some studies computed their FC measures without regressing out the stimulus-evoked component (e.g., Song et al., 2021) or relying on stimulus-evoked parametric measures (e.g., beta series correlation; Bein et al., 2020). Future work might further examine whether these types of FC-based measures also preferentially capture state-related aspects of the cognitive process.

The Utility of Feature Selection in Whole-brain Voxel-wise FC Analyses

The current study used full correlation matrix analysis (FCMA; Kumar et al., 2022; Wang et al., 2015) to explore whether cognitive states are encoded in whole-brain voxel-wise background FC patterns. Our approach is systematically different from those used in previous studies, such as connectome-based predictive modeling (Shen et al., 2017) in two ways. First, FCMA operates on voxel-level connectivity matrices instead of the commonly-used, lower-dimensional parcel-averaged time series. Second, FCMA uses a nested leave-one-subject-out cross validation framework that enables more efficient feature selection to reduce large

connectivity matrix to a tractable size. Here we discuss the potential trade-off regarding these two distinctions. First, our results suggest that FCMA identified regions that, even after clustering over contiguous voxels, retained a higher sensitivity for differences in cognitive states compared to parcel-level analyses (**Figure S2.3B right**). This finding is consistent with previous research suggesting that voxel-/vertex-level FC patterns are more sensitive to other cognitive measures (concerning intelligence) compared to relatively coarse-grained parcel-level analysis (Feilong et al., 2021). The differences in sensitivity could be due to the fact that many parcellation schemes were defined from whole-brain resting-state functional connectivity profiles rather than task-based connectivity and previous work has suggested that the functional architecture of the brain might change across resting and task states (Cole et al., 2014) and may also vary across different task states (Krienen et al., 2014). It is worth mentioning that the use of predefined parcellation schemes can significantly improve sensitivity (as measured by effect size) in other types of analyses (e.g., univariate analyses) compared to voxel-/vertex-level analysis (Li et al., 2021). Thus, future studies need to further investigate the tradeoffs for predefined parcellation schemes in connectivity analyses.

The second way the current approach differs from prior approaches is in terms of interpretability. That is, machine learning models often face a trade-off between prediction accuracy and model interpretability (Feilong et al., 2021). In the context of FC-based models, previous work has primarily focused on constructing a model for making the most accurate predictions on trait-like demographic variation (Finn et al., 2015), behavioral performance (Rosenberg et al., 2016, 2020), or task conditions (Gonzalez-Castillo et al., 2015; Shirer et al., 2012). Despite high prediction accuracies in these models, it is often hard to interpret the FC configuration given the vast number of connections. For example, Rosenberg et al. (2016)

identified a "high-attention network", consisted of 757 edges across the entire brain, whose pattern of connectivity reliably predicted better performance on a sustained attention task. Indeed, such an approach likely captures many nuances in the neuronal distributed process of attention and has high predictive accuracy. However, it is possible that such high accuracy comes at the expense of interpretability. That is, constraining the number of edges and nodes in the descriptive network might sacrifice some degree of prediction accuracy, but the resulting FC configuration might be more easily interpreted. The current study attempted to do this by combining a whole-brain voxel-level FC model with feature selection using a nested cross-validation framework. Specifically, we quantified the "utility" of each connection using the machine learning training and testing framework (See **Method**: ***Full Correlation Matrix Analysis on Residual Activity***; **Figure S2.1**). As a result, we were able to select the most useful connections in an unbiased, automated fashion, reducing large correlation matrices to a tractable size. Remarkably, the model based on connections among only a set of 16 regions retained comparable AUC scores compared to models based on connections among 3000 voxels (Figure 2a; 0.83 vs. 0.87)[3]. Thus, the current study demonstrates the value of using the FCMA voxel-to-cluster pipeline in order to yield the most relevant and interpretable FC configuration profile while largely maintaining prediction performance.

Ideas and Speculation: How Specialized are Retrieval and Perception States?

The nature of this experiment along with the brain regions implicated in our data-driven approach are broadly consistent with the framework of cognitive control. That is, in terms of experimental demands, the same type of information from the outside world (images of scenes or

[3] Note that there was overlap between the feature selection process and the final testing process (both used all subjects) in the 16 cluster analysis. Thus, the performance of the 16 clusters is slightly biased towards higher performance.

faces) had to be flexibly routed to a limited number of response options based on the task goals (Posner & Snyder, 1975). Consistent with multi-faceted involvement of cognitive control across conditions, our analysis identified a series of frontal and parietal regions falling within the control network (Miller & Cohen, 2001). Per this perspective, initiation and maintenance of retrieval and perception states would be supported by the ability of prefrontal control regions to represent task goals and to dynamically update connectivity of the control network and beyond (Cole, Reynolds, et al., 2013; Stokes et al., 2017). In this perspective, this control mechanism would enable perceptual- or memory-based processing similar to how it might promote a large range of other complex cognitive states, with, e.g., the added involvement of DMN regions here likely related to the involvement of memory retrieval.

What awaits future research is if and how these general properties of frontoparietal cognitive control dovetail with mechanisms posited to play a role in external/perceptual versus internal/mnemonic processing specifically. For example, the retrieval and perception states indexed here might be thought of as forms of internal and external attention respectively (Chun et al., 2011), but the current study did not explicitly manipulate selection demands during either state, making a full comparison to the different forms of attention incomplete. Another rich vein of theoretical and empirical work suggests the hippocampus might play a central role in how the brain switches between environmentally-oriented encoding processes and memory-based retrieval processes (Duncan et al., 2014; Hasselmo et al., 1996; Honey et al., 2017; Poskanzer & Aly, 2022), but our approach did not find its significant involvement. We speculate that this absence might stem from design-related (use of previously encountered items in the 'Perceive' condition) and/or analysis-related (lack of subject-specific subfield data) issues. Nevertheless, a critical step moving forward will be to understand the bridge between such process-specific

mechanisms and how such processes are flexibly controlled and maintained in the service of ongoing behavior.

Data and Code Availability

Processed fMRI data including both the stimulus-evoked and residual time series supporting the primary findings of this study are available on the Open Science Framework (OSF) at https://osf.io/yfwc7/. Scripts for performing and reproducing the specific analyses described in this paper can be found through Github at https://github.com/peetal/Decode_AttenStates.

Funding and Acknowledgement

This work was supported by the Intel Corporation, the John Templeton Foundation, and NIH R01 EY021755. We express our deepest thanks for the feedback we received from Dr. Ken Norman and Dr. Sam Nastase. We are also grateful for helpful discussions and support from members of the Hutchinson Lab of Cognitive Neuroscience, the Dubrow Lab, and the Kuhl Lab.

CHAPTER III

BACKGROUND CONNECTIVITY AND EVOKED ACTIVITY PATTERNS REFLECT ONGOING ATTENTIONAL GOALS DURING MULTITASKING

This chapter contains unpublished co-authored material. I am the primary author of this chapter, and I incorporated editing advice from Dr. Ben Hutchinson. Dr. Hutchinson and I designed the study together. I conducted all data collection, and wrote the scripts for experiment presentation, data analysis, and figure creation. I wrote the manuscript with editorial assistance from Dr. Hutchinson.

Introduction

A major challenge for human cognition stems from the rapid shifts in the behavioral relevance of diverse and ambiguous information sources within complex environments. To effectively navigate this challenge, our attentional control system possesses two vital capabilities. Firstly, it allocates attentional resources to prioritize goal-relevant information and filter out distractions (Desimone & Duncan, 1995; Posner & Petersen, 1990). Second, it is capable of allocating attentional resources across multiple demands and to complete a variety of goals simultaneously (J. Duncan, 2010). For instance, during an engaging conversation, individuals naturally focus on both the conversation content and relevant memory episodes while filtering out irrelevant ambient noises.

In human fMRI research, it has been proposed that the neural mechanisms underlying this control system are evident in both evoked activity and functional connectivity estimates within the recorded signal. The guided activation account posits that specific brain regions, particularly those centered at the lateral prefrontal cortex (lPFC), exhibit meaningful evoked activity patterns that represent behavioral goals. These patterns then guide activations in other brain regions to align with the behavioral objectives via neuronal pathways (Miller & Cohen, 2001).

Complementarily, the switching train tracks account suggests that neuronal pathways themselves also undergo meaningful modulations to prioritize processing streams of goal-relevant information amidst the background of evoked activity (Al-Aidroos et al., 2012; Turk-Browne, 2013). These pathways are quantified through functional connectivity (FC), computed as the statistical dependence (i.e., correlation) between the time series of two brain regions (Friston, 1994). Notably, both evoked activity and FC patterns demonstrate *compositional coding* during multitasking, where the brain represents complex compound tasks by combining the neural representations of individual constituent tasks (Cole et al., 2011; Cole, Reynolds, et al., 2013; Reverberi et al., 2012). Compositional coding is deemed critical for humans' ability to swiftly adapt to novel multitasking scenarios by facilitating the transfer of knowledge and skills (Cole, Laurent, et al., 2013). Specifically, existing work has suggested that classifiers trained on evoked activity patterns of the lPFC and FC maps of the frontoparietal network (i.e., the FC measure between regions in this network and all other regions in the brain) can decode constituent tasks of multitasking conditions (Cole et al., 2011; Cole, Laurent, et al., 2013; Reverberi et al., 2012).

Despite the evidence supporting compositional coding as a pivotal neural mechanism for multitasking, several aspects of this phenomenon remain unknown. One such aspect pertains to the potentially distinct information contained within different neural measures (i.e., activity vs. connectivity). Previous literature suggests that the blood oxygen level dependent (BOLD) signal in human fMRI research comprises two distinct sources of information: stimulus-related information, best captured by evoked activity patterns, and task state-related information, reflected in FC patterns (Otten et al., 2002; Summerfield et al., 2006; Turk-Browne, 2013). Consistent with this view, empirical studies have indicated that combining these two neural measures can provide additional insights (Li et al., 2023; Manning et al., 2018). Consequently,

questions arise regarding whether compositional coding of activity- and FC-based neural measures contributes to comparable or disparate neural processing during multitasking. If activity- and FC-based compositional coding reflects non-identical neural processing during multitasking, it is hypothesized that different brain regions and networks may exhibit preferences for specific neural measures in demonstrating compositional coding.

Another aspect that remains unclear regarding compositional coding is whether this property persists when the compound task involves tasks from dichotomized attentional domains. Attention can be divided into external and internal domains, with external attention involving perceptually driven information and internal attention involving mnemonically driven episodes (Chun et al., 2011). Previous studies have suggested that externally and internally oriented processing often engage distinct processing modes (Chun & Johnson, 2011; Honey et al., 2017; Poskanzer & Aly, 2022), which may be somewhat conflicting (K. Duncan et al., 2014; Rolls, 2013). Therefore, it is likely that compositional coding of components within the same attentional domain (e.g., two perceptual tasks) differs from that of components across attentional domains (e.g., one perceptual and one memory retrieval task). However, previous task paradigms only allowed for examining compositional coding of multitasking conditions within the same attentional domain. It is hypothesized that certain brain regions or networks may specialize in compositional coding for within- or across-domain multitasking goals, while others may exhibit a more general property.

This study aims to systematically investigate the compositional coding property of every brain region and network as it relates to supporting multitasking. Specifically, we compared this property reflected in both activity- and connectivity-based measures for every brain region. Importantly, we computed background functional connectivity (BGFC) to isolate the

connectivity-based measure from evoked activity signals and co-activation confounds (Al-Aidroos et al., 2012; Cole et al., 2019; Córdova et al., 2016; Li et al., 2023). Additionally, we compared the compositional coding property of each brain region when multitasking conditions engage constituent tasks within or across attention domains (i.e., external and internal). In summary, we report three main findings: 1) brain regions beyond the PFC and frontoparietal control network demonstrate compositional coding property with both activity- and connectivity-based neural measures; 2) assembling the two neural measures significantly improves compositional coding accuracy, suggesting they contribute to non-identical aspects neural processing during multitasking; and 3) while some regions demonstrate measure- and domain-specificity, compositional coding of most regions does not exhibit such preferences.

Methods

Participants

Thirty-seven right-handed young adults aged between 18 and 35, with normal or corrected-to-normal vision, were recruited from the University of Oregon community to participate in exchange for monetary compensation. One participant was excluded due to incomplete participation, another due to excessive head motion, and three due to poor behavioral performance (defined as average accuracy below two standard deviations from the sample mean). This resulted in a final sample size of 32 subjects. Informed consent was obtained following procedures approved by the University of Oregon Institutional Review Board. The sample size aligns with that of previous studies investigating functional connectivity (FC) during perception and memory retrieval (Li et al., 2023) and multitasking (Cole, Reynolds, et al., 2013).

Materials

The visual stimuli used in the experiment comprised 48 images of well-known scenes and 48 images of celebrity faces, sourced from the stimulus set utilized by Lee and Kuhl (2016). The scene images contain equal number of natural (e.g., Crater Lake) and man-made scenes (e.g., Golden Gate Bridge) and the face images include qual number of male and female faces. To regulate brightness, the contrast parameter in Psychopy was adjusted, ranging from 0 to 1. A value of 1 represented the original color of the image, while smaller values resulted in progressively dimmer and greyer images. Initially, the contrast parameter was set to 0.5 but varied throughout each trial's duration. The auditory stimuli consisted of high-pitched tones generated using the Psychopy sound module, commencing at 440 Hz and also varying during each trial. Refer to the following section for a detailed description of the titration procedure.

Experimental design and procedure

Memory formation phase. During the pre-scan behavioral training phase, occurring one hour before scanning, participants were presented with randomly assigned pairs of face and scene images (**Figure 3.1A**). Initially, they viewed all 48 pairs twice in a random order, followed by a series of 2-alternative forced choice (2-AFC) trials. In these trials, a face image appeared at the top of the screen, followed by two scene images below, one of which was the correct pair for the face image while the other was randomly selected. Participants were instructed to select the scene image paired with the face. This 2-AFC process continued until participants correctly identified the paired scene image for each face image twice.

Titration phase. After memorizing the associations between image pairs, participants were introduced to each of the three sub-tasks of the main task. In the Tone sub-task trials, participants heard a tone starting at 440hz that either increased or decreased in pitch. The objective of the Tone sub-task was to identify the direction of the pitch change (**Figure 3.1B,**

tone task). For each trial of the Face sub-task, participants were presented with face images from the memory formation phase one at a time. The brightness of the face image either increased or decreased, and participants were required to identify the direction of the brightness change (**Figure 3.1B, face task**). In the Scene sub-task trials, participants were again presented with face images from the memory formation phase one at a time, though with the brightness of the image remaining constant. The task objective was to recall the associated scene image for each face and indicate whether it depicted a natural or manmade scene (**Figure 3.1B, scene task**). Visual or auditory stimuli were presented for 2-s in each trial of the three sub-tasks, with changes occurring every 0.5-s for the Tone and Face sub-tasks, and participants were given 2-s respond window for each trial. This titration phase aimed to ensure that all three sub-tasks were matched in difficulty for each participant, so that they differed primarily in terms of the nature of the information attended to and not in terms of overall difficulty. To achieve this, participants initially performed the Scene sub-task alone, and their accuracy performance was used to adjust the difficulties of the Tone and Face sub-tasks. This adjustment involved setting the stride of pitch/brightness change, taking into account each participant's sensitivity to detecting such changes. For instance, while a 5Hz change may be easily detectable for a participant, a 2Hz change significantly increases the difficulty of the Tone sub-task. The titration phase was conducted individually for each participant due to variations in performance on the scene retrieval sub-tasks and differences in sensitivity to pitch and brightness changes.

fMRI tasks. Each trial in the fMRI main tasks encompassed all three sub-task components. During each 2-s stimuli presentation, participants encountered a tone with changing pitch every 0.5-s and a face image with changing brightness also every 0.5-s (**Figure 3.1B**). It's crucial to note that trials in the main tasks consistently provided information relevant for all three

sub-tasks. That is, in contrast to the titration phase where only task-relevant information was presented, participants were presented with sufficient information to perform the Tone, Face, and Scene sub-tasks for each trial. However, participants were directed to engage in only one or two sub-tasks depending on the condition (**Figure 3.1C**). In the 3 non-multitasking conditions, participants focused on a single sub-task while disregarding information related to the others. They then responded during a subsequent 2-s response window, prompted by the task being performed. For instance, in the Face task non-multitasking condition, participants concentrated on the image brightness changes for 2-s and disregarded both tone pitch changes and face-associated scene images. Following this, they had a 2-s window to respond with a "Face task" prompt displayed on the screen. Conversely, in the 3 multitasking conditions, participants attended to two sub-tasks simultaneously but responded only to the prompted task during the response window. For instance, in the Face/Tone task multitasking condition, participants tracked changes in image brightness and tone pitch concurrently during the 2-s stimulus presentation of each trial. Subsequently, during the ensuing 2-s response window, participants responded to prompts being either "Face task" or "Tone task," indicating the direction of pitch or brightness change, respectively, while disregarding the face-associated scene image's properties. Each functional run started with a 6-s blank lead-in period, followed by 8 task epochs (i.e., blocks) and concluded with a 6-s lead-out period. Within each epoch, participants received 4-s of instruction presentation followed by six 4-s trials. Each trial included a 2-s stimulus presentation, where stimuli changed every 0.5-s, and a subsequent 2-s response window with a presented prompt. Following each sequence of stimuli, there was a 12-s inter-block interval (IBI). Each condition comprises two functional runs, with all epochs within a run belonging to the same condition. Each participant completed in total of 96 epochs evenly distributed among the 6 task

conditions. The duration of each trial, epoch, and run was 4-s, 40-s, and 332-s, respectively. To ensure counterbalancing, task conditions were organized using a Latin square method, resulting in six sets of counterbalanced orders. These orders were randomly assigned to participants, who then completed the first six functional runs according to their assigned order, followed by the remaining runs in the same sequence.

Image acquisition and preprocessing

The fMRI data were acquired on a 3T scanner (Siemens Prisma) with a 64-channel coil at Lewis Center for Neuroimaging (LCNI) at the University of Oregon. Functional data were acquired using a T2*-weighted multiband EPI sequence (2.5 mm isotropic resolution, repetition time = 1 s, echo time = 28 ms, flip angle = 54°, bandwidth = 2590Hz/pixel, multiband acceleration factor = 4) with 60 axial slices aligned to the anterior commissure/posterior commissure. A whole-brain T1-weighted MPRAGE 3D anatomical volume (1 mm isotropic resolution, repetition time = 2.5 s, echo time = 3.43 ms, flip angle = 7°) was collected to improve registration. One phase and two magnitude field maps were collected to correct field inhomogeneities.

The preprocessing steps closely mirrored those outlined in our prior work (Li et al., 2023). Image preprocessing was conducted using fMRIPrep 20.1.0rc1 (Esteban et al., 2019). Functional images underwent correction for slice acquisition time, head motion, and susceptibility distortion, followed by normalization to both standard (MNI152NLin2009cAsym) and native (T1w) spaces. As for post fMRIPrep processing, the minimally preprocessed functional runs were further handled using FSL (Woolrich et al., 2001) with a Nipype implementation (Gorgolewski et al., 2011). A Gaussian kernel with a full-width half-maximum (FWHM) of 5.0 mm was applied for spatial smoothing, and a high-pass filter with a cutoff

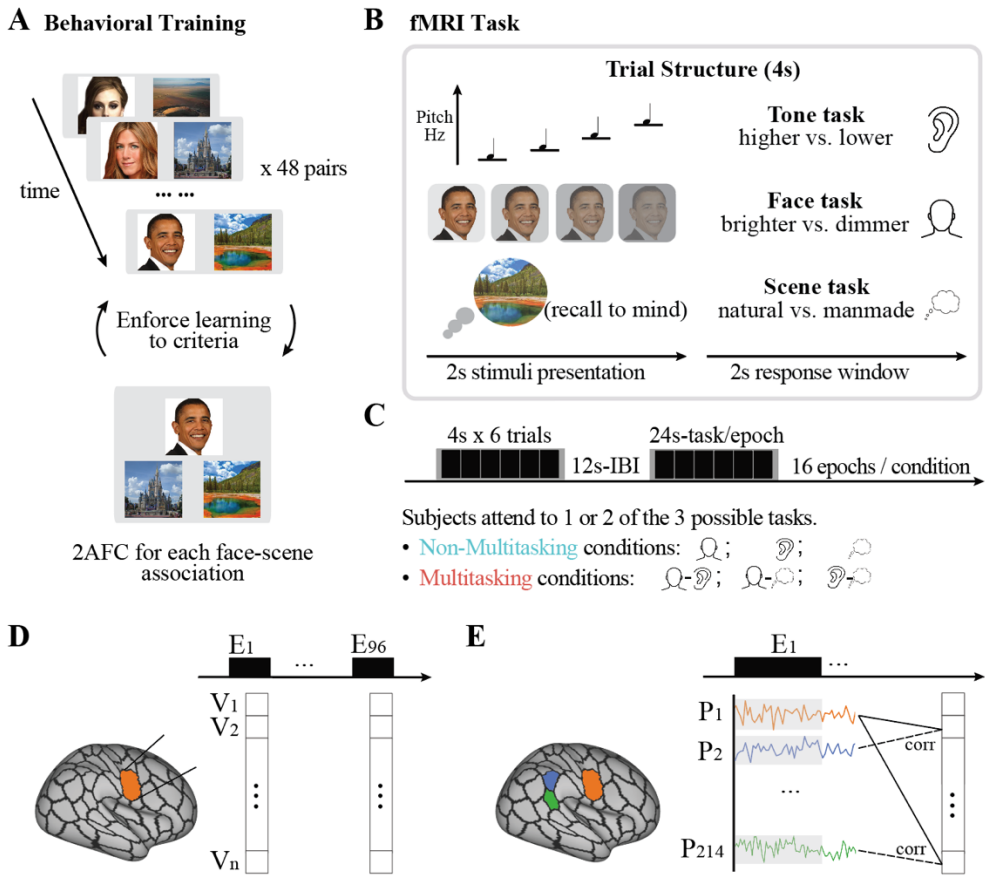

Figure 3.1. Task paradigm for multitasking and non-multitasking attention conditions. **A**) Memory formation phase. Participants established mental associations between face and scene one hour before entering the scanner. **B**) Trial structure for all fMRI task conditions. Every trail comprised a tone with changing pitch and a face image with changing brightness in each trial. Participants determined the direction of pitch change for tone sub-tasks, brightness change for face sub-tasks, and identified whether the face-associated scene image depicted a natural or manmade scene for the scene retrieval task. **C**) Participants engaged in one or two of the three available sub-tasks cross different conditions, yielding three non-multitasking conditions and three multitasking conditions. The titration phase is not depicted in this diagram. **D**) Evoked activity patterns at the parcel level were measured. Within each epoch, the *evoked activities* were averaged across the 24-second tasks (averaged across the time dimension), yielding a singular value for each voxel. Consequently, for each parcel, the evoked activity pattern for each epoch was depicted as an n-vector, where n represents the number of voxels within that parcel. **E**) Background functional connectivity (BGFC) patterns at the parcel level were measured. Within each epoch, the *residual activities* were averaged across all voxels within a parcel (averaged across the spatial dimension), resulting in a 36-s residual activity for each parcel per epoch. The BGFC pattern of each parcel was computed as the Fisher's z-transformed correlation coefficient between this parcel (e.g., the orange parcel) and every other parcel in the brain (e.g., the blue and green parcels). For each parcel, the BGFC pattern of each epoch was represented by a 214-vector, with 214 being the total number of parcels in the brain.

frequency of 0.01 Hz was employed. A confound regression was performed for each functional run to minimize the effect of the confounds by fMRIprep, including the 6 motion parameters, white matter (WM) and cereberospinal fluid (CSF). Next, normalization of intensity values in each voxel across the 12 functional runs was performed using the mean and standard deviation of the resting period for each subject. The resting period comprised the 6 lead-out volumes plus all 12-second inter-block intervals of each run, adjusted for a 4-TR hemodynamic delay. This normalization aimed to mitigate BOLD signal variations across runs, enabling concatenation of all 6 runs into a single time series for subsequent modeling.

Next, to mitigate the impact of head motion on subsequent neural measures, we performed cleaning on the concatenated timeseries using the framewise displacement (FD) data estimated by fMRIprep. A spike was identified as any frame with an FD exceeding 2 mm. We eliminated the spike along with its preceding and succeeding frames by manually setting all voxel intensity values to np.nan. Consequently, these frames were ignored when computing activity- and connectivity-based measures. Additionally, we removed runs if over 5% of their frames exhibited an FD exceeding 0.5 mm. Each participant had at least one run per condition, with no more than two runs being excluded in total. The unqualified runs were not subjected to modeling in any of the subsequent analyses.

Evoked activity and background functional connectivity (BGFC)

Parcel-level evoked activity pattern. The concatenated timeseries after regressing out the confound regressors are denoted as the evoked activity. These timeseries are fully preprocessed and retain stimulus-evoked signals. We employed the Schaefer predefined parcellation scheme to divide the cortical area into 200 parcels across 7 functional networks (Schaefer et al., 2018). For subcortical regions, we utilized the Harvard Oxford parcellation scheme to define 14 regions of

interest, encompassing bilateral thalamus, caudate, putamen, pallidum, hippocampus, amygdala, and accumbens (Desikan et al., 2006). Subsequently, we estimated the evoked activity pattern for each parcel for each epoch, excluding those in the unqualified runs. Specifically, the evoked activity of each voxel within a parcel was averaged over 24 task TRs, capturing the peak evoked BOLD response (adjusted 4 s for hemodynamic delay), yielding a single value per voxel per epoch. Therefore, each parcel was represented by an n-voxel long vector quantifying its evoked activity pattern for each epoch (**Figure 3.1D**). For example, if a parcel contained 300 voxels, then its evoked activity pattern would be represented by a 300-long vector for each of the 96 epochs (assuming no unqualified runs). Notably, to ensure consistency in voxel count within each parcel across participants, these procedures were conducted in standard space (MNI152NLin2009cAsym) using a shared brain mask, maintaining uniform brain shape across all participants prior to parcellation.

Parcel-level background functional connectivity pattern. We proceeded to estimate and eliminate the stimulus-evoked signals from the fully preprocessed time series utilizing a Finite Impulse Response (FIR) model. The FIR regressors were constructed to model the initial 36 TRs for each epoch, resulting in 36 (TR) x 6 (conditions) = 216 regressors. FIR is considered the optimal General Linear Model (GLM) for eliminating stimulus-evoked responses because it does not presuppose the shape of the hemodynamic response function (Al-Aidroos et al., 2012; Cole et al., 2019). The resulting residual timeseries data were termed as the residual activity and employed for calculating background functional connectivity (BGFC). Employing the same parcellation schemes, the brain was divided into 200 cortical parcels across 7 functional networks and 14 subcortical parcels, after which the residual activities were averaged across all voxels within each parcel. The BGFC pattern of each parcel was determined by the statistical

dependence (i.e., correlation) of residual activities between the given parcel and every other parcel in the brain, resulting in a 214-dimensional vector for each epoch (**Figure 3.1E**). To ensure precise BGFC measures, the residual activities were computed and parcellated in each participant's native space (T1w).

Activity- and connectivity-based compositional coding score

In the current experimental design, compositional coding refers to the observation the activity- or connectivity-based neural representations of a multitasking condition (e.g., Face/Tone multitasking condition) is built on those of its simple constituent conditions (e.g., Face and Tone non-multitasking conditions; Cole, Reynolds, et al., 2013; Reverberi et al., 2012). Here, we calculated the compositional coding score (CCS) to examine the extent to which activity- and connectivity-based neural representations exhibit compositional coding properties for each parcel and network. Employing a leave-one-participant-out cross-validation framework, we estimated a CCS score for each parcel and participant. In each fold, one participant's data were withheld for testing, while the data from the remaining participants were used as training data. Using the training data, we trained regularized Softmax models (with L2 regularization and C=0.1) implemented in Scikit-learn (Pedregosa et al., 2011) on only the non-multitasking epochs (i.e., Face, Tone, and Scene epochs). Subsequently, the trained model was tested on multitasking epochs (i.e., Face/Tone, Face/Scene, and Scene/Tone epochs) in the testing set (**Figure 3.3A left**). An epoch in the testing set was considered correct if the Softmax model assigned the two relevant labels the highest decision function output values (i.e., probability). For instance, during testing of a Face/Tone multitasking epoch, the epoch was deemed correct only if the output probability for the Face and Tone classes exceeded that for the Scene class. The CCS score was

calculated as the number of correctly predicted epochs divided by the total number of testing epochs (48 epochs if no disqualified runs were present; **Figure 3.3A right**.).

Importantly, we calculated the CCS for each parcel using both evoked activity patterns and background connectivity patterns. Specifically, for the activity-based CCS estimations of each parcel, the training and testing inputs of the models were the n-long vectors, where n represents the number of voxels within the respective parcel (See **Methods**: *Evoked activity and background functional connectivity* for details). It is important to note that due to the utilization of standard space and a shared brain mask, the dimensions of these n-vectors were consistent across participants, rendering this cross-validation framework feasible. On the other hand, for the connectivity-based CCS estimations of each parcel, the training and testing inputs of the models were the 214-long vectors, which encapsulated the correlation of residual activities between the current parcel and every other parcel in the brain (See **Methods**: *Evoked activity and background functional connectivity* for details). Moreover, we derived an ensembled CCS using an ensemble model that integrated decision function outputs (i.e., probability) from both the activity- and connectivity-based Softmax models. Specifically, for each testing epoch within each fold, both the activity- and connectivity-based models outputted an estimated probability value for each class (i.e., Face, Tone, and Scene). The ensemble model then computed the weighted average of the probability outputs from the two models (weight=0.5) and assessed the accuracy of the current epoch's prediction using the same approach as introduced above. Together, we obtained a CCS score for each parcel within each participant, incorporating activity-based, connectivity-based, and ensemble neural measures.

Examining measure- and domain-specificity of parcels

Measure-specific and general parcels. We hypothesized that some parcels may demonstrate stronger compositional coding properties when a specific neural measure was used (i.e., measure-specific) whereas other parcels may not exhibit this preference (i.e., measure-general). To identify parcels that are either measure-specific or measure-general, one sample t-tests were performed to first select parcels that had ensemble CCS significantly above chance level (33.33%; $p < 0.05$). Within this subset, a paired sample t-test was performed to identify parcels exhibiting significantly higher activity-based CCS scores compared to connectivity-based CCS scores, or vice versa ($p < 0.05$), termed as measure-specific parcels. Measure-general parcels encompassed the remaining parcels.

Domain-specific and general parcels. Moreover, we posited that the degree of compositional coding in a parcel might differ based on whether the multitasking condition involves tasks from the same attentional domain (i.e., external/perceptual vs. internal/mnemonic). For instance, certain parcels might exhibit a stronger compositional coding tendency when multitasking conditions entail two tasks from the same attentional domain (i.e., Face/Tone condition; both tasks are perceptual related), as opposed to conditions involving tasks from different attentional domains (i.e., Face/Scene and Scene/Tone conditions; one perceptual task and one memory retrieval task). Parcels demonstrating such preferences, or the reverse, were designated as domain-specific parcels, while others were classified as domain-general parcels. To identify these parcels, one-sample t-tests were initially conducted to select parcels with ensemble CCS scores significantly exceeding chance level (33.33%; $p < 0.05$). Within this subset, the ensembled CCS for each multitasking condition was individually assessed within each testing fold. This was quantified as the ratio of correctly predicted epochs by the ensembled CCS to the total number of epochs in each multitasking condition (i.e., 16 epochs if no

unqualified runs occurred). Subsequently, the within-domain CCS referred to the CCS for the Face/Tone condition, while the across-domain CCS was computed as the average of the CCS for the Face/Scene and Scene/Tone conditions. Paired-sample t-tests were then employed to identify domain-specific parcels whose within-domain CCS was significantly greater than the across-domain CCS, or vice versa ($p < 0.05$). Parcels remaining in the subset were classified as domain-general.

Statistical tests

All statistical analyses were performed using Pingouin 0.5.1 with Python3. Statistical significances were assessed at the 0.05 alpha threshold. Bonferroni corrections were made for multiple comparisons.

Results

Behavioral results

We devised a behavioral task where participants were simultaneously exposed to information for three sub-tasks: the Face task (requiring brightness judgment on visual stimuli), the Tone task (requiring pitch judgment on auditory stimuli), and the Scene task (requiring naturalness judgment on recalled images). In the non-multitasking conditions (**blue dots in Figure 3.2**), participants focused on one piece of information and executed one sub-task at a time, whereas in the multitasking conditions (**red dots in Figure 3.2**), they attended to two information sources and performed two sub-tasks concurrently. Overall, participants exhibited higher accuracy (**Figure 3.2 top**) and quicker reaction times (**Figure 3.2 bottom**) during non-multitasking conditions compared to multitasking conditions. Specifically, two-way repeated measures ANOVAs with tasks (Face-, Tone- and Scene-tasks) and conditions (non-multitasking vs. multitasking) on behavioral accuracy and reaction time revealed significant main effects of

condition (Acc: $F_{(1,31)} = 73.03$, $p < 0.001$, $\eta^2 = 0.70$; RT: $F_{(1,31)} = 748{,}70$, $p < 0.001$, $\eta^2 = 0.96$), suggesting that multitasking incurred substantial *costs* in both accuracy and reaction time.

Additionally, the ANOVA on accuracy showed no main effect of tasks ($F_{(2,62)} = 1.78$, $p = 0.18$, $\eta^2 = 0.05$) but revealed an interaction between tasks and conditions ($F_{(2,62)} = 6.04$, $p = 0.004$, $\eta^2 = 0.16$). The ANOVA on reaction time revealed a main effect of tasks ($F_{(2,62)} = 34.20$, $p < 0.001$, $\eta^2 = 0.52$) and an interaction between task and conditions ($F_{(2,62)} = 26.18$, $p < 0.001$, $\eta^2 = 0.46$). Subsequent analyses indicated that these interactions were driven by the scene task exhibiting greater *costs* caused by multitasking in both accuracy and reaction time compared to the face and tone tasks (Acc *cost* in Scene- vs. Face tasks: $t_{(31)} = 2.85$, $p = 0.008$, 95% CI = [0.01, 0.06], Cohen's $d = 0.64$; Acc *cost* in Scene- vs. Tone tasks: $t_{(31)} = 2.78$, $p = 0.009$, 95% CI = [0.01, 0.06], Cohen's $d = 0.71$; RT *cost* in Scene- vs. Face tasks: $t_{(31)} = 4.60$, $p < 0.001$, 95% CI = [0.06, 0.15], Cohen's $d = 0.92$; RT *cost* in Scene- vs. Tone tasks: $t_{(31)} = 7.40$, $p < 0.001$, 95% CI = [0.10, 0.17], Cohen's $d = 1.11$).

Crucially, preceding fMRI tasks, the three sub-tasks underwent titration processes (see Methods: *Experimental design and procedure* for details) to ensure comparable task difficulties for each participant. As a result, during non-multitasking conditions, participants demonstrated similar accuracy and reaction times across the three sub-tasks (**Figure 3.2 blue dots**). A repeated measure one-way ANOVA on tasks of the non-multitasking conditions showed neither differences in accuracy ($F_{(2,62)} = 0.86$, $p = 0.43$, $\eta^2 = 0.03$) nor reaction time ($F_{(2,62)} = 1.41$, $p = 0.25$, $\eta^2 = 0.04$). This finding is pivotal as it suggests that subsequent examination of compositional coding properties is unlikely influenced by varying neural responses resulting from different cognitive demands or motor responses.

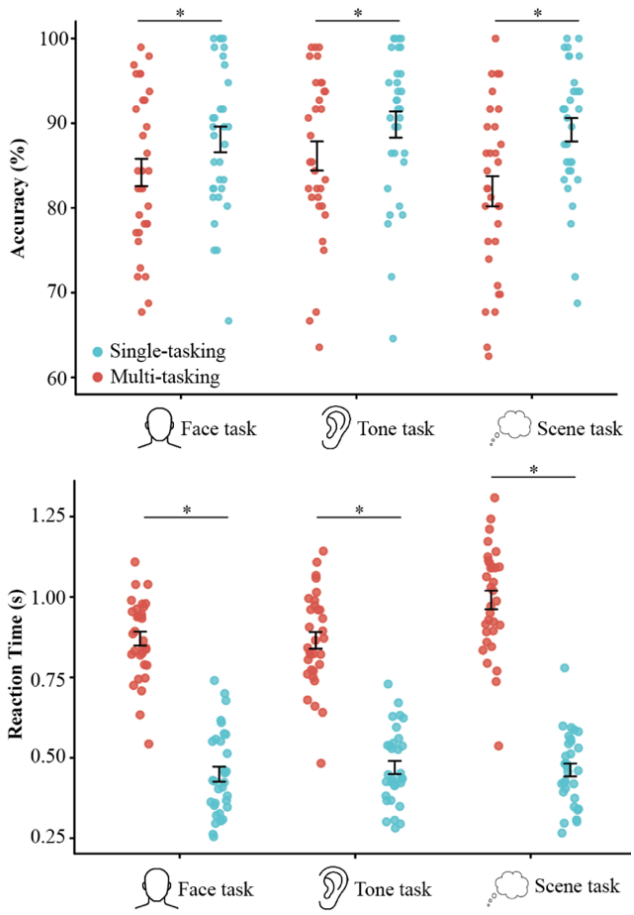

Figure 3.2. Behavioral results.
Accuracy and reaction time performance for each sub-task under non-multitasking and multi-tasking conditions. Each data point represents an individual participant. Multi-tasking performances (i.e., accuracy or reaction time) for each sub-task were calculated as the average performances when it was performed alongside another sub-task in the multitasking conditions. For instance, the multi-tasking accuracy of the Face task was determined by averaging its accuracy across the Face/Tone and Face/Scene conditions. Error bars depict the standard error of the mean across all participants, with asterisks indicating statistical significance at $p < 0.05$.

Activity- and connectivity-based compositional coding

Initially, we investigated the extent to which each parcel and network embodies the compositional coding property. This property denotes that a parcel represents a multitasking scenario by combining the neural representations of its constituent tasks, with the neural representations being either evoked activity or background functional connectivity (BGFC)

patterns. A compositional coding score (CCS) was computed for each parcel per participant, measuring how well the two individual tasks of the multitasking conditions can both be successfully detected from classifiers trained solely on neural representations of the non-multitasking conditions (**Figure 3.3A**; see Methods: *Activity- and connectivity-based compositional coding score* for details). CCS were averaged within each cortical network, and bilateral subcortical regions of interests (**Figure 3.3B**). One sample t-tests were performed on the CCS of each network against the chance level (33.33%).

Our findings indicate that all seven cortical networks and the hippocampus exhibited significantly off-chance evoked activity-based CCS (Bonferroni corrected at $p < 0.003$). The putamen and thalamus also displayed off-chance evoked activity-based CCS (ps < 0.05), but did not withstand multiple comparison correction. One the other hand, the control, default mode, dorsal-attention, ventral-attention, and visual networks demonstrated significantly off-chance BGFC-based CCS (Bonferroni corrected at $p < 0.003$). Additionally, the limbic network, putamen, hippocampus, and amygdala exhibited off-chance BGFC-based CCS (ps < 0.05), albeit failing to survive multiple correction (**Figure 3.3B**). One potential counterargument to the BGFC-based CCS results is that the FIR preprocessing procedures might not entirely remove all evoked activities (See methods: *Evoked activity and background functional connectivity* for details). Consequently, the off-chance performance of the BGFC-based CCS could be solely driven by the remaining stimulus-evoked signals in the residual activity. To address this concern, we also computed the CCS using the residual activity pattern. As illustrated in **Figure 3.3B**, the residual activity-based CCS for both cortical networks and subcortical ROIs were not significantly off-chance (ps > 0.2). Importantly, however, when BGFC measures were derived from the residual activity, they effectively demonstrated how a parcel integrates multitasking

objectives with their underlying components. This suggests that the information conveyed in BGFC is not driven by and independent from stimulus-evoked signals.

Next, we compared the CCS based on evoked activity and connectivity (i.e., BGFC) across brain regions. A two-way repeated measures ANOVA with neural measure (evoked activity, BGFC) and cortical networks (seven cortical networks) revealed a main effect of neural measure ($F_{(1,31)} = 8.44$, $p < 0.01$, $\eta^2 = 0.21$), highlighting the overall greater sensitivity of evoked-activity patterns for compositional coding. There was also a main effect of networks ($F_{(6,186)} = 10.58$, $p < 0.001$, $\eta^2 = 0.25$). Notably, the ANOVA revealed a significant interaction between the two factors ($F_{(6,186)} = 4.37$, $p < 0.001$, $\eta^2 = 0.12$), suggesting varying sensitivity of activity- and connectivity-based CCS across networks. Post-hoc t-tests (**Figure 3.3B**) further indicated that this interaction was driven by the default mode and ventral-attention networks, which displayed numerically higher connectivity-based CCS compared to activity-based CCS, while the opposite pattern was observed in all other cortical networks. Similarly, a repeated measures ANOVA involving neural measure and subcortical ROIs revealed a main effect of ROI ($F_{(6,186)} = 3.27$, $p = 0.004$, $\eta^2 = 0.10$), but no main effect of neural measure ($F_{(1,31)} = 1.11$, $p = 0.30$, $\eta^2 = 0.03$) or interaction ($F_{(6,186)} = 1.18$, $p = 0.32$, $\eta^2 = 0.04$) was observed.

Evoked activity and BGFC capture non-identical aspects of compositional coding

The findings thus far indicate that both the evoked activity patterns and background functional connectivity (BGFC) patterns of a parcel can exhibit compositional coding properties. However, a lingering question persists: as a parcel represents a multitasking condition by combining the neural representations of its constituent tasks, do the composite activity-based neural representation and the composite connectivity-based neural representation yield similar or disparate insights into cognitive processes during multitasking? To address this inquiry, we ran a

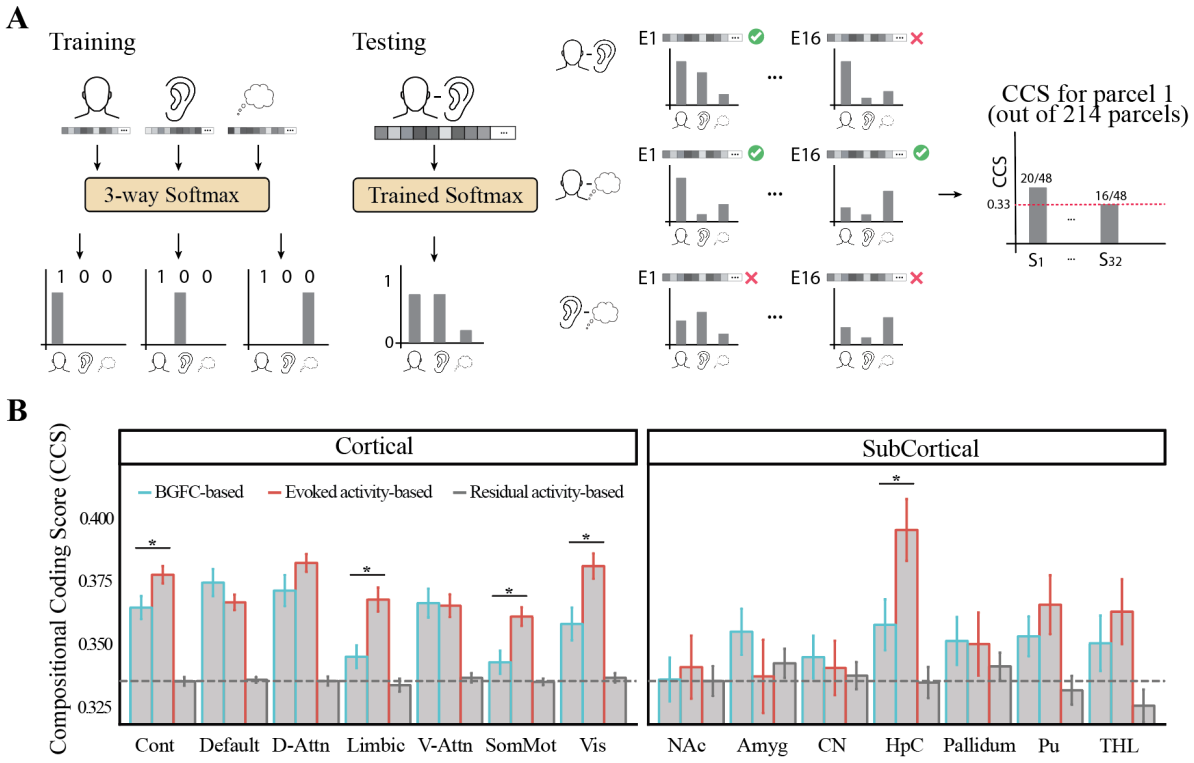

Figure 3.3. Activity- and connectivity-based compositional coding scores (CCS). **A)** Classifiers were trained on parcel-level neural representations (i.e., either activity patterns or background functional connectivity seedmaps) of non-multitasking conditions and tested on those of multitasking conditions. Correct labeling in the testing set was based on the model assigning higher probability scores to both relevant tasks (e.g., greater probability for both the Face and Tone classes compared to the scene class for a Face/Tone multitasking epoch). Compositional coding scores were calculated as the percentage of correctly predicted epochs in the testing set. **B)** Comparison of activity- and connectivity-based CCS across cortical networks and subcortical ROIs. Error bars represent the standard error of the mean across all subjects, with the dashed line indicating chance level.

mixed-effects linear regression model to explore the association between CCS scores derived from activity and connectivity across all parcels, with participants treated as a random effect. The premise is that if compositional coding of evoked activity and BGFC largely depict overlapping facets of cognitive processing in multitasking, then the two scores should exhibit a robust positive relationship, consistent across participants. Conversely, we would not anticipate observing a significant group-level relationship if the compositional coding of the two neural

measures predominantly encapsulate distinct information. As depicted in **Figure 3.4A**, the model did not reveal a robust relationship between CCS obtained from the two neural measures (group-level $\beta = 0.013$, $p = 0.14$, 95% CI = [-0.004, 0.031]). We also examined the model for parcels within each cortical network; however, none of the models exhibited a significant relationship between the two CCS measures (ps > 0.07).

These results indicate that the composite activity patterns and BGFC patterns signify separate dimensions of multitasking. Consequently, we hypothesized that a composite model, integrating both activity- and connectivity-based neural measures during both training and testing, would yield higher CCS compared to using a single neural measure (See Methods: *Activity- and connectivity-based compositional coding score* for details). The CCS was averaged across all parcels within each participant for each neural measure (i.e., BGFC, evoked activity, and ensembled). As anticipated, a one-way repeated measures ANOVA revealed a significant main effect of neural measures (**Figure 3.4B**; $F_{(2,62)} = 13.33$, $p < 0.001$, $\eta^2 = 0.30$). Post-hoc t-tests indicated that the ensembled CCS is significantly higher than both BGFC-based CCS ($t_{(31)} = 3.86$, $p < 0.001$, 95% CI = [0, 0.01], Cohen's $d = 0.43$) and activity-based CCS ($t_{(31)} = 5.30$, $p < 0.001$, 95% CI = [0.01, 0.02], Cohen's $d = 0.81$). Subsequently, one-sample t-tests were performed on each parcel's ensembled CCS against the chance level to identify all parcels demonstrating significantly off-chance ensembled CCS ($p < 0.05$), with Figure 4C displaying the t-stats of all off-chance parcels. These parcels play a crucial role in supporting the brain's multitasking abilities by aiding in the achievement of multitasking objectives and facilitating neural processing through meaningful evoked activity patterns or background connectivity patterns. It's important to note that computing the ensemble enables the identification of parcels that may not individually surpass the threshold based on either activity

or connectivity patterns alone, but still significantly contribute to multitasking when both neural measures are taken into account. Overall, 133 out of 214 parcels exhibited significantly off-chance ensembled CCS. The parcels with the highest t-estimates were primarily located in the lateral prefrontal cortex (lPFC), intraparietal sulcus (IPS), precuneus (PCUN), post cingulate cortex (PCC), and fusiform area (FFA). Notably, among the 14 subcortical ROIs, only the left thalamus (THL) and bilateral hippocampus (HPC) displayed off-chance ensembled CCS.

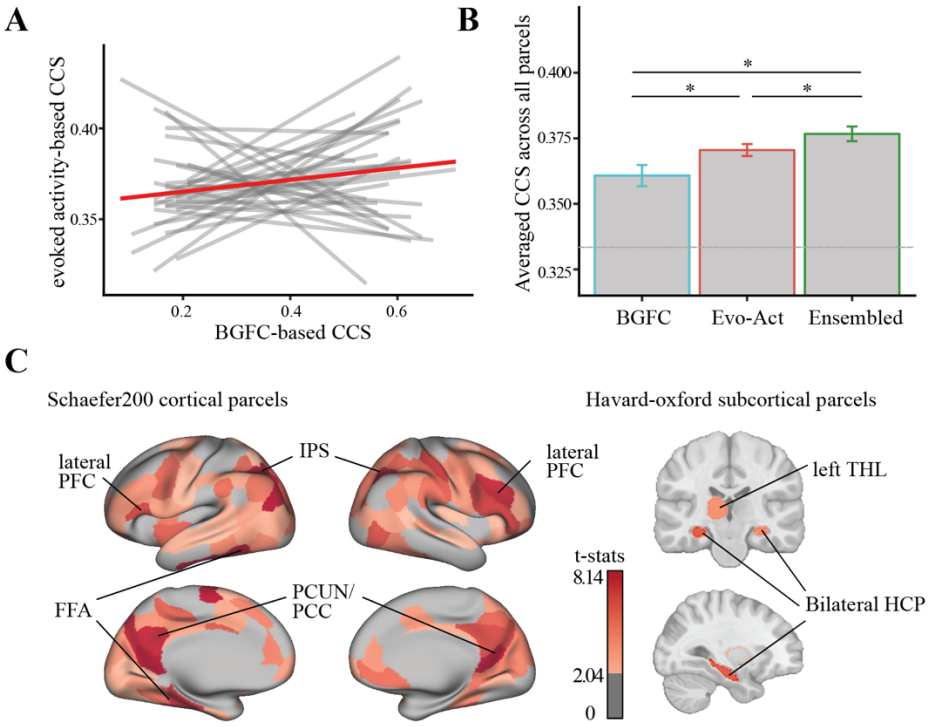

Figure 3.4. Ensemble-based compositional coding scores (CCS) outperform CCS based on a single measure.
A) The relationship between connectivity (BGFC) and activity-based CCS across 214 brain parcels. Each gray line represents the regression line for an individual participant, while the red line represents the group-level regression line. **B**) CCS values were averaged across all parcels, resulting in a single value for each participant per neural measure. The dotted gray line indicates the chance level. Error bars represent the standard error of the mean across all participants, with asterisks indicating statistical significance at $p < 0.05$. **C**) Parcels displaying significantly off-chance ensemble CCS. The color map illustrates t-stats from one-sample t-tests.

Measure and attentional domain specificity of compositional coding

The preceding findings have pinpointed parcels that play a role in multitasking. However, the extent of their involvement in multitasking may vary depending on the neural measure and the attentional domain of multitasking. Regarding neural measures, a parcel's off-chance performance in the ensemble CCS can be influenced by either activity- or connectivity-based measures alone. In other words, a parcel might exhibit significant changes in connectivity patterns that reflect neural processing during multitasking, while its evoked activity pattern may not convey meaningful information, or vice versa. On the other hand, while attention can be generally dichotomized into external and internal attention (Chun et al., 2011), multitasking can involve tasks within the same attentional domain (Face/Tone condition) and across attentional domains (Face/Scene and Scene/Tone conditions). Consequently, parcels may demonstrate selectivity in representing within- and across-domain multitasking.

To explore the measure specificity of parcels, we conducted paired sample t-tests comparing activity- and connectivity-based CCS scores for each parcel with off-chance ensembled CCS (see Methods: *Examining measure- and domain-specificity of parcels* for details). The findings indicate that the majority of parcels exhibiting compositional coding properties are measure-general (**Figure 3.5A**). This implies that both their evoked activity and BGFC patterns similarly represent multitasking through compositional coding. Notably, nearly all parcels demonstrating compositional coding property within the dorsal attention network are measure-general. Moreover, all cortical networks consist of parcels that exhibit activity-specific compositional coding, indicating significantly stronger properties when examining evoked activity compared to BGFC. In contrast, only five parcels demonstrate BGFC-specificity, showing significantly stronger compositional coding when considering BGFC over evoked

activity. These five parcels encompass the prefrontal cortex (PFC) and superior parietal lobule (SPL) from the frontoparietal control network, as well as the parahippocampal cortex (PHC) and bilateral medial PFC from the default mode network (**Figure 3.5A**).

To investigate the attentional domain specificity of parcels, we computed the ensembled CCS separately for each multitasking condition instead of averaging across conditions. Within-domain CCS refers to the CCS for the Face/Tone condition, while across-domain CCS refers to the averaged CCS for the Face/Scene and Scene/Tone conditions (see Methods: *Examining measure- and domain-specificity of parcels* for details). Paired sample t-tests were conducted to compare within- and across-domain CCS. Our findings suggest that most parcels are domain general when representing multitasking goals and neural processing (**Figure 3.5B,C**). In particular, nearly all parcels in the dorsal attention network that demonstrate compositional coding properties are domain-general. This means that, with the neural measure that encompasses both evoked activity and BGFC, these parcels do not differentiate in representing multitasking conditions that involve tasks that are both perceptual compared to one perceptual and one retrieval task. Furthermore, as depicted in **Figure 3.5B**, parcels located in the dorsal lateral prefrontal cortex (dlPFC), PCUN, IPL, PHC, and hippocampus (HPC) demonstrated enhanced compositional coding when multitasking involved tasks within the same attentional domain. Conversely, parcels situated in the lateral prefrontal cortex (lPFC), superior frontal gyrus (SFG), anterior cingulate cortex (ACC), visual and somatosensory cortex, as well as the left thalamus (THL), exhibited a stronger compositional coding property when multitasking occurred across attentional domains. In supplementary analyses, we explored whether the domain specificity of a parcel or network might differ based on the neural measure utilized. Our findings indicate that parcels in the control and salience/ventral attention networks tend to

exhibit increased within-domain specificity when assessed using BGFC-based measures compared to activity-based measures. Conversely, parcels in the dorsal attention networks and the visual networks tend to demonstrate heightened across-domain specificity when assessed using BGFC-based measures compared to activity-based measures (**Figure S3.1**).

Discussion

The goal of the current study was to investigate the compositional coding characteristics of individual brain parcels and networks in order to elucidate the neural mechanisms involved in effective multitasking. Notably, we assessed this property using both evoked activity-based measures and intrinsic functional connectivity measures (i.e., BGFC). Additionally, we compared these measures across multitasking conditions within and across attentional domains. Firstly, we observed robust compositional coding properties in the patterns of background functional connectivity (FC) across multiple networks, even in cases where the residual activity,

Figure 3.5. Measure- and domain-specificity of parcels exhibiting compositional coding property.
A) Criteria for categorizing parcels as evoked-activity-specific (red), BGFC-specific (blue), and measure-general (gray). Parcels with significantly off-chance ensembled CCS were selected. For each parcel within this subset, t-stats were computed between its activity- and BGFC-based CCS, with positive values indicating greater activity-based CCS and negative values suggesting the opposite. **B)** Criteria for categorizing parcels as within-domain-specific (green), across-domain-specific (purple), and domain-general (white). Parcels with significantly off-chance ensembled CCS were selected. For each parcel within this subset, t-stats were computed between its ensembled within-domain- and ensembled across-domain-CCS, with positive values indicating greater ensembled within-domain-CCS and negative values suggesting the opposite. Here, attentional domain specificity refers to whether the cognitive task requires external or internal attention. Within-domain indicates that the multitasking condition involves two subtasks of the same attentional domain, while across-domain means that the multitasking condition involves subtasks from different domains. **C)** The t-stats of each parcel showing significantly off-chance ensembled CCS, grouped by networks. The x-axis displays the t-stats of the domain-specificity estimates and the y-axis shows the t-stats of the measure-specificity estimates. Each dot represents a parcel, and the dotted lines represent the t threshold for being statistically significant ($p < 0.05$).

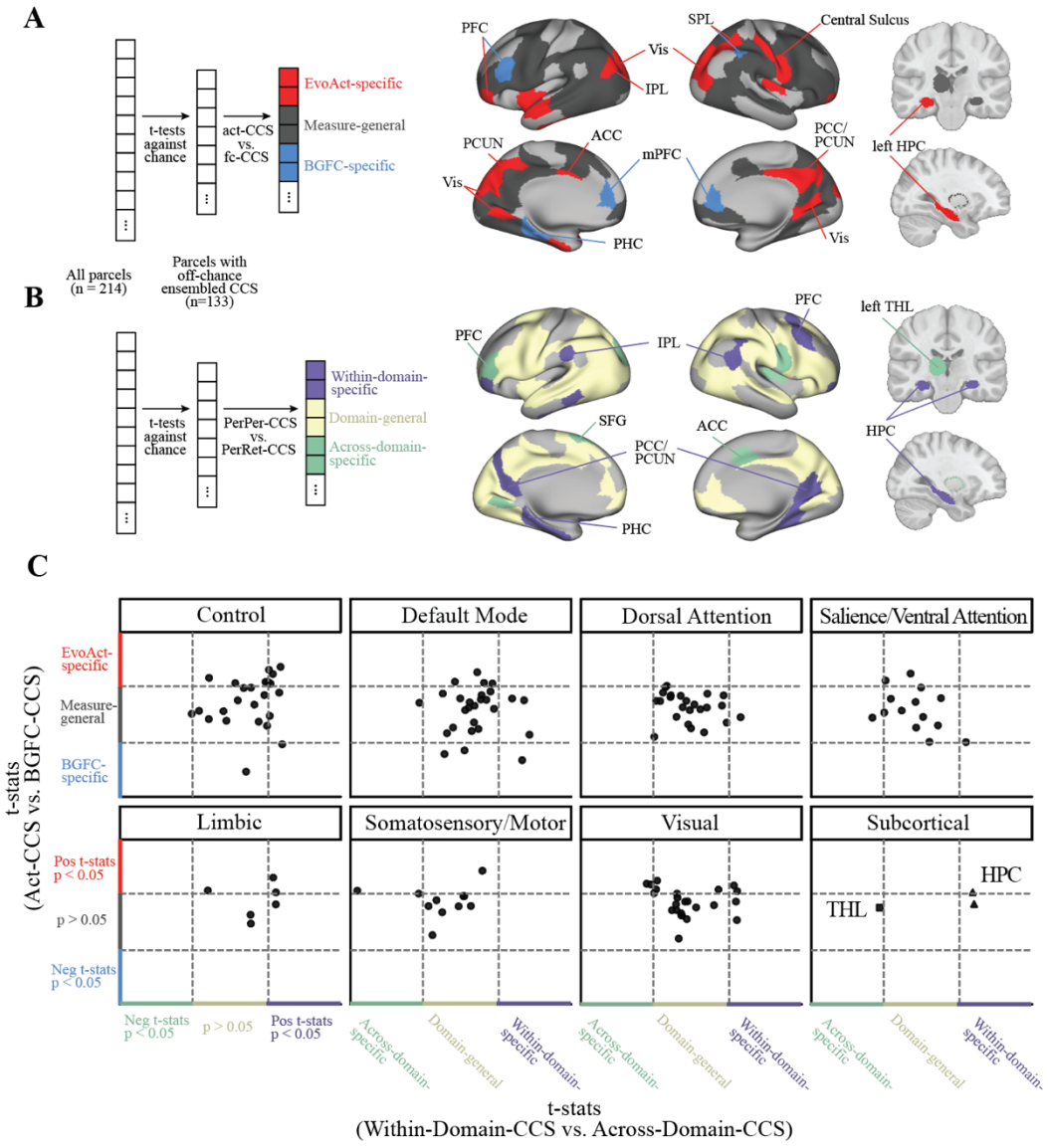

from which BGFC was computed, did not exhibit compositional coding (**Figure 3.3**). Secondly, our findings suggest that compositional coding is not limited to the lateral prefrontal cortex (lPFC) and the frontoparietal network; instead, it involves other networks such as the dorsal attention network in facilitating efficient multitasking (**Figure 3.3**). Thirdly, our results indicate that compositional coding of evoked activity and background FC likely represent distinct facets of multitasking neural processes, with certain brain networks relying more on one aspect than the

other (**Figure 3.4 and 3.5**). Additionally, the compositional coding of background FC, compared to evoked activity, exhibits stronger preferences for either within- or across-domain multitasking conditions, which vary across different brain networks (**Figure S3.1**).

BGFC robustly reveals constituent task-states during multitasking

In human fMRI research, previous studies have demonstrated that functional connectivity patterns can effectively reflect ongoing cognitive processes, including current behavioral goals, sustained attention levels, and targets of selective attention (Al-Aidroos et al., 2012; Cole, Reynolds, et al., 2013; Gonzalez-Castillo et al., 2015; Rosenberg et al., 2020; Shirer et al., 2012). Additionally, functional connectivity patterns have been proposed to capture cognitive processes independently of stimulus-evoked activities (Fox & Raichle, 2007; J. Kim & Horwitz, 2008; Summerfield et al., 2006). In line with these perspectives, findings from our study indicate that even after modeling and removing stimulus-evoked activities, multivariate pattern analyses (MVPA) of the residual activity within a parcel did not successfully identify the constituent tasks of multitasking (Norman et al., 2006). However, when pearson correlations were computed between the residual activities of that parcel and those of every other parcel, MVPA of this BGFC seed map still retained information about the ongoing multitasking components. It is essential to note that due to the individually tailored titration procedure (see Methods: *Experimental design and procedure* for details task difficulty in terms of accuracy and reaction time was matched across the three sub-tasks. Therefore, the success of BGFC in reflecting the constituent tasks being performed cannot be attributed to differences in cognitive demands or stimulus-evoked signals remaining in the residual activity.

We posit that the observed compositional coding property of BGFC stems from the fact that multitasking necessitates the interaction of multiple brain networks (Bressler & Menon,

2010; Santangelo, 2018) and such interaction is manifested in the form of noise correlation captured by BGFC but not by evoked activity (Al-Aidroos et al., 2012; Bejjanki et al., 2017). Specifically, due to the parcel-level analysis approach employed in our study, evoked activity was measured as the pattern of activity across voxels within a parcel, primarily reflecting local signals concerning the behavior of a specific brain area. In contrast, connectivity was measured as the pattern of BGFC between a parcel and every other parcel in the brain, thus containing more global signals regarding communication between brain regions (see Methods: *Evoked activity and background functional connectivity* for details). With the removal of stimulus-evoked activity, the seeming task-induced reactions of the brain parcels were no longer apparent, leading to the absence of compositional coding property in the local signal of residual activity. Yet information regarding the ongoing multitasking condition was not solely reliant on the local reactions of parcels but was also evident in the global communication pattern between parcels. This communication, facilitated through noise correlation, persisted in the residual activity, enabling BGFC to capture components of multitasking (Al-Aidroos et al., 2012).

Previous studies exploring the relationship between FC patterns and task-states have typically focused on identifying connectivity edges that differ between task states (Li et al., 2023; Shirer et al., 2012). However, the current findings suggest that task-states, instead of being independent and detached from each other, actually share resemblance and even interdependency. Specifically, the results of our study suggest that such interdependency represents the transfer of skills and knowledge. Consequently, it is meaningful to study how task-states resemble each other in terms of functional connectivity patterns to identify the neural mechanisms underlying the repertoire of the key cognitive functions that are widely applied across multiple task states.

Compositional coding of evoked activity and connectivity reflect non-identical aspects of multitasking

In line with prior research, we first established that the brain integrates regional reactions of individual brain regions (assessed through evoked activity) and global communication patterns between regions (assessed through BGFC) of constituent tasks to effectively represent a multitasking condition (Cole et al., 2011; Cole, Reynolds, et al., 2013; Reverberi et al., 2012). Earlier studies have proposed that such compositional coding during multitasking plays a vital role in knowledge and skill transfer, enabling humans to swiftly learn instructed tasks and adapt flexibly to new situations (Cole, Laurent, et al., 2013). Yet it remains unknown that whether this compositional encoding of evoked activity and BGFC reflects similar or distinct neural processes linked to knowledge and skill transfer during multitasking. Prior research has suggested that evoked activity and BGFC patterns capture at least partially different aspects of neural processes when representing a single task state. Specifically, combining these two neural measures using ensemble methods has been shown to significantly enhance classification accuracy in distinguishing between task states (Li et al., 2023; Manning et al., 2018). Building on this, our study expands on these findings, demonstrating that the ensemble model combining both neural measures could decode constituent tasks with significantly greater accuracy, as evidenced by higher CCS scores (**Figure 3.4B**). Furthermore, our results indicate that the extent to which evoked activity reflects the multitasking process does not predict the extent to which BGFC reflects the same process. Taken together, these findings suggest that during multitasking, the compositional encoding of evoked activity and BGFC reflects distinct aspects of top-down attentional control.

Notably, findings from the current study suggest that the disparities between evoked activity and BGFC in reflecting multitasking processes depend on their sensitivities to whether the subtasks being multitasked belong to the same attentional domain (i.e., external and internal). Specifically, most brain regions exhibit composite evoked activity patterns regardless of whether the subtasks are both perceptual (i.e., within attentional domain) or one perceptual and one retrieval (i.e., across attentional domain). In contrast, a greater number of brain regions demonstrate selectivity when examining BGFC patterns. Some regions only display composite BGFC patterns when the attentional domain of subtasks is the same, while others show meaningful BGFC patterns only when subtasks are of different domains. This effect is particularly pronounced for brain regions in the control, default mode, dorsal attention, ventral attention, and visual networks (**Figure S3.1**). Consequently, it appears that evoked activity patterns convey transferable skills and knowledge that are more universally applicable across attentional domains, while BGFC patterns facilitate learning that is more specific to either perceptually or mnemonically driven information.

Networks beyond the prefrontal cortex contribute to multitasking

Our findings indicate that both the evoked activity and the BGFC patterns within the prefrontal cortex (PFC) and the control network are crucial for facilitating the transfer of skills and knowledge during multitasking (**Figure 3.3B**). his discovery aligns with the guided activation account, which posits that the evoked activity pattern of the prefrontal cortex delineates goals and rules, subsequently directing the activation of other brain regions (Miller & Cohen, 2001). Furthermore, our results are consistent with prior research indicating that the frontoparietal control network modulates its functional connectivity (FC) patterns with other brain regions to optimize the guided activation process (Braun et al., 2015; Cole, Reynolds, et

al., 2013). These findings suggest that when faced with multitasking comprising familiar constituent goals, the guided activation process in the frontal cortex is achieved through compositional coding.

Importantly, employing a whole-brain, data-driven approach, our study also identified brain regions within the default mode network (DMN), dorsal attention network (DAN), and visual networks, alongside the thalamus and hippocampus (HPC). In particular, our findings indicated the involvement of the evoked activity and BGFC patterns of these regions in facilitating and achieving attentional control during multitasking (**Figure 3.3B**). In this context, we discuss previous research and theories regarding significant attentional control mechanisms beyond the PFC. Firstly, a body of work suggests that the thalamus plays a crucial role in integrating multimodal information through the PFC-thalamus-hippocampus circuit (Theyel et al., 2010; Weel et al., 2019). This circuit is implicated in supporting various behavioral functions, including memory organization and executive functions (Chudasama et al., 2012; Jayachandran et al., 2019), and lesions in the thalamus can result in impairments in high-level cognitive functioning (de Bourbon-Teles et al., 2014). It has been postulated that following the integration of multimodal information, this circuit facilitates the maintenance and coordination of task-relevant cortical representations by modulating the FC pathways within the cortex (Nakajima & Halassa, 2017). Secondly, evidence suggests that switching between external- and internal-oriented attention requires control mechanisms extending beyond the PFC. Several studies propose that the hippocampus serves as a pivotal switchboard in transitioning between these attentional domains. Specifically, the HPC-DAN coupling is stronger during external attention, while the HPC-DMN coupling is stronger during internal attention (H. Kim, 2015; Poskanzer & Aly, 2022). Moreover, evidence from our previous work indicates that sustained

BGFC within the DMN characterizes internal attention, whereas stable patterns of BGFC within the DAN/frontoparietal control network characterize external attention (Li et al., 2023). Thirdly, research suggests that the visual network itself also engages in low-level attentional control. Particularly, the BGFC pattern of early visual regions shifts from coupling to face-specialized areas to coupling to scene-specialized areas when the behavioral goal transitions from perceiving faces to perceiving scenes (Al-Aidroos et al., 2012; Córdova et al., 2016; Norman-Haignere et al., 2012; Tompary et al., 2018). Collectively, these pieces of evidence suggest that the substantial compositional coding scores (CCS) observed in the DMN, DAN, visual network, HPC, and thalamus, akin to those in the PFC, reflect the combination of critical attentional control processes within these regions for the purpose of multitasking.

Conclusion

This chapter aimed to understand how the top-down attentional control system concurrently represent two attentional goals, whether externally or internally driven. Specifically, the study focused on examining the compositional coding property reflected in the evoked activity and intrinsic functional connectivity (FC) patterns across all brain cortical and subcortical regions. The chapter provided strong evidence suggesting that multitasking attentional goals are represented by merging the neural representations of their individual tasks, which can be either activity- or connectivity-based. Notably, our findings indicated that the strength of compositional coding varied across different networks and neural measures. Additionally, activity- and connectivity-based neural measures showed distinct preferences in compositional coding for tasks within the same or different attentional domains. In sum, the results from this chapter offered valuable insights into understanding how top-down attentional control manages complex attentional goals.

CHAPTER IV

BACKGROUND FUNCTIONAL CONNECTIVITY KIT: A PUBLIC PYTHON LIBRARY DEVELOPED FOR BGFC ANALYSES

Introduction

In human fMRI, functional connectivity (FC) is a neural measure that examines distributed neural interactions between brain regions that are functionally homogenous but anatomically separated (Friston, 1994). FC is operationalized as the statistical dependence (e.g. correlation) between time series of preprocessed blood oxygen level-dependent (BOLD) signals across distinct brain regions. Resting-state functional connectivity (RSFC) is the measure of FC when neither explicit cognitive tasks nor external stimuli were presented to the participants. RSFC has been used to reflect endogenous functional structures of the brain (e.g., Damoiseaux et al., 2006; Gratton et al., 2018; Yeo et al., 2011). One the other hand, task-state functional connectivity measures FC when the brain is performing an explicit behavioral task. Previous studies have indicated that engaging in a behavioral task leads to subtle but significant changes in the functional structure of the brain, as observed through FC pattern modualtions (Cole et al., 2014). As task-state functional connectivity becomes a popular neural measure of the brain during task, a main challenge of this approach is to exclude the "co-activation confounds" during the preprocessing stage of the measured human fMRI signals. Specifically, co-activation confounds are introduced by stimulus-related activity in multiple brain regions, thus creating spurious connectivity even though having no real functional interactions among them (Cole et al., 2019). Background functional connectivity (BGFC) is a variant of functional connectivity analysis with the goal being to remove the stimulus-evoked responses, using various techniques,

leaving only the residual timeseries for subsequent connectivity analyses (Al-Aidroos et al., 2012; Cole et al., 2019; Fair et al., 2007; Frank & Zeithamova, 2023).

One dominant approach to model and remove the stimulus-evoked responses is to use a finite impulse (FIR) basis function to model the mean evoked responses of every time point across blocks (Al-Aidroos et al., 2012; Córdova et al., 2016; Norman-Haignere et al., 2012). Such approach has been shown to be able to remove almost all coactivation confounds (Cole et al., 2019). However, although the approach has been conceptually introduced in several previous works, there remains neither thorough and detailed guide on its operation nor any standard open-source tools to conduct such analyses. Here we introduce the background functional connectivity kit (BGFC-kit), an open-source python library developed to facilitate and standardize the preprocessing and computation of background functional connectivity (https://github.com/peetal/bgfc_kit). Importantly, BGFC-kit provides pipelines that can perfectly connect to fMRIprep, a popular fMRI preprocessing tool (Esteban et al., 2019) and leverages available fMRI analyses libraries such as FSL and AFNI, integrated in a workflow using Nipype (https://nipype.readthedocs.io/en/latest/). Specifically, BGFC-kit presents tools that cover four important stages of BGFC analyses: 1) tools that intake key experimental design parameters and generate FIR model design matrix, 2) tools that model and remove co-activation confounds and output both the modeling parameters and residual activities, 3) tools that divide timeseries into epochs (blocks) and compute background connectivity matrices, and 4) tools for potential subsequent analyses using the computed connectivity measures. Each of these features will be further introduced in the following sections. We present an accompanying notebook that applies these tools in BGFC-kit to an available dataset, serving as a guidance for using the library (https://github.com/peetal/bgfc_kit/blob/main/bgfc_kit/demo/).

Main features in BGFC-kit

Finite impulse response (FIR) model

BGFC-kit uses a FIR task regression approach to model and then remove the task-evoked activities. In this approach, the cross-block mean response is calculated for each time point using within a specified window length, synchronized with the block onset for a given task condition. For example, if the first 20 time points were being modeled for a task condition consisted of 5 blocks, the mean response of each of the 20 time point would be modeled across the 5 blocks, leading up to 20 beta estimates (Al-Aidroos et al., 2012; Cole et al., 2019; Cooper & Ritchey, 2019; K. Duncan et al., 2014; Norman-Haignere et al., 2012). This approach is apart from the traditional modeling approach that it does not make any assumption regarding to the hemodynamic response function (HRF), but determine the best fitting shape empirically, allowing for more precise modeling of the task-evoked activity (Cole et al., 2019; Fair et al., 2007).

BGFC-kit includes a module to generate the design matrix that be used for performing FIR task regression. Specifically, this module allows user defined configuration files containing their specific experimental design parameters, such as the number of task conditions, the number of blocks within a condition, the number of timepoints to model etc. Using the configuration file, this module will be able to generate a design matrix that includes a binary regressor for every time point in the task blocks that the user aims to model, which can be used again by BGFC-kit during the modeling stage.

Notably, analyses of human fMRI data can be influenced by head motion, leading to the exclusion of time points with noticeable spikes in head motion from the design matrix. As in the previous example, the usual practice involves modeling the mean evoked responses of a time

point across 5 blocks of a specific condition. However, if a head motion spike is detected at this time point in one of the blocks, the mean evoked response for this time point will only be modeled across the remaining 4 blocks. In the block with the motion spike, the binary regressor for this time point will be set to 0. BGFC-kit achieves this by referring to the framewise displacement confound parameter measured by fMRIprep, and drops the time points using a user defined spike cutoff optionally specified in the configuration file.

Extracting residual timeseries

The module within BGFC-kit responsible for extracting the residual timeseries is intended to complement the preprocessing pipeline of fMRIprep (Esteban et al., 2019). Utilizing the minimally preprocessed NIFTI files and the confound parameter estimates generated by fMRIprep, BGFC-kit carries out additional preprocessing steps. These steps include: 1) smoothing and filtering, 2) applying a first general linear model (GLM) to eliminate nuisance regressors, 3) demeaning and concatenation, and 4) employing a second GLM to eliminate stimulus-evoked activities.

Smoothing and filtering (**Figure 4.1 purple and orange boxes**). BGFC-kit initiates the preprocessing by applying spatial smoothing and high-pass filtering to each fMRIprep preprocessed image, utilizing user-defined parameters such as smoothing kernel size and high-pass filter cutoff. Spatial smoothing was done using FSL SUSAN workflow implemented in Nipype, and high-pass filtering was performed using fsl.ImageMaths. *The first GLM* (**Figure 4.1 blue box**). The first GLM aims to remove selected confound estimates from the each timeseries, including the 6 motion parameters as well as white matter (MW) and cerebrospinal fluid (CSF) estimated by fMRIprep. BGFC-kit performs the first GLM using FSL FEAT implemented in Nipype (Woolrich et al., 2001). *Demeaning and concatenation* (**Figure 4.1 green box**). BOLD

signals often exhibit arbitrary units, introducing potential biases when comparing different runs. To address this issue, BGFC-kit employs a normalization step for the BOLD signal within each run and concatenates runs before modeling the task-evoked response. More precisely, BGFC-kit normalizes each run using the mean and standard deviation of the BOLD signals during the inter-block interval of that run. This normalization is based on the rationale that the BOLD signals during the "resting" period should remain consistent across runs. Subsequently, the demeaned timeseries are concatenated together using a shared brain masks across all runs. *The second GLM* (**Figure 4.1 pink box**). The second GLM takes in the previously generated design matrix and compute both the parameter estimates for each regressor and residual timeseries. *BGFC-kit outputs.* The outputs of BGFC-kit preprocessing pipeline includes 4 important components: 1) the residual timeseries, which can then be used for computing background functional connectivity, 2) the “evoked” timeseries, which is the concatenated timeseries prior to the second GLM, 3) the parameter estimates of the second GLM, which can be used to perform sanity check, and 4) a brain mask for the subject shared across all fMRI functional runs.

Computing BGFC from residual activities

BGFC-kit encompasses various functions designed to operate on the residual timeseries resulting from the post-fMRIprep preprocessing pipeline. These functions are instrumental in computing whole-brain background functional connectivity matrices. Given the extensive number of voxels in the brain, calculating a voxel-level whole-brain correlation matrix can be impractical. To address this, BGFC-kit employs dimension reduction through parcellation, using a predefined parcellation mask (e.g., Gratton et al., 2018; Schaefer et al., 2018; Yeo et al., 2011) to divide the brain into a manageable number of parcels with each parcel reflecting the averaged neural activity across all voxels within it. Additionally, BGFC-kit provides tools to unpack the

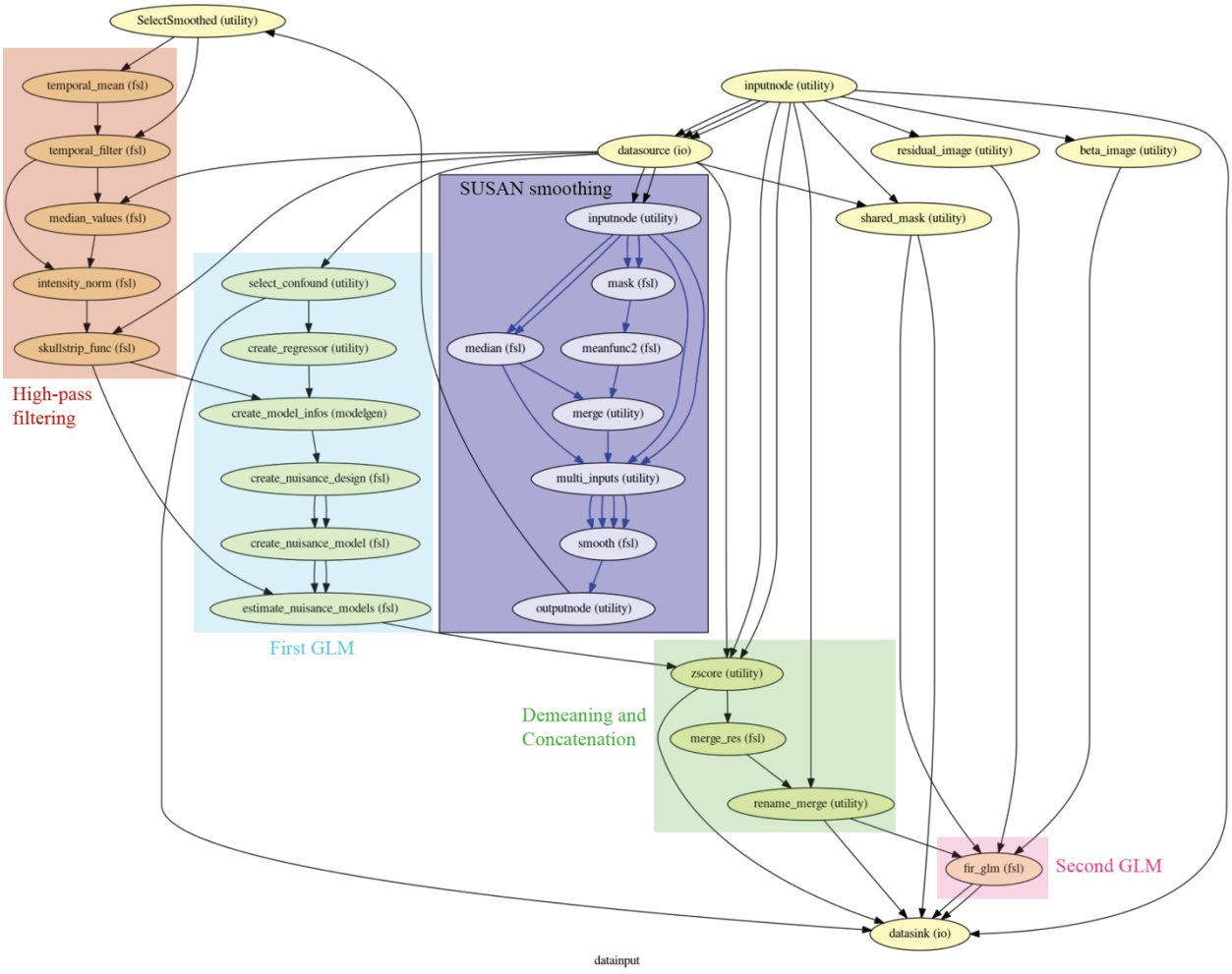

Figure 4.1. BGFC-kit post-fMRIprep processing pipeline.
This graph is modified based on the workflow graph automatically generated from Nipype. Each circle represents a Nipype node, which consists of an input field, a function that can be built-in (e.g., a FSL function) or user-defined (i.e., utility), and an output field. The name of each circle represents the name of the function contains within each node. The arrows connect the output field on the previous node to the input field of the next node, representing the order of the workflow. Some nodes can take inputs from multiple nodes and pass outputs to multiple nodes. The colored boxes represent the key components within this pipeline, including smoothing and filtering, the nuisance regression, de-meaning and concatenation, and the FIR model regression.

residual timeseries into epochs (i.e., blocks) for each condition. For instance, in an experiment with 2 conditions, each consisting of 5 epochs, and modeling the first 20 timepoints of each epoch with the FIR regressors, BGFC-kit returns a 10 by 20 NumPy array. In this array, the first

dimension represents the total number of epochs, and the second dimension represents the residual activity with the task-evoked activity removed by the model.

Following this, BGFC-kit offers a function to compute background connectivity matrices from these epoch-level residual timeseries using numpy.corrcoef. Subsequently, it performs Fisher z-transformation through numpy.arctanh to derive the final connectivity measure. The function provides flexibility in producing either epoch-level or condition-level outputs. Epoch-level matrices enable the examination of connectivity matrices for each epoch individually. On the other hand, condition-level matrices are computed by averaging across all matrices of epochs within the same condition. The availability of both epoch- and condition-level matrices allows researchers to conduct diverse analyses to address various types of questions. For instance, epoch-level data can be particularly valuable for training and testing machine learning models to discern neural differences between conditions. In contrast, condition-level data proves useful for investigating neural-behavioral relationships across participants, especially when the number of trials within an epoch is too limited to be considered in isolation.

It's essential to acknowledge that BGFC measures can be influenced by head motion spikes. Specifically, because the stimulus-evoked activities were not modeled at the time points of motion spikes when constructing the design matrix for FIR regressors, the residual timeseries near the spike may contain a mix of stimulus-evoked and motion-distorted signals. Consequently, in certain cases, researchers may prefer to exclude specific time points associated with head motion spikes when computing connectivity measures. BGFC-kit implements this operation by incorporating a function that systematically scans the residual timeseries, identifying and masking the time points near a head motion spike based on framewise displacements measured by fMRIprep. Subsequently, motion-corrected BGFC matrices are

computed using numpy.ma.corrcoef followed by Fisher z-transformation, and this operation is available for both epoch- and condition-level analyses.

Potential subsequent analyses

As recommended by previous studies, both the residual timeseries and the BGFC matrices offer avenues for diverse subsequent analyses, tailored to specific research inquiries. BGFC furnishes tools and illustrative examples for several of these potential analyses, conveniently accessible in the accompanying notebook demonstration (see https://github.com/peetal/bgfc_kit/blob/main/bgfc_kit/demo/).

Sanity check. A fundamental assumption underpinning BGFC analyses is the efficacy of the FIR model in capturing most of the stimulus-evoked neural activity. Therefore, it is important to conduct sanity checks to validate this assumption and ensure the absence of task-evoked components that may have eluded removal by the GLM models. BGFC-kit offers a suite of tools for this purpose. Firstly, it provides functions to plot the parameter estimates of the FIR regressors for each parcel of the interest to examine each whether the estimates capture the block design structure within the task paradigm. In these plots, one should observe regressors capturing inter-block intervals reflecting baseline neural activity, while those modeling task should depict either activation (e.g., in control network regions) or deactivation (e.g., in default mode network regions), resulting in a discernible boxcar or inverted boxcar function. Secondly, BGFC-kit assesses whether residual timeseries retain any informative activity patterns, as successful removal of stimulus-evoked activities should render these patterns incongruent with external stimuli and processing. Specifically, BGFC-kit can conduct multi-voxel pattern analyses on both residual and pre-FIR timeseries to discriminate between selected task conditions (Norman et al.,

2006). Chance-level performance in the former and a deviation from chance in the latter would signify successful modeling and removal of task-evoked activities.

BGFC based machine learning classifiers. One subsequent analysis within the realm of BGFC analyses involves scrutinizing the extent to which stimulus-independent, endogenous functional connectivity (FC) reflect ongoing task states (e.g., Gonzalez-Castillo et al., 2015; Li et al., 2023). To conduct this analysis, cross-subject classification could be performed upon the BGFC matrices computed by BGFC-kit to differentiate between task conditions. Specifically, the notebook demonstration employs a leave-one-subject-out cross-validation framework, utilizing all epochs of the excluded subject as the testing set for each fold. Given the abundance of features within a connectivity matrix, principal component analysis (PCA) is initially performed on all BGFC matrices in the training set. The top 500 principal components are then utilized to train a regularized generalized linear model (e.g., softmax) to distinguish between selected task conditions, which is subsequently tested on epochs from the left-out subject in each fold. Machine learning performance can be averaged across folds to assess overall performance. Previous studies have suggested that the endogenous BGFC pattern associated with task states can be modulated to prioritize goal-relevant information processing (Chun et al., 2011; Turk-Browne, 2013).

Graph theory analyses. Another popular approach in subsequent BGFC analyses involves employing graph theory measures (Bullmore & Bassett, 2011; Fornito et al., 2013), as each BGFC matrix can often serve as the basis for constructing a graph (Barnett et al., 2021; Cohen & D'Esposito, 2016; Richiardi et al., 2011). BGFC-kit is seamlessly integrated with NetworkX (https://networkx.org/) and offers wrapper functions for computing graph theory measures across various thresholds. Previous studies in graph theory analyses have often opted to generate binary

graphs by considering only the top percentage of edges instead of constructing graphs from all connectivity edges (e.g., Cohen & D'Esposito, 2016). BGFC-kit facilitates this approach by computing various graph theory measures, such as degrees, participation coefficients, and modularity, using graphs generated from the top 25%, 20%, 15%, 10%, and 5% of edges. These analyses offer a macro-level understanding of how the brain reconfigures itself to accommodate different behavioral task goals.

Conclusion

This chapter introduces a self-developed public Python library designed to streamline background functional connectivity (BGFC) analyses. The library offers wrapped functions and pipelines that cover various stages such as: 1) FIR modeling for evoked activity, 2) preprocessing for extracting residual time series, 3) calculating BGFC measures, and 4) performing potential subsequent analyses with BGFC. We hope this library will make it easier and more appealing for researchers to conduct BGFC analyses, thus enabling more studies to explore the neural mechanisms of top-down attentional control through intrinsic functional connectivity modulations.

CHAPTER V

GENERAL DISCUSSION

A major line of work in cognitive neuroscience has been directed toward understanding the neural mechanism underlying top-down attention control, which refers to the voluntary allocation of attentional resources to goal-relevant information (Corbetta & Shulman, 2002; Hopfinger et al., 2000). One line of works primarily focuses on investigating the operations performed upon the stimulus, such as the processes of monitoring, selection, and modulation, by examining brain regions showing increased neural activity evoked by these operations (Corbetta et al., 2000; Kastner et al., 1999). Yet recent theories propose that in the presence of behavioral tasks and goals, the brain not only demonstrates evoked activities related to stimulus processing but also maintains a sustained task-state in the background of activation (Otten et al., 2002; Summerfield et al., 2006). Building upon this notion, another line of research has emerged to explore the neural mechanisms underlying the sustained maintenance of task states (Turk-Browne, 2013). The present dissertation aligns with this line of inquiry and focuses on utilizing background functional connectivity (BGFC) as the neural measure to investigate the neural basis of top-down attentional control.

The research presented in this dissertation aimed to enhance our comprehension and support future studies on top-down attentional control from various perspectives. Firstly, I conducted whole-brain exploratory approach using whole-brain BGFC, revealing neural mechanisms that enable flexible transitions between external and internal attentional states (**Chapter 2**), as well as the concurrent maintenance of multiple attentional states, whether external or internal (**Chapter 3**). These data-driven approaches allow for the identification of crucial top-down attentional control mechanisms often overlooked in previous seed-based human

fMRI studies but consistent with theories proposed in rodent literature. Secondly, I examined the similarities and distinctions between BGFC and evoked activity in reflecting top-down attention control mechanisms. I presented evidence indicating that their differentiation lies in their preference for capturing either stimulus- or state-related signals (**Chapter 2**), and that various brain networks preferentially employ top-down attentional control via either stimulus- or state-related signal (**Chapter 3**). Lastly, I developed and introduced an open-source Python library aimed at streamlining and standardizing the preprocessing stage of BGFC analyses (**Chapter 4**).

Bridging top-down attentional control theories

It is a fundamental principle that the brain is inherently competitive. Various pathways within it, each carrying distinct sources of information, compete for dominance in shaping behavior. Multiple top-down attentional control accounts have been proposed to explain how attention can influence this competitive dynamic. First introduced by Desimone and Duncan (1995), the theory of biased competition elucidates top-down attentional control at the individual neuron level. This theory posits that the neuronal reaction to stimuli presented simultaneously is a weighted average of the reaction to individual stimuli, with attention influencing the weighting in favor of the attended stimulus. Subsequently, this theory was expanded beyond the single-neuron level, with evidence indicating that attention effectively biases population-level multivariate activation patterns in object representation (Reddy et al., 2009). Building upon the theory of biased competition, Miller and Cohen (2001) proposed the guided activation account, emphasizing the prefrontal cortex's (PFC) role in biased competition. According to this account, the evoked activity patterns of the PFC represent current behavioral goals and rules, guiding activation patterns across neural pathways to other brain regions. It was suggested that activation patterns in the PFC are acquired over time to establish mappings between goals and necessary

actions. As a result, the PFC can orchestrate brain-wide activation to bias competition in alignment with the behavioral objective. The guided activation account finds support in the specialized functions of the PFC, which include multimodal convergence, adaptive plasticity, and robust feedback pathways enabling control over other brain regions (Cole et al., 2012; Friedman & Robbins, 2022; Menon & D'Esposito, 2022; Miller & Cohen, 2001). In addition to the modulations of evoked activity patterns, the guided activation account also suggests potential changes in the neural pathways. That is, the evoked activity pattern of the PFC dictates which neural pathways to traverse and subsequently influences the behavior of other brain regions (Miller & Cohen, 2001). Building upon this concept, the switching train tracks account asserts that top-down attentional control does not solely depend on managing evoked activation patterns from the PFC to bias competition and influence behavior. Instead, competition is also shaped by intrinsic functional connectivity (FC) modulation that are independent from evoked activities in the PFC, where goal-relevant information processing pathways are strengthened and irrelevant ones are weakened (Al-Aidroos et al., 2012; Turk-Browne, 2013). This account is supported by previous research indicating that intrinsic FC patterns engage in goal-oriented modulation both before and after the presence of actual behavioral tasks, even without guidance signals from the PFC (Gruber et al., 2016; Murty et al., 2017; Ploner et al., 2010; Sadaghiani et al., 2015; Tambini et al., 2017)

The findings from this dissertation align with these theories of top-down attentional control. Consistent outcomes from Chapters 2 and 3 show that intrinsic FC patterns, as measured by BGFC, exhibit goal-oriented modulations even after removing whole-brain evoked activity patterns. These results imply that the attentional control mechanisms reflected by FC modulations operate independently of those reflected by evoked activity pattern modulations. As

a result, biased competition can arise through two distinct pathways: firstly, via guided activation through PFC-generated activation patterns, and secondly, through intrinsic FC modulations in the background of activation (Al-Aidroos et al., 2012; Miller & Cohen, 2001; Turk-Browne, 2013). Therefore, a comprehensive understanding of the neural mechanisms of top-down attentional control requires an integrative approach that combines these two lines of research. Additionally, the findings from this dissertation also offer insights that could potentially guide future research beyond established theories. The guided activation account primarily focuses on the PFC's role in initiating FC pathway modulations. However, the dissertation's results suggest the involvement of additional neural circuits, such as those involving the retrosplenial cortex (RSC) and thalamus, which have been highlighted in rodent studies. These circuits may also play a role in initiating FC pathway modulations alongside the PFC.

Differences between activity- and connectivity-based neural measures

As depicted in the previous session, research on the neural mechanisms of top-down attentional control typically adopts two distinct approaches. The first approach, following the guided activation account, focuses on evoked activity patterns to identify brain regions activated during attentional control processes or to decode information revealing how they influence competition (Corbetta & Shulman, 2002; Long & Kuhl, 2018). The second approach, aligned with the switching train tracks account, concentrates on intrinsic FC patterns to unveil FC modulations induced by behavioral goals that bias competition in favor of goal-relevant information processing (Al-Aidroos et al., 2012; Cooper & Ritchey, 2019; K. Duncan et al., 2014; Tompary et al., 2015). However, there has been limited exploration into whether activity- and connectivity-based neural measures reveal similar or distinct neural mechanisms of top-down attentional control. The studies presented in this dissertation are among the first to

systematically compare the use of these two neural measures and shed light on the distinctions between the two perspectives.

Firstly, I provided evidence that both evoked activity and intrinsic FC (measured by BGFC) robustly reflect aspects of ongoing cognitive tasks. This is demonstrated by their ability to differentiate task conditions when only one task is being performed (Chapter 2) and to identify constituent tasks during multitasking (Chapter 3). Secondly, results from both chapters indicate that evoked activity generally contains more information than BGFC, as evidenced by the higher accuracy of machine learning models trained on evoked activity. However, Chapter 3 reveals evidence that this superiority of evoked activity may not always hold for certain brain networks such as the default mode network (DMN). Specifically, our findings suggest that BGFC of brain regions in the DMN may better reflect attentional control processes during multitasking compared to evoked activity patterns of these regions. These results suggest that while some brain networks tend to engage top-down attentional control more via evoked activity patterns, others preferentially engage this process via modulations in intrinsic FC patterns. Lastly, the studies in this dissertation consistently provide evidence that evoked activity and BGFC patterns reflect distinct aspects of top-down attentional control processes. Results from both Chapters indicate that an ensemble model combining both neural measures outperforms models using a single measure. In particular, Chapter 2 suggests that the differences between the two measures lie in the sensitivity of evoked activity patterns to stimulus-related signals, while BGFC patterns are more specific to state-related signals. In other words, evoked activity patterns exhibit greater sensitivity to variations in stimuli (e.g., intact vs. scrambled), whereas BGFC demonstrates heightened sensitivity to differences in states (e.g., perception vs. retrieval states) compared to evoked activity patterns.

Overall, the findings from this dissertation align with theoretical propositions suggesting that evoked activity and intrinsic FC patterns are independent from each other, reflecting non-identical processes of top-down attentional control. Specifically, evoked activity captures more transient signals (stimulus-related), while intrinsic FC reflects relatively sustained signals (state-related; (Otten et al., 2002; Summerfield et al., 2006).

Neural mechanisms underlying externally- and internally oriented attention

Investigating top-down attentional control poses an inherent challenge due to its multifaceted and pervasive nature. Previous human fMRI research focusing on intrinsic FC modulations tends to narrow its scope to specific aspects of this cognitive process. For instance, some studies delve into intrinsic FC modulations associated with the control process of attending to face versus scene stimuli (Al-Aidroos et al., 2012; Córdova et al., 2016; Norman-Haignere et al., 2012; Tompary et al., 2015; Turk-Browne et al., 2010). Other studies concentrate on intrinsic FC modulations related to individual differences in specific cognitive functions, such as maintaining focus on pertinent information over prolonged periods (sustained attention) and attending to relevant details from past episodes (memory retrieval; Cooper & Ritchey, 2019; Rosenberg et al., 2020; Song & Rosenberg, 2021). Undoubtedly, these studies provide valuable insights into particular facets of top-down attentional control, illuminating how intrinsic FC modulations mirror such control systems. However, there is also merit in exploring the neural mechanisms underlying broader categories of top-down attention control based on specific taxonomies.

This dissertation undertook such an investigation by adopting the taxonomy of external and internal attention (Chun et al., 2011). This taxonomy categorizes top-down attentional control mechanisms into either externally-oriented attention, such as visual perception and

sustained attention, or internally-oriented attention, such as memory retrieval. Works in this dissertation explored the neural mechanisms underlying this taxonomy of top-down attentional control in two scenarios: 1) the mechanism for flexibly switching between external and internal attention states (**Chapter 2**), and 2) the mechanism for concurrently representing tasks of external or internal attention states (**Chapter 3**). These investigations yielded multiple findings that will be discussed in the context of previous literature. Firstly, findings from both chapters underscored the involvement of the frontoparietal control network in both external and internal attentional control processes. In Chapter 2, it was observed that regions within the control network displayed heightened BGFC during external attention tasks compared to internal ones. Furthermore, Chapter 3 revealed that BGFC patterns of the control network regions effectively captured the task conditions concurrently represented during multitasking. These results align with established theories proposing the control network as a flexible connector hub (Cole, Reynolds, et al., 2013; Gordon et al., 2018; Gratton, Sun, et al., 2018). Specifically, this theory posits that the control network not only demonstrates coordinated activity within its network but also swiftly adapts its brain-wide FC patterns to facilitate attentional control across various tasks.

Furthermore, the results from Chapter 2 suggest that the retrosplenial cortex (RSC) acts as a switchboard in alternating between externally (perception) and internally (memory retrieval) oriented attention. Specifically, the RSC exhibited stronger coupling with regions in the default mode network (DMN) during external attention, but with regions in the frontoparietal control and dorsal attention network (DAN) during internal attention. This constitutes among the first evidence in human fMRI studies suggesting the role of intrinsic FC modulations centered on RSC in switching between external and internal attentional control. We posit that this finding is attributed to our non-seed-based, data-driven approach, without presuming network allegiance.

Previous works typically rely on a priori regions of interest, and the RSC is often included as part of the DMN network, making it challenging to identify the important role of the sole RSC region. (Cooper & Ritchey, 2019; Yeshurun et al., 2021). Moreover, our indication of the role of RSC aligns with rodent literature, such as its involvement in integrating sensory inputs and mnemonic information (Bicanski & Burgess, 2018), and in integrating animals' actual location in the external world (allocentric mapping) with their internal representations of location (egocentric mapping) during maze navigation (Alexander & Nitz, 2015).

Lastly, findings from Chapter 3 indicate that effective top-down attentional control during concurrent tasks, whether external or internal, involves the coordinated activity of multiple brain networks and subcortical regions. This cortical and subcortical engagement aligns with various circuits proposed in previous literature for controlling external and internal attentional processes. Notably, previous studies have suggested the existence of a thalamus-centered circuit responsible for managing memory and executive functions (Weel et al., 2019). Specifically, the thalamus has been identified as a highly adaptable connector hub, exhibiting extensive connectivity with various cortical functional networks within the human brain (Hwang et al., 2017). It plays a pivotal role in integrating multimodal information across the cortex (de Bourbon-Teles et al., 2014), and in facilitating the maintenance and coordination of task-relevant cortical representations by adjusting functional connectivity strengths within the cortex (Nakajima & Halassa, 2017). Additionally, a hippocampus (HPC)-centered circuit has been proposed to regulate both externally and internally oriented processing through pattern separation and completion, respectively (Norman, 2010). Consequently, intrinsic FC modulation within HPC subregions and between the HPC and cortical and other subcortical structures have

been demonstrated to influence attentional control. (K. Duncan et al., 2014; H. Kim, 2015; Poskanzer & Aly, 2022).

Together, this dissertation serves as an exploration into the intrinsic FC modulations that underlie the mechanisms of top-down control across externally and internally oriented attention, utilizing a comprehensive, data-driven approach spanning the entire brain. Our discoveries not only pinpoint significant FC pathways consistent with established theories but also those overlooked in previous seed-based human fMRI research, yet aligned with findings from rodent studies.

The prospect and challenge of whole-brain BGFC analyses

This dissertation places particular emphasis on data-driven, whole-brain background functional connectivity (BGFC) analyses, coupled with machine learning models and feature selection methods. It's important to acknowledge that BGFC encompasses any FC analyses that address coactivation confounds, such as through methods like gPPI and low-pass filtering (Frank & Zeithamova, 2023; McLaren et al., 2012). However, the BGFC analysis undertaken in this dissertation specifically focuses on employing the finite impulse response model to eliminate stimulus-evoked signals from the recorded timeseries (see Cole et al., 2019 and Frank & Zeithamova, 2023 for comparisons between various approaches for computing BGFC). In this section, we delve into the benchmarks, challenges, and future directions associated with performing exploratory analyses on whole-brain BGFC.

This dissertation attempted to conducted whole-brain BGFC analyses on both voxel-level, utilizing full correlation matrix analyses (FCMA; Wang et al., 2015) and parcel-level, employing predefined parcellation schemes and network structure (Schaefer et al., 2018). Evidence was presented indicating that both methodologies successfully identified meaningful

BGFC modulations associated with top-down attentional control. However, these analyses encountered a trade-off between precision and complexity. Chapter 2 findings suggested that machine learning classifiers trained on voxel-level BGFC patterns achieved notably higher accuracy compared to those trained on parcel-level BGFC patterns. This outcome implies that, by avoiding predefined parcels, voxel-level BGFC analyses could pinpoint clusters of voxels wherein BGFC modulation more accurately capture the top-down attention control process. Nonetheless, the enhanced precision of voxel-level analysis is offset by increased computational demands and the need for sophisticated feature selection techniques to delineate clusters of interest, which could be circumvented through parcel-level analyses.

Following the computation of BGFC from the recorded timeseries, there are multiple pathways that subsequent analyses can pursue. The current dissertation focused on building machine learning models using BGFC patterns to distinguish between different attentional states (**Chapter 2**) and to decode concurrent tasks (**Chapter 3**). Feature selection methods were then applied to pinpoint brain regions influencing classifier performance based on BGFC patterns. While this approach undoubtedly yields meaningful and interpretable results, future studies could explore additional avenues complementary to the current approach. Firstly, researchers could consider conducting graph theory analyses on whole-brain BGFC alongside predefined parcellation schemes. The advantage of the graph theory approach lies in its interpretability, with each measure indicating specific properties of the functional network structure (Bullmore & Bassett, 2011; Rubinov & Sporns, 2011). Additionally, graph theory measures, such as the participation coefficient, could help identify brain parcels or networks with unique characteristics, like connector hubs (e.g., connector hubs; Cole, Reynolds, et al., 2013; Gordon et al., 2018). However, a downside of the graph theory approach is the challenge of pinpointing

specific FC pathways and circuits underlying top-down attentional control. Secondly, while the current dissertation focused on identifying BGFC modulations related to different attentional states, another direction could involve examining BGFC modulation in relation to individual differences in behavioral performance. Connectome-based predictive modeling (CPM) was developed for this purpose (Shen et al., 2017). Hence, it would be valuable to investigate the extent to which BGFC modulation underlying behavioral performances overlaps with or differs from those characterizing attentional states. In summary, future studies could explore BGFC analyses along any of these directions, employing different granularities (i.e., voxel or parcel levels), to better elucidate the neural mechanisms underlying top-down attentional control.

Conclusion

The present dissertation employs whole-brain background functional connectivity (BGFC) analysis to delve into the neural mechanisms underpinning top-down attentional control as manifested in the intrinsic functional organization of the brain. It moves beyond the exploration of specific aspects or functions of top-down attentional control to unveil general neural circuits governing the taxonomy of externally- and internally-oriented control systems. Notably, this dissertation introduces innovative methodologies for conducting non-seed-based, data-driven BGFC analyses and develops tools to facilitate future research in this area. Collectively, works in this dissertation broaden our current comprehension of the neural mechanisms of top-down attentional control and pave the way for further exploration in the field.

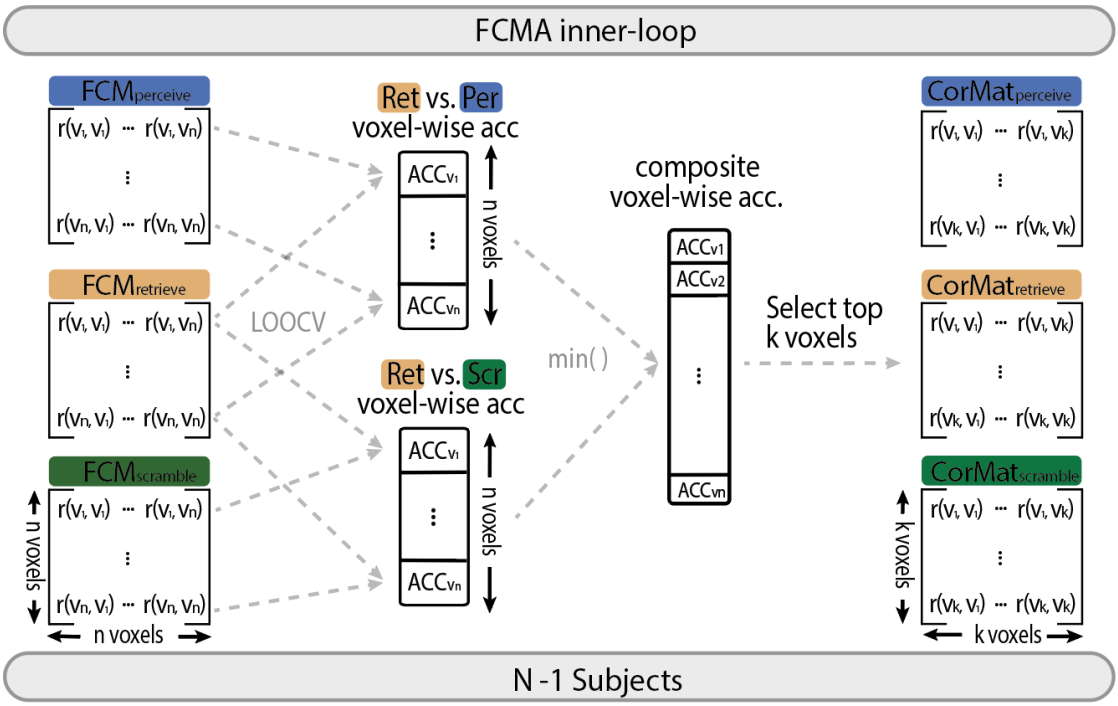

Figure S2.1. FCMA feature selection process.
The FCMA inner-loop used a leave-one-subject-out cross validation (LOOCV) framework to quantify the utility of each voxel. Within each training fold, we examined the degree to which each voxel's background functional connectivity patterns (seed map) can be used to differentiate *Retrieve* vs. *Perceive* conditions and *Retrieve* vs. *Scramble* conditions. This leads to two *n*-vector accuracy measures across voxels, one for each task condition comparison. A composite voxel-wise accuracy score was computed by taking the minimum of the two accuracy values for each voxel. The top *k* voxels in terms of composite accuracy score were selected to construct dimensionality reduced FC patterns (**Figure 2.1F**). Because each fold's training data differed by one subject, a different (but typically highly overlapping) set of *k* voxels could be selected for each training fold. As a result, the full cross-validation framework create 24 masks of selected voxels for each choice of *k*.

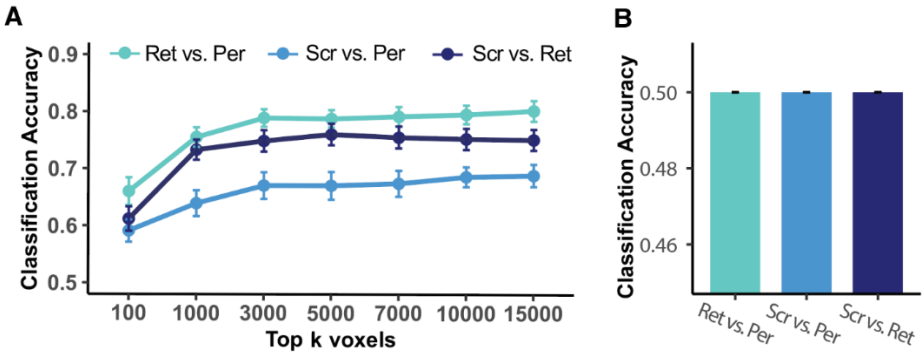

Figure S2.2. Background FCMA and MVPA classifier accuracies.
A) Background FC classification accuracy for each task comparison across different numbers of voxels selected by FCMA. Performance asymptoted when k = 3,000: *Perceive-Scramble*, M_{acc} = 67% ± 11%; *Perceive-Retrieve*, M_{acc} = 79% ± 8%; *Retrieve-Scramble*, M_{acc} = 75% ± 9%. **B)** Using the k = 3,000 mask, MVPA classifiers trained on residual activity patterns from the background FC processing pipeline failed to differentiate task conditions.

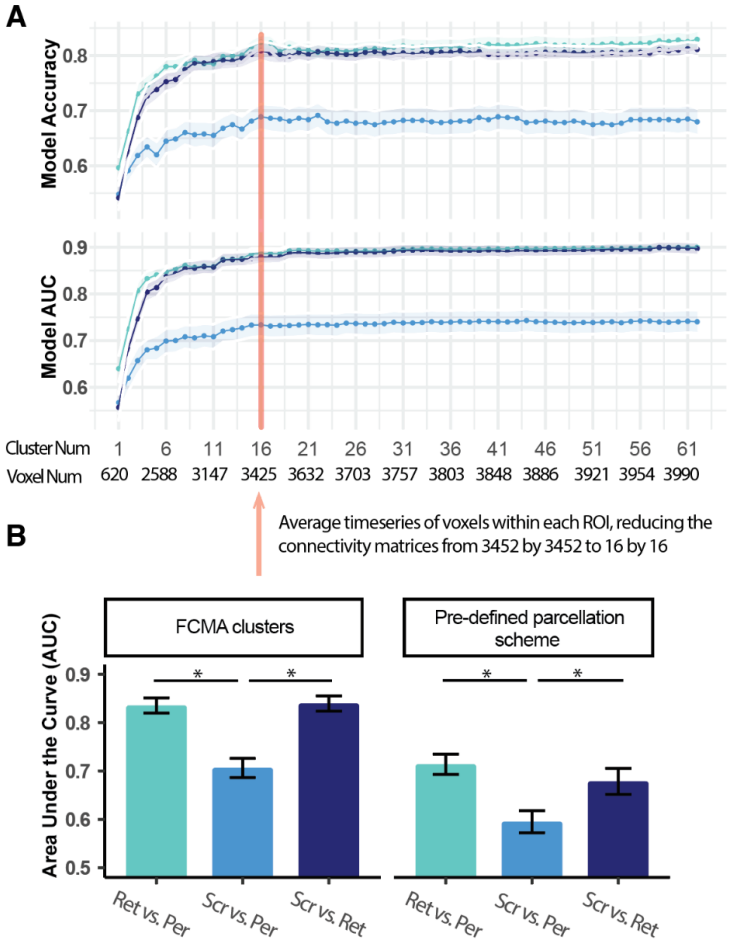

Figure S2.3. Cluster selection process.
A) Model performance as measured by both proportion correct accuracy and area under the curve (AUC) when sequentially adding in all voxels from the next largest cluster. The semi-transparent bands indicate the standard error of the mean across all testing folds. For example, we started by using the background FC matrices of all voxels only in the largest cluster (i.e., shaped 620 x 620) to differentiate each task condition comparison. Then we added in all voxels (519; **Table S2.1**) from the next largest cluster and estimated the model performances of the combined background FC matrices (now shaped 1139 x 1139), and so forth. We selected a cluster number that, for either AUC or ACC, was significantly greater than the preceding number and not significantly less than the maximal number of clusters. **B**) **Left**: We averaged all voxels within a cluster, thus reducing the dimensions of the FC matrices from 3452 x 3452 to 16 x 16 and examined the performances of the models for the reduced matrices. **Right:** Instead of defining clusters using the FCMA-then-clustering pipeline, we selected the top-performing 16 parcels (from the Schaefer 1000 parcellation scheme) based on separating perception from retrieval states using the same cross-validation framework (**Figure S2.1**). We then examined the performance of models trained using FC matrices among predefined Schaefer parcels for differentiating each task condition comparison. The error bars represent the standard errors of the mean across all testing folds.

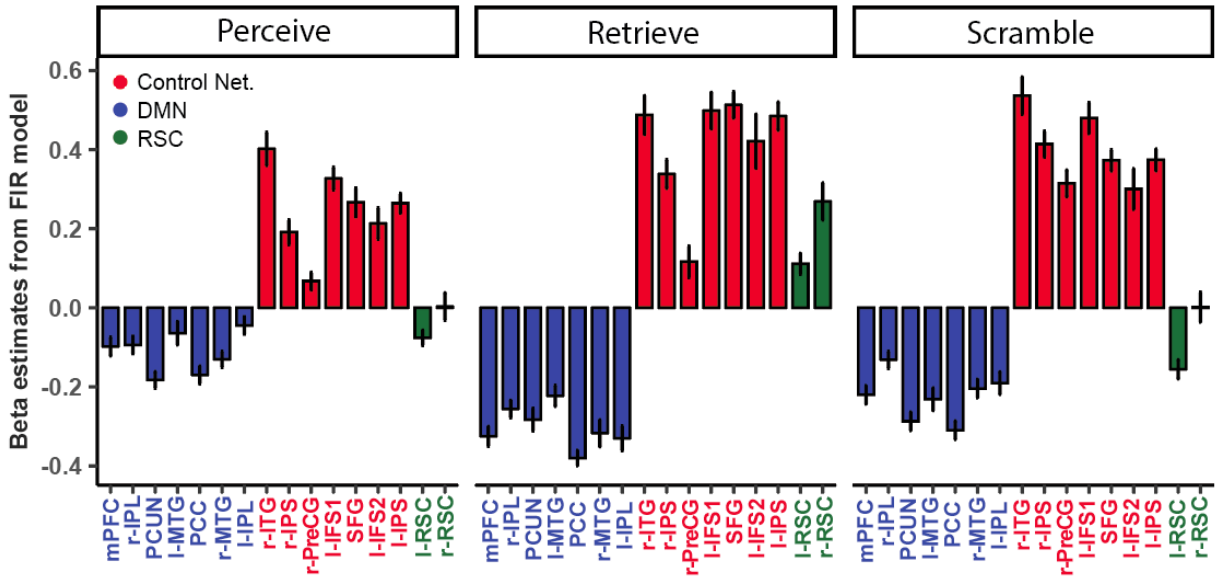

Figure S2.4. Univariate activation profiles of the 16 clusters across 3 functional communities during each task condition.

The FIR model consists of 36 (4 TR instruction + 24 TR task + 8 TR inter-block interval) x 2 (epoch category) x 3 (condition) = 216 regressors. Thus, 24 (TR task) x 2 (epoch category) = 48 regressors modeled task activations for each condition. Here for each subject, we computed the averaged beta estimates (of the 48 regressors) for all voxels within a cluster per condition. Error bars indicates the standard error of the mean of beta estimates across subjects. The color indicates the functional community assignment of each cluster. mPFC: medial prefrontal cortex; IPL: inferior parietal lobule; PCUN: precuneus; MTG: middle temporal gyrus; PCC: posterior cingulate cortex; ITG: inferior temporal gyrus; IPS: Intraparietal sulcus; PreCG: precentral gyrus; IFS: inferior frontal sulcus; SFG: superior frontal gyrus; RSC: retrosplenial cortex

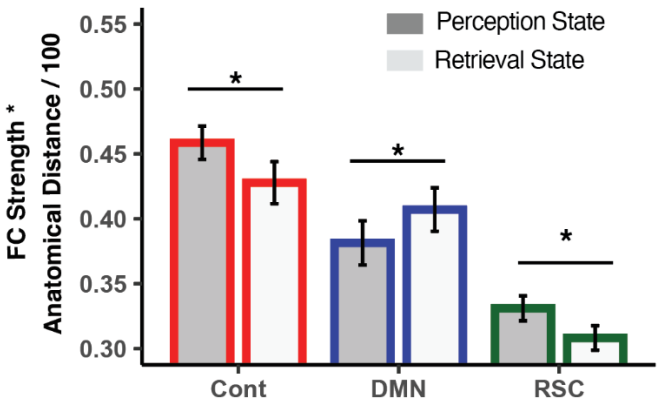

Figure S2.5. Background FC strength averaged across all pairwise connections within the same functional community across perception and retrieval states after factoring in anatomical distance.

Using MNI coordinates in **Table S2.1**, anatomical distance was quantified as the Euclidean distance between each pair of clusters (divided by 100 to make the y-axis unit comparable to **Figure 2.5B**). The adjusted background FC strength was computed as $FC\ strength \times anatomical\ distance$, thus closer anatomical distance (e.g., the two RSC cluster) would lead to smaller adjusted FC strength. After factoring in anatomical distance, clusters within the Control network retained overall stronger connectivity density compared to the DMN ($t_{(23)} = 4.03$, $p < 0.001$, 95% CI = [0.02, 0.07], Cohen's d = 0.70). On the other hand, the strong coupling strength between RSC regions observed in **Figure 2.5B** could be largely attributed to the short anatomical distance between the two RSC clusters.

ClusterIdx	Brain Region	Volume	X	Y	Z	MaxInt
1	Medial prefrontal cortex	620	-0.5	44.3	-1.0	9.14
2	R-Inferior parietal lobule	519	60.1	-26.4	49.0	8.03
3	L-Retrosplenial cortex	400	-18.2	-69.3	24.0	7.88
4	L-Intraparietal sulcus	377	-33.3	-59.2	41.5	8.30
5	R-Intraparietal sulcus	364	29.8	-66.8	36.5	7.09
6	Precuneus	308	-10.6	-54.2	44.0	7.47
7	L-Middle temporal gyrus	117	-66.2	-51.7	9.0	5.96
8	R-Precentral gyrus	116	52.5	9.0	19.0	6.43
9	L-Inferior frontal sulcus1	116	-53.6	16.5	31.5	7.30
10	Posterior cingulate cortex	107	2.0	-18.8	44.0	7.37
11	R Retrosplenial cortex	103	14.6	-54.2	14.0	7.06
12	Superior frontal gyrus/ Pre-supplementary motor area	82	-3.0	16.5	51.5	7.27
13	L-Inferior frontal sulcus2	64	-48.5	29.2	24.0	6.23
14	R-Middle temporal gyrus	58	62.6	-16.3	-11.0	6.30
15	L-Inferior parietal lobule	52	-61.1	-49.1	44.0	7.00
16	R-Inferior temporal gyrus	49	55.1	-56.7	-13.5	5.83

Table S2.1. Sizes and locations (MNI coordinates) of the clusters of interest.
The *Volume* column indicates the number of voxels included in each cluster. The *MaxInt* column indicates the maximum z-score within each cluster.

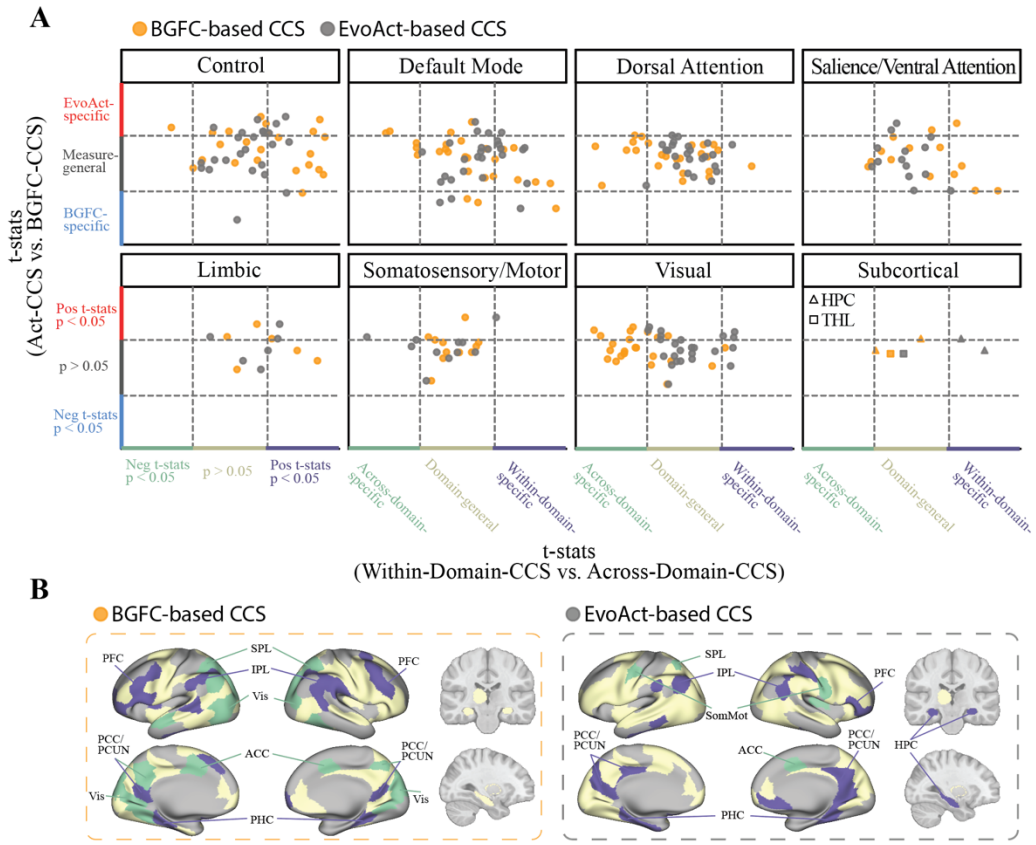

Figure S3.1. Measure- and domain-specificity of parcels exhibiting compositional coding property.
A) The t-stats of each parcel showing significantly off-chance ensembled CCS, grouped by networks. The x-axis displays the t-stats of the domain-specificity estimates, with neural measures being either evoked activity (gray) or BGFC (orange). The y-axis shows the t-stats of the domain-specificity estimates. Each dot represents a parcel, and the dotted lines represent the t threshold for being statistically significant ($p < 0.05$). **B)** Within-domain-specific (green), across-domain-specific (purple), and domain-general (white) parcels when either BGFC- or evoked activity was used as the neural measure.

REFERENCE CITED

Addante, R. J., Watrous, A. J., Yonelinas, A. P., Ekstrom, A. D., & Ranganath, C. (2011). Prestimulus theta activity predicts correct source memory retrieval. *Proceedings of the National Academy of Sciences of the United States of America*, *108*(26), 10702–10707. https://doi.org/10.1073/pnas.1014528108

Al-Aidroos, N., Said, C. P., & Turk-Browne, N. B. (2012). Top-down attention switches coupling between low-level and high-level areas of human visual cortex. *Proceedings of the National Academy of Sciences*, *109*(36), 14675–14680. https://doi.org/10.1073/pnas.1202095109

Alexander, A. S., & Nitz, D. A. (2015). Retrosplenial cortex maps the conjunction of internal and external spaces. *Nature Neuroscience*, *18*(8), Article 8. https://doi.org/10.1038/nn.4058

Barnett, A. J., Reilly, W., Dimsdale-Zucker, H. R., Mizrak, E., Reagh, Z., & Ranganath, C. (2021). Intrinsic connectivity reveals functionally distinct cortico-hippocampal networks in the human brain. *PLoS Biology*, *19*(6), e3001275–e3001275. https://doi.org/10.1371/journal.pbio.3001275

Bein, O., Duncan, K., & Davachi, L. (2020). Mnemonic prediction errors bias hippocampal states. *Nature Communications*, *11*(1), Article 1. https://doi.org/10.1038/s41467-020-17287-1

Bejjanki, V. R., Silveira, R. A. da, Cohen, J. D., & Turk-Browne, N. B. (2017). Noise correlations in the human brain and their impact on pattern classification. *PLOS Computational Biology*, *13*(8), e1005674. https://doi.org/10.1371/journal.pcbi.1005674

Ben-Yakov, A., & Dudai, Y. (2011). Constructing realistic engrams: Poststimulus activity of hippocampus and dorsal striatum predicts subsequent episodic memory. *Journal of Neuroscience*, *31*(24), 9032–9042. https://doi.org/10.1523/JNEUROSCI.0702-11.2011

Bicanski, A., & Burgess, N. (2018). A neural-level model of spatial memory and imagery. *eLife*, *7*, e33752. https://doi.org/10.7554/eLife.33752

Biswal, B., Zerrin Yetkin, F., Haughton, V. M., & Hyde, J. S. (1995). Functional connectivity in the motor cortex of resting human brain using echo-planar mri. *Magnetic Resonance in Medicine*, *34*(4), 537–541. https://doi.org/10.1002/mrm.1910340409

Blondel, V. D., Guillaume, J.-L., Lambiotte, R., & Lefebvre, E. (2008). Fast unfolding of communities in large networks. *Journal of Statistical Mechanics: Theory and Experiment*, *2008*(10), P10008. https://doi.org/10.1088/1742-5468/2008/10/P10008

Bosch, S. E., Jehee, J. F. M., Fernández, G., & Doeller, C. F. (2014). Reinstatement of associative memories in early visual cortex is signaled by the hippocampus. *The Journal*

of Neuroscience: The Official Journal of the Society for Neuroscience, *34*(22), 7493–7500. https://doi.org/10.1523/JNEUROSCI.0805-14.2014

Braun, U., Schäfer, A., Walter, H., Erk, S., Romanczuk-Seiferth, N., Haddad, L., Schweiger, J. I., Grimm, O., Heinz, A., Tost, H., Meyer-Lindenberg, A., & Bassett, D. S. (2015). Dynamic reconfiguration of frontal brain networks during executive cognition in humans. *Proceedings of the National Academy of Sciences*, *112*(37), 11678–11683. https://doi.org/10.1073/pnas.1422487112

Bressler, S. L., & Menon, V. (2010). Large-scale brain networks in cognition: Emerging methods and principles. *Trends in Cognitive Sciences*, *14*(6), 277–290. https://doi.org/10.1016/j.tics.2010.04.004

Buckner, R. L., Andrews-Hanna, J. R., & Schacter, D. L. (2008). The brain's default network. *Annals of the New York Academy of Sciences*, *1124*(1), 1–38. https://doi.org/10.1196/annals.1440.011

Bullmore, E. T., & Bassett, D. S. (2011). Brain graphs: Graphical models of the human brain connectome. *Annual Review of Clinical Psychology*, *7*(1), 113–140. https://doi.org/10.1146/annurev-clinpsy-040510-143934

Chanales, A. J. H., Dudukovic, N. M., Richter, F. R., & Kuhl, B. A. (2019). Interference between overlapping memories is predicted by neural states during learning. *Nature Communications*, *10*(1), 5363. https://doi.org/10.1038/s41467-019-13377-x

Chudasama, Y., Doobay, V. M., & Liu, Y. (2012). Hippocampal-prefrontal cortical circuit mediates inhibitory response control in the rat. *Journal of Neuroscience*, *32*(32), 10915–10924. https://doi.org/10.1523/JNEUROSCI.1463-12.2012

Chun, M. M., Golomb, J. D., & Turk-Browne, N. B. (2011). A taxonomy of external and internal attention. *Annual Review of Psychology*, *62*(1), 73–101. https://doi.org/10.1146/annurev.psych.093008.100427

Chun, M. M., & Johnson, M. K. (2011). Memory: Enduring traces of perceptual and reflective attention. *Neuron*, *72*(4), 520–535. https://doi.org/10.1016/j.neuron.2011.10.026

Cohen, J. R., & D'Esposito, M. (2016). The segregation and integration of distinct brain networks and their relationship to cognition. *Journal of Neuroscience*, *36*(48), 12083–12094. https://doi.org/10.1523/JNEUROSCI.2965-15.2016

Cole, M. W., Bassett, D. S., Power, J. D., Braver, T. S., & Petersen, S. E. (2014). Intrinsic and task-evoked network architectures of the human brain. *Neuron*, *83*(1), 238–251. https://doi.org/10.1016/j.neuron.2014.05.014

Cole, M. W., Etzel, J., Zacks, J., Schneider, W., & Braver, T. (2011). Rapid transfer of abstract rules to novel contexts in human lateral prefrontal cortex. *Frontiers in Human Neuroscience*, *5*. https://www.frontiersin.org/articles/10.3389/fnhum.2011.00142

Cole, M. W., Ito, T., Bassett, D. S., & Schultz, D. H. (2016). Activity flow over resting-state networks shapes cognitive task activations. *Nature Neuroscience*, *19*(12), 1718–1726. https://doi.org/10.1038/nn.4406

Cole, M. W., Ito, T., Cocuzza, C., & Sanchez-Romero, R. (2021). The functional relevance of task-state functional connectivity. *The Journal of Neuroscience*, JN-RM-1713-20. https://doi.org/10.1523/JNEUROSCI.1713-20.2021

Cole, M. W., Ito, T., Schultz, D., Mill, R., Chen, R., & Cocuzza, C. (2019). Task activations produce spurious but systematic inflation of task functional connectivity estimates. *NeuroImage*, *189*, 1–18. https://doi.org/10.1016/j.neuroimage.2018.12.054

Cole, M. W., Laurent, P., & Stocco, A. (2013). Rapid instructed task learning: A new window into the human brain's unique capacity for flexible cognitive control. *Cognitive, Affective & Behavioral Neuroscience*, *13*(1), 1–22. https://doi.org/10.3758/s13415-012-0125-7

Cole, M. W., Reynolds, J. R., Power, J. D., Repovs, G., Anticevic, A., & Braver, T. S. (2013). Multi-task connectivity reveals flexible hubs for adaptive task control. *Nature Neuroscience*, *16*(9), Article 9. https://doi.org/10.1038/nn.3470

Cooper, R. A., & Ritchey, M. (2019). Cortico-hippocampal network connections support the multidimensional quality of episodic memory. *eLife*, *8*, e45591. https://doi.org/10.7554/eLife.45591

Corbetta, M., Kincade, J. M., Ollinger, J. M., McAvoy, M. P., & Shulman, G. L. (2000). Voluntary orienting is dissociated from target detection in human posterior parietal cortex. *Nature Neuroscience*, *3*(3), 292–297. https://doi.org/10.1038/73009

Corbetta, M., & Shulman, G. L. (2002). Control of goal-directed and stimulus-driven attention in the brain. *Nature Reviews Neuroscience*, *3*(3), 201–215. https://doi.org/10.1038/nrn755

Córdova, N. I., Tompary, A., & Turk-Browne, N. B. (2016). Attentional modulation of background connectivity between ventral visual cortex and the medial temporal lobe. *Neurobiology of Learning and Memory*, *134*, 115–122. https://doi.org/10.1016/j.nlm.2016.06.011

Damoiseaux, J. S., Rombouts, S. a. R. B., Barkhof, F., Scheltens, P., Stam, C. J., Smith, S. M., & Beckmann, C. F. (2006). Consistent resting-state networks across healthy subjects. *Proceedings of the National Academy of Sciences of the United States of America*, *103*(37), 13848–13853. https://doi.org/10.1073/pnas.0601417103

Daselaar, S., Prince, S., Dennis, N., Hayes, S., Kim, H., & Cabeza, R. (2009). Posterior midline and ventral parietal activity is associated with retrieval success and encoding failure. *Frontiers in Human Neuroscience*, *3*. https://www.frontiersin.org/articles/10.3389/neuro.09.013.2009

de Bourbon-Teles, J., Bentley, P., Koshino, S., Shah, K., Dutta, A., Malhotra, P., Egner, T., Husain, M., & Soto, D. (2014). Thalamic control of human attention driven by memory and learning. *Current Biology: CB*, *24*(9), 993–999. https://doi.org/10.1016/j.cub.2014.03.024

Desikan, R. S., Ségonne, F., Fischl, B., Quinn, B. T., Dickerson, B. C., Blacker, D., Buckner, R. L., Dale, A. M., Maguire, R. P., Hyman, B. T., Albert, M. S., & Killiany, R. J. (2006). An automated labeling system for subdividing the human cerebral cortex on MRI scans into gyral based regions of interest. *NeuroImage*, *31*(3), 968–980. https://doi.org/10.1016/j.neuroimage.2006.01.021

Desimone, R., & Duncan, J. (1995). Neural Mechanisms of Selective Visual Attention. *Annual Review of Neuroscience*, *18*(Volume 18, 1995), 193–222. https://doi.org/10.1146/annurev.ne.18.030195.001205

Dosenbach, N. U. F., Fair, D. A., Cohen, A. L., Schlaggar, B. L., & Petersen, S. E. (2008). A dual-networks architecture of top-down control. *Trends in Cognitive Sciences*, *12*(3), 99–105. https://doi.org/10.1016/j.tics.2008.01.001

Dosenbach, N. U. F., Visscher, K. M., Palmer, E. D., Miezin, F. M., Wenger, K. K., Kang, H. C., Burgund, E. D., Grimes, A. L., Schlaggar, B. L., & Petersen, S. E. (2006). A core system for the implementation of task sets. *Neuron*, *50*(5), 799–812. https://doi.org/10.1016/j.neuron.2006.04.031

Duncan, J. (2010). The multiple-demand (MD) system of the primate brain: Mental programs for intelligent behaviour. *Trends in Cognitive Sciences*, *14*(4), 172–179. https://doi.org/10.1016/j.tics.2010.01.004

Duncan, K., Sadanand, A., & Davachi, L. (2012). Memory's penumbra: Episodic memory decisions induce lingering mnemonic biases. *Science*, *337*(6093), 485–487. https://doi.org/10.1126/science.1221936

Duncan, K., Tompary, A., & Davachi, L. (2014). Associative encoding and retrieval are predicted by functional connectivity in distinct hippocampal area ca1 pathways. *Journal of Neuroscience*, *34*(34), 11188–11198. https://doi.org/10.1523/JNEUROSCI.0521-14.2014

Esteban, O., Markiewicz, C. J., Blair, R. W., Moodie, C. A., Isik, A. I., Erramuzpe, A., Kent, J. D., Goncalves, M., DuPre, E., Snyder, M., Oya, H., Ghosh, S. S., Wright, J., Durnez, J., Poldrack, R. A., & Gorgolewski, K. J. (2019). fMRIPrep: A robust preprocessing pipeline

for functional MRI. *Nature Methods*, *16*(1), 111–116. https://doi.org/10.1038/s41592-018-0235-4

Ezzyat, Y., Kragel, J. E., Burke, J. F., Levy, D. F., Lyalenko, A., Wanda, P., O'Sullivan, L., Hurley, K. B., Busygin, S., Pedisich, I., Sperling, M. R., Worrell, G. A., Kucewicz, M. T., Davis, K. A., Lucas, T. H., Inman, C. S., Lega, B. C., Jobst, B. C., Sheth, S. A., … Kahana, M. J. (2017). Direct brain stimulation modulates encoding states and memory performance in humans. *Current Biology*, *27*(9), 1251–1258. https://doi.org/10.1016/j.cub.2017.03.028

Fair, D. A., Schlaggar, B. L., Cohen, A. L., Miezin, F. M., Dosenbach, N. U. F., Wenger, K. K., Fox, M. D., Snyder, A. Z., Raichle, M. E., & Petersen, S. E. (2007). A method for using blocked and event-related fMRI data to study "resting state" functional connectivity. *NeuroImage*, *35*(1), 396–405. https://doi.org/10.1016/j.neuroimage.2006.11.051

Favila, S. E., Kuhl, B. A., & Winawer, J. (2022). Perception and memory have distinct spatial tuning properties in human visual cortex. *Nature Communications*, *13*(1), Article 1. https://doi.org/10.1038/s41467-022-33161-8

Favila, S. E., Lee, H., & Kuhl, B. A. (2020). Transforming the concept of memory reactivation. *Trends in Neurosciences*, *43*(12), 939–950. https://doi.org/10.1016/j.tins.2020.09.006

Favila, S. E., Samide, R., Sweigart, S. C., & Kuhl, B. A. (2018). Parietal representations of stimulus features are amplified during memory retrieval and flexibly aligned with top-down goals. *The Journal of Neuroscience*, *38*(36), 7809–7821. https://doi.org/10.1523/JNEUROSCI.0564-18.2018

Feilong, M., Guntupalli, J. S., & Haxby, J. V. (2021). The neural basis of intelligence in fine-grained cortical topographies. *eLife*, *10*, e64058. https://doi.org/10.7554/eLife.64058

Felleman, D. J., & Van Essen, D. C. (1991). Distributed hierarchical processing in the primate cerebral cortex. *Cerebral Cortex*, *1*(1), 1–47. https://doi.org/10.1093/cercor/1.1.1

Fernandez, C., Madore, K. P., & Wagner, A. D. (2022). *Encoding and the medial temporal lobe. to appear in: Oxford handbook of human memory (m. j. kahana & a. d. wagner, eds). oxford university press.* PsyArXiv. https://doi.org/10.31234/osf.io/za6gw

Finc, K., Bonna, K., He, X., Lydon-Staley, D. M., Kühn, S., Duch, W., & Bassett, D. S. (2020). Dynamic reconfiguration of functional brain networks during working memory training. *Nature Communications*, *11*(1), 2435. https://doi.org/10.1038/s41467-020-15631-z

Finn, E. S., Shen, X., Scheinost, D., Rosenberg, M. D., Huang, J., Chun, M. M., Papademetris, X., & Constable, R. T. (2015). Functional connectome fingerprinting: Identifying individuals using patterns of brain connectivity. *Nature Neuroscience*, *18*(11), Article 11. https://doi.org/10.1038/nn.4135

Fong, A. H. C., Yoo, K., Rosenberg, M. D., Zhang, S., Li, C.-S. R., Scheinost, D., Constable, R. T., & Chun, M. M. (2019). Dynamic functional connectivity during task performance and rest predicts individual differences in attention across studies. *NeuroImage*, *188*, 14–25. https://doi.org/10.1016/j.neuroimage.2018.11.057

Fornito, A., Harrison, B. J., Zalesky, A., & Simons, J. S. (2012). Competitive and cooperative dynamics of large-scale brain functional networks supporting recollection. *Proceedings of the National Academy of Sciences*, *109*(31), 12788–12793. https://doi.org/10.1073/pnas.1204185109

Fornito, A., Zalesky, A., & Breakspear, M. (2013). Graph analysis of the human connectome: Promise, progress, and pitfalls. *NeuroImage*, *80*, 426–444. https://doi.org/10.1016/j.neuroimage.2013.04.087

Fox, M. D., & Raichle, M. E. (2007). Spontaneous fluctuations in brain activity observed with functional magnetic resonance imaging. *Nature Reviews Neuroscience*, *8*(9), 700–711. https://doi.org/10.1038/nrn2201

Frank, L. E., Preston, A. R., & Zeithamova, D. (2019). Functional connectivity between memory and reward centers across task and rest track memory sensitivity to reward. *Cognitive, Affective & Behavioral Neuroscience*, *19*(3), 503–522. https://doi.org/10.3758/s13415-019-00700-8

Frank, L. E., & Zeithamova, D. (2023). Evaluating methods for measuring background connectivity in slow event-related functional magnetic resonance imaging designs. *Brain and Behavior*, *13*(6), e3015. https://doi.org/10.1002/brb3.3015

Friston, K. J. (1994). Functional and effective connectivity in neuroimaging: A synthesis. *Human Brain Mapping*, *2*(1–2), 56–78. https://doi.org/10.1002/hbm.460020107

Fritch, H. A., Spets, D. S., & Slotnick, S. D. (2021). Functional connectivity with the anterior and posterior hippocampus during spatial memory. *Hippocampus*, *31*(7), 658–668. https://doi.org/10.1002/hipo.23283

Fruchterman, T. M. J., & Reingold, E. M. (1991). Graph drawing by force-directed placement. *Software: Practice and Experience*, *21*(11), 1129–1164. https://doi.org/10.1002/spe.4380211102

Geib, B. R., Stanley, M. L., Dennis, N. A., Woldorff, M. G., & Cabeza, R. (2017). From hippocampus to whole-brain: The role of integrative processing in episodic memory retrieval. *Human Brain Mapping*, *38*(4), 2242–2259. https://doi.org/10.1002/hbm.23518

Gilmore, A. W., Nelson, S. M., & McDermott, K. B. (2016). The contextual association network activates more for remembered than for imagined events. *Cerebral Cortex*, *26*(2), 611–617. https://doi.org/10.1093/cercor/bhu223

Golland, Y., Bentin, S., Gelbard, H., Benjamini, Y., Heller, R., Nir, Y., Hasson, U., & Malach, R. (2007). Extrinsic and Intrinsic Systems in the Posterior Cortex of the Human Brain Revealed during Natural Sensory Stimulation. *Cerebral Cortex*, *17*(4), 766–777. https://doi.org/10.1093/cercor/bhk030

Golland, Y., Golland, P., Bentin, S., & Malach, R. (2008). Data-driven clustering reveals a fundamental subdivision of the human cortex into two global systems. *Neuropsychologia*, *46*(2), 540–553. https://doi.org/10.1016/j.neuropsychologia.2007.10.003

Gonzalez-Castillo, J., Hoy, C. W., Handwerker, D. A., Robinson, M. E., Buchanan, L. C., Saad, Z. S., & Bandettini, P. A. (2015). Tracking ongoing cognition in individuals using brief, whole-brain functional connectivity patterns. *Proceedings of the National Academy of Sciences*, *112*(28), 8762–8767. https://doi.org/10.1073/pnas.1501242112

Gordon, E. M., Laumann, T. O., Adeyemo, B., Huckins, J. F., Kelley, W. M., & Petersen, S. E. (2016). Generation and Evaluation of a Cortical Area Parcellation from Resting-State Correlations. *Cerebral Cortex (New York, N.Y.: 1991)*, *26*(1), 288–303. https://doi.org/10.1093/cercor/bhu239

Gordon, E. M., Lynch, C. J., Gratton, C., Laumann, T. O., Gilmore, A. W., Greene, D. J., Ortega, M., Nguyen, A. L., Schlaggar, B. L., Petersen, S. E., Dosenbach, N. U. F., & Nelson, S. M. (2018). Three distinct sets of connector hubs integrate human brain function. *Cell Reports*, *24*(7), 1687-1695.e4. https://doi.org/10.1016/j.celrep.2018.07.050

Gorgolewski, K., Burns, C. D., Madison, C., Clark, D., Halchenko, Y. O., Waskom, M. L., & Ghosh, S. S. (2011). Nipype: A flexible, lightweight and extensible neuroimaging data processing framework in python. *Frontiers in Neuroinformatics*, *5*. https://doi.org/10.3389/fninf.2011.00013

Gratton, C., Laumann, T. O., Nielsen, A. N., Greene, D. J., Gordon, E. M., Gilmore, A. W., Nelson, S. M., Coalson, R. S., Snyder, A. Z., Schlaggar, B. L., Dosenbach, N. U. F., & Petersen, S. E. (2018). Functional brain networks are dominated by stable group and individual factors, not cognitive or daily variation. *Neuron*, *98*(2), 439-452.e5. https://doi.org/10.1016/j.neuron.2018.03.035

Gratton, C., Sun, H., & Petersen, S. E. (2018). Control networks and hubs. *Psychophysiology*, *55*(3). https://doi.org/10.1111/psyp.13032

Greene, A. S., Gao, S., Scheinost, D., & Constable, R. T. (2018). Task-induced brain state manipulation improves prediction of individual traits. *Nature Communications*, *9*(1), 2807. https://doi.org/10.1038/s41467-018-04920-3

Gruber, M. J., & Otten, L. J. (2010). Voluntary control over prestimulus activity related to encoding. *Journal of Neuroscience*, *30*(29), 9793–9800. https://doi.org/10.1523/JNEUROSCI.0915-10.2010

Gruber, M. J., Ritchey, M., Wang, S.-F., Doss, M. K., & Ranganath, C. (2016). Post-learning hippocampal dynamics promote preferential retention of rewarding events. *Neuron*, *89*(5), 1110–1120. https://doi.org/10.1016/j.neuron.2016.01.017

Guderian, S., Schott, B. H., Richardson-Klavehn, A., & Düzel, E. (2009). Medial temporal theta state before an event predicts episodic encoding success in humans. *Proceedings of the National Academy of Sciences*, *106*(13), 5365–5370. https://doi.org/10.1073/pnas.0900289106

Hanley, J. A., & McNeil, B. J. (1982). The meaning and use of the area under a receiver operating characteristic (ROC) curve. *Radiology*, *143*(1), 29–36. https://doi.org/10.1148/radiology.143.1.7063747

Hanslmayr, S., Staresina, B. P., & Bowman, H. (2016). Oscillations and episodic memory: Addressing the synchronization/desynchronization conundrum. *Trends in Neurosciences*, *39*(1), 16–25. https://doi.org/10.1016/j.tins.2015.11.004

Hanslmayr, S., Volberg, G., Wimber, M., Dalal, S. S., & Greenlee, M. W. (2013). Prestimulus oscillatory phase at 7 Hz gates cortical information flow and visual perception. *Current Biology: CB*, *23*(22), 2273–2278. https://doi.org/10.1016/j.cub.2013.09.020

Hasselmo, M. E., Wyble, B. P., & Wallenstein, G. V. (1996). Encoding and retrieval of episodic memories: Role of cholinergic and GABAergic modulation in the hippocampus. *Hippocampus*, *6*(6), 693–708. https://doi.org/10.1002/(SICI)1098-1063(1996)6:6<693::AID-HIPO12>3.0.CO;2-W

Haxby, James. V. (2012). Multivariate pattern analysis of fMRI: The early beginnings. *Neuroimage*, *62*(2), 852–855. https://doi.org/10.1016/j.neuroimage.2012.03.016

Honey, C. J., Newman, E. L., & Schapiro, A. C. (2017). Switching between internal and external modes: A multiscale learning principle. *Network Neuroscience*, *1*(4), 339–356. https://doi.org/10.1162/NETN_a_00024

Hopfinger, J. B., Buonocore, M. H., & Mangun, G. R. (2000). The neural mechanisms of top-down attentional control. *Nature Neuroscience*, *3*(3), Article 3. https://doi.org/10.1038/72999

Huijbers, W., Schultz, A. P., Vannini, P., McLaren, D. G., Wigman, S. E., Ward, A. M., Hedden, T., & Sperling, R. A. (2013). The encoding/retrieval flip: Interactions between memory performance and memory stage and relationship to intrinsic cortical networks. *Journal of Cognitive Neuroscience*, *25*(7), 1163–1179. https://doi.org/10.1162/jocn_a_00366

Huijbers, W., Vannini, P., Sperling, R., Pennartz, C., Cabeza, R., & Daselaar, S. (2012). Explaining the encoding/retrieval flip: Memory-related deactivations and activations in the posteromedial cortex. *Neuropsychologia*, *50*(14),

10.1016/j.neuropsychologia.2012.08.021. https://doi.org/10.1016/j.neuropsychologia.2012.08.021

Hutchinson, J. B., Uncapher, M. R., Weiner, K. S., Bressler, D. W., Silver, M. A., Preston, A. R., & Wagner, A. D. (2014). Functional heterogeneity in posterior parietal cortex across attention and episodic memory retrieval. *Cerebral Cortex*, *24*(1), 49–66. https://doi.org/10.1093/cercor/bhs278

Hwang, K., Bertolero, M. A., Liu, W. B., & D'Esposito, M. (2017). The human thalamus is an integrative hub for functional brain networks. *The Journal of Neuroscience*, *37*(23), 5594–5607. https://doi.org/10.1523/JNEUROSCI.0067-17.2017

James, G., Witten, D., Hastie, T., & Tibshirani, R. (2013). *An introduction to statistical learning* (Vol. 103). Springer New York. https://doi.org/10.1007/978-1-4614-7138-7

Jayachandran, M., Linley, S. B., Schlecht, M., Mahler, S. V., Vertes, R. P., & Allen, T. A. (2019). Prefrontal pathways provide top-down control of memory for sequences of events. *Cell Reports*, *28*(3), 640-654.e6. https://doi.org/10.1016/j.celrep.2019.06.053

Ji, J. L., Spronk, M., Kulkarni, K., Repovš, G., Anticevic, A., & Cole, M. W. (2019). Mapping the human brain's cortical-subcortical functional network organization. *NeuroImage*, *185*, 35–57. https://doi.org/10.1016/j.neuroimage.2018.10.006

Kahana, M. J. (2006). The cognitive correlates of human brain oscillations. *Journal of Neuroscience*, *26*(6), 1669–1672. https://doi.org/10.1523/JNEUROSCI.3737-05c.2006

Kanwisher, N. (2010). Functional specificity in the human brain: A window into the functional architecture of the mind. *Proceedings of the National Academy of Sciences*, *107*(25), 11163–11170. https://doi.org/10.1073/pnas.1005062107

Kastner, S., Pinsk, M. A., De Weerd, P., Desimone, R., & Ungerleider, L. G. (1999). Increased activity in human visual cortex during directed attention in the absence of visual stimulation. *Neuron*, *22*(4), 751–761. https://doi.org/10.1016/S0896-6273(00)80734-5

Kim, D.-Y., Yoo, S.-S., Tegethoff, M., Meinlschmidt, G., & Lee, J.-H. (2015). The inclusion of functional connectivity information into fMRI-based neurofeedback improves its efficacy in the reduction of cigarette cravings. *Journal of Cognitive Neuroscience*, *27*(8), 1552–1572. https://doi.org/10.1162/jocn_a_00802

Kim, H. (2013). Differential neural activity in the recognition of old versus new events: An activation likelihood estimation meta-analysis. *Human Brain Mapping*, *34*(4), 814–836. https://doi.org/10.1002/hbm.21474

Kim, H. (2015). Encoding and retrieval along the long axis of the hippocampus and their relationships with dorsal attention and default mode networks: The HERNET model. *Hippocampus*, *25*(4), 500–510. https://doi.org/10.1002/hipo.22387

Kim, J., & Horwitz, B. (2008). Investigating the neural basis for fMRI-based functional connectivity in a blocked design: Application to interregional correlations and psycho-physiological interactions. *Magnetic Resonance Imaging*, *26*(5), 583–593. https://doi.org/10.1016/j.mri.2007.10.011

King, D. R., Chastelaine, M. de, Elward, R. L., Wang, T. H., & Rugg, M. D. (2015). Recollection-related increases in functional connectivity predict individual differences in memory accuracy. *Journal of Neuroscience*, *35*(4), 1763–1772. https://doi.org/10.1523/JNEUROSCI.3219-14.2015

Kompus, K., Eichele, T., Hugdahl, K., & Nyberg, L. (2011). Multimodal imaging of incidental retrieval: The low route to memory. *Journal of Cognitive Neuroscience*, *23*(4), 947–960. https://doi.org/10.1162/jocn.2010.21494

Konkle, T., Brady, T. F., Alvarez, G. A., & Oliva, A. (2010). Scene memory is more detailed than you think: The role of categories in visual long-term memory. *Psychological Science*, *21*(11), 1551–1556. https://doi.org/10.1177/0956797610385359

Kosslyn, S. M., Thompson, W. L., Klm, I. J., & Alpert, N. M. (1995). Topographical representations of mental images in primary visual cortex. *Nature*, *378*(6556), Article 6556. https://doi.org/10.1038/378496a0

Krienen, F. M., Yeo, B. T. T., & Buckner, R. L. (2014). Reconfigurable task-dependent functional coupling modes cluster around a core functional architecture. *Philosophical Transactions of the Royal Society of London. Series B, Biological Sciences*, *369*(1653), 20130526. https://doi.org/10.1098/rstb.2013.0526

Kumar, M., Anderson, M. J., Antony, J. W., Baldassano, C., Brooks, P. P., Cai, M. B., Chen, P.-H. C., Ellis, C. T., Henselman-Petrusek, G., Huberdeau, D., Hutchinson, J. B., Li, Y. P., Lu, Q., Manning, J. R., Mennen, A. C., Nastase, S. A., Richard, H., Schapiro, A. C., Schuck, N. W., … Norman, K. A. (2022). Brainiak: The brain imaging analysis kit. *Aperture Neuro*, *2021*(4), 42. https://doi.org/10.52294/31bb5b68-2184-411b-8c00-a1dacb61e1da

LaBar, K. S., & Cabeza, R. (2006). Cognitive neuroscience of emotional memory. *Nature Reviews Neuroscience*, *7*(1), Article 1. https://doi.org/10.1038/nrn1825

Lee, H., & Kuhl, B. A. (2016). Reconstructing perceived and retrieved faces from activity patterns in lateral parietal cortex. *Journal of Neuroscience*, *36*(22), 6069–6082. https://doi.org/10.1523/JNEUROSCI.4286-15.2016

Lepsien, J., & Nobre, A. C. (2006). Cognitive control of attention in the human brain: Insights from orienting attention to mental representations. *Brain Research*, *1105*(1), 20–31. https://doi.org/10.1016/j.brainres.2006.03.033

Li, Y. P., Cooper, S. R., & Braver, T. S. (2021). The role of neural load effects in predicting individual differences in working memory function. *NeuroImage*, *245*, 118656. https://doi.org/10.1016/j.neuroimage.2021.118656

Li, Y. P., Wang, Y., Turk-Browne, N. B., Kuhl, B. A., & Hutchinson, J. B. (2023). Perception and memory retrieval states are reflected in distributed patterns of background functional connectivity. *NeuroImage*, *276*, 120221. https://doi.org/10.1016/j.neuroimage.2023.120221

Long, N. M., & Kuhl, B. A. (2018). Bottom-Up and Top-Down Factors Differentially Influence Stimulus Representations Across Large-Scale Attentional Networks. *The Journal of Neuroscience*, *38*(10), 2495–2504. https://doi.org/10.1523/JNEUROSCI.2724-17.2018

Long, N. M., & Kuhl, B. A. (2019). Decoding the tradeoff between encoding and retrieval to predict memory for overlapping events. *NeuroImage*, *201*, 116001. https://doi.org/10.1016/j.neuroimage.2019.07.014

Long, N. M., & Kuhl, B. A. (2021). Cortical representations of visual stimuli shift locations with changes in memory states. *Current Biology: CB*. https://doi.org/10.1016/j.cub.2021.01.004

Manning, J. R., Zhu, X., Willke, T. L., Ranganath, R., Stachenfeld, K., Hasson, U., Blei, D. M., & Norman, K. A. (2018). A probabilistic approach to discovering dynamic full-brain functional connectivity patterns. *NeuroImage*, *180*, 243–252. https://doi.org/10.1016/j.neuroimage.2018.01.071

Marek, S., & Dosenbach, N. U. F. (2018). The frontoparietal network: Function, electrophysiology, and importance of individual precision mapping. *Dialogues in Clinical Neuroscience*, *20*(2), 133–140.

McClelland, J. L., McNaughton, B. L., & O'Reilly, R. C. (1995). Why there are complementary learning systems in the hippocampus and neocortex: Insights from the successes and failures of connectionist models of learning and memory. *Psychological Review*, *102*(3), 419–457. https://doi.org/10.1037/0033-295X.102.3.419

McCormick, E. M., Arnemann, K. L., Ito, T., Hanson, S. J., & Cole, M. W. (2022). Latent functional connectivity underlying multiple brain states. *Network Neuroscience (Cambridge, Mass.)*, *6*(2), 570–590. https://doi.org/10.1162/netn_a_00234

McLaren, D. G., Ries, M. L., Xu, G., & Johnson, S. C. (2012). A generalized form of context-dependent psychophysiological interactions (gPPI): A comparison to standard approaches. *NeuroImage*, *61*(4), 1277–1286. https://doi.org/10.1016/j.neuroimage.2012.03.068

Mesulam, M. (1990). Large-scale neurocognitive networks and distributed processing for attention, language, and memory. *Annals of Neurology*, *28*(5), 597–613. https://doi.org/10.1002/ana.410280502

Miller, E. K., & Cohen, J. D. (2001). An integrative theory of prefrontal cortex function. *Annual Review of Neuroscience*, *24*(1), 167–202. https://doi.org/10.1146/annurev.neuro.24.1.167

Murty, V. P., Tompary, A., Adcock, R. A., & Davachi, L. (2017). Selectivity in postencoding connectivity with high-level visual cortex is associated with reward-motivated memory. *Journal of Neuroscience*, *37*(3), 537–545. https://doi.org/10.1523/JNEUROSCI.4032-15.2016

Nakajima, M., & Halassa, M. M. (2017). Thalamic control of functional cortical connectivity. *Current Opinion in Neurobiology*, *44*, 127–131. https://doi.org/10.1016/j.conb.2017.04.001

Norman, K. A. (2010). How hippocampus and cortex contribute to recognition memory: Revisiting the Complementary Learning Systems model. *Hippocampus*, *20*(11), 1217–1227. https://doi.org/10.1002/hipo.20855

Norman, K. A., Polyn, S. M., Detre, G. J., & Haxby, J. V. (2006). Beyond mind-reading: Multi-voxel pattern analysis of fMRI data. *Trends in Cognitive Sciences*, *10*(9), 424–430. https://doi.org/10.1016/j.tics.2006.07.005

Norman-Haignere, S. V., McCarthy, G., Chun, M. M., & Turk-Browne, N. B. (2012). Category-selective background connectivity in ventral visual cortex. *Cerebral Cortex*, *22*(2), 391–402. https://doi.org/10.1093/cercor/bhr118

Nyhus, E., & Curran, T. (2010). Functional role of gamma and theta oscillations in episodic memory. *Neuroscience & Biobehavioral Reviews*, *34*(7), 1023–1035. https://doi.org/10.1016/j.neubiorev.2009.12.014

Oppenheim, A. V., & Lim, J. S. (1981). The importance of phase in signals. *Proceedings of the IEEE*, *69*(5), 529–541. https://doi.org/10.1109/PROC.1981.12022

O'Reilly, R. C., & McClelland, J. L. (1994). Hippocampal conjunctive encoding, storage, and recall: Avoiding a trade-off. *Hippocampus*, *4*(6), 661–682. https://doi.org/10.1002/hipo.450040605

Otten, L. J., Henson, R. N. A., & Rugg, M. D. (2002). State-related and item-related neural correlates of successful memory encoding. *Nature Neuroscience*, *5*(12), Article 12. https://doi.org/10.1038/nn967

Pantazatos, S. P., Talati, A., Pavlidis, P., & Hirsch, J. (2012). Decoding unattended fearful faces with whole-brain correlations: An approach to identify condition-dependent large-scale

functional connectivity. *PLOS Computational Biology*, *8*(3), e1002441. https://doi.org/10.1371/journal.pcbi.1002441

Parasuraman, R. (2000). *The Attentive Brain*. MIT Press.

Pedregosa, F., Varoquaux, G., Gramfort, A., Michel, V., Thirion, B., Grisel, O., Blondel, M., Prettenhofer, P., Weiss, R., Dubourg, V., Vanderplas, J., Passos, A., Cournapeau, D., Brucher, M., Perrot, M., & Duchesnay, É. (2011). Scikit-learn: Machine learning in python. *Journal of Machine Learning Research*, *12*(85), 2825–2830.

Petersen, S. E., & Posner, M. I. (2012). The attention system of the human brain: 20 years after. *Annual Review of Neuroscience*, *35*, 73–89. https://doi.org/10.1146/annurev-neuro-062111-150525

Ploner, M., Lee, M. C., Wiech, K., Bingel, U., & Tracey, I. (2010). Prestimulus functional connectivity determines pain perception in humans. *Proceedings of the National Academy of Sciences of the United States of America*, *107*(1), 355–360. https://doi.org/10.1073/pnas.0906186106

Polyn, S. M., Natu, V. S., Cohen, J. D., & Norman, K. A. (2005). Category-specific cortical activity precedes retrieval during memory search. *Science (New York, N.Y.)*, *310*(5756), 1963–1966. https://doi.org/10.1126/science.1117645

Poskanzer, C., & Aly, M. (2022). *Switching between external and internal attention in hippocampal networks* (p. 2022.12.20.521285). bioRxiv. https://doi.org/10.1101/2022.12.20.521285

Poskanzer, C., & Aly, M. (2023). Switching between External and Internal Attention in Hippocampal Networks. *Journal of Neuroscience*, *43*(38), 6538–6552. https://doi.org/10.1523/JNEUROSCI.0029-23.2023

Posner, M. I., & Petersen, S. E. (1990). The attention system of the human brain. *Annual Review of Neuroscience*, *13*(1), 25–42. https://doi.org/10.1146/annurev.ne.13.030190.000325

Posner, M. I., & Snyder, C. R. R. (1975). Attention and cognitive control. In R. L. Solso (Ed.), *Information Processing and Cognition: The Loyola Symposium*. Lawrence Erlbaum.

Power, J. D., Cohen, A. L., Nelson, S. M., Wig, G. S., Barnes, K. A., Church, J. A., Vogel, A. C., Laumann, T. O., Miezin, F. M., Schlaggar, B. L., & Petersen, S. E. (2011). Functional network organization of the human brain. *Neuron*, *72*(4), 665–678. https://doi.org/10.1016/j.neuron.2011.09.006

Preti, M. G., Bolton, T. A., & Van De Ville, D. (2017). The dynamic functional connectome: State-of-the-art and perspectives. *NeuroImage*, *160*, 41–54. https://doi.org/10.1016/j.neuroimage.2016.12.061

Ranganath, C., & Ritchey, M. (2012). Two cortical systems for memory-guided behaviour. *Nature Reviews Neuroscience*, *13*(10), Article 10. https://doi.org/10.1038/nrn3338

Reddy, L., Kanwisher, N. G., & VanRullen, R. (2009). Attention and biased competition in multi-voxel object representations. *Proceedings of the National Academy of Sciences*, *106*(50), 21447–21452. https://doi.org/10.1073/pnas.0907330106

Reverberi, C., Görgen, K., & Haynes, J.-D. (2012). Compositionality of rule representations in human prefrontal cortex. *Cerebral Cortex (New York, N.Y.: 1991)*, *22*(6), 1237–1246. https://doi.org/10.1093/cercor/bhr200

Richiardi, J., Eryilmaz, H., Schwartz, S., Vuilleumier, P., & Van De Ville, D. (2011). Decoding brain states from fMRI connectivity graphs. *NeuroImage*, *56*(2), 616–626. https://doi.org/10.1016/j.neuroimage.2010.05.081

Ritchey, M., & Cooper, R. A. (2020). Deconstructing the posterior medial episodic network. *Trends in Cognitive Sciences*, *24*(6), 451–465. https://doi.org/10.1016/j.tics.2020.03.006

Rolls, E. (2013). The mechanisms for pattern completion and pattern separation in the hippocampus. *Frontiers in Systems Neuroscience*, *7*. https://doi.org/10.3389/fnsys.2013.00074

Rosen, M. L., Stern, C. E., Devaney, K. J., & Somers, D. C. (2018). Cortical and subcortical contributions to long-term memory-guided visuospatial attention. *Cerebral Cortex*, *28*(8), 2935–2947. https://doi.org/10.1093/cercor/bhx172

Rosen, M. L., Stern, C. E., Michalka, S. W., Devaney, K. J., & Somers, D. C. (2016). Cognitive control network contributions to memory-guided visual attention. *Cerebral Cortex*, *26*(5), 2059–2073. https://doi.org/10.1093/cercor/bhv028

Rosenberg, M. D., Finn, E. S., Scheinost, D., Papademetris, X., Shen, X., Constable, R. T., & Chun, M. M. (2016). A neuromarker of sustained attention from whole-brain functional connectivity. *Nature Neuroscience*, *19*(1), Article 1. https://doi.org/10.1038/nn.4179

Rosenberg, M. D., Scheinost, D., Greene, A. S., Avery, E. W., Kwon, Y. H., Finn, E. S., Ramani, R., Qiu, M., Constable, R. T., & Chun, M. M. (2020). Functional connectivity predicts changes in attention observed across minutes, days, and months. *Proceedings of the National Academy of Sciences*, *117*(7), 3797–3807. https://doi.org/10.1073/pnas.1912226117

Rubinov, M., & Sporns, O. (2011). Weight-conserving characterization of complex functional brain networks. *NeuroImage*, *56*(4), 2068–2079. https://doi.org/10.1016/j.neuroimage.2011.03.069

Rugg, M. D., & Vilberg, K. L. (2013). Brain networks underlying episodic memory retrieval. *Current Opinion in Neurobiology*, *23*(2), 255–260. https://doi.org/10.1016/j.conb.2012.11.005

Sadaghiani, S., Poline, J.-B., Kleinschmidt, A., & D'Esposito, M. (2015). Ongoing dynamics in large-scale functional connectivity predict perception. *Proceedings of the National Academy of Sciences*, *112*(27), 8463–8468. https://doi.org/10.1073/pnas.1420687112

Santangelo, V. (2018). Large-Scale Brain Networks Supporting Divided Attention across Spatial Locations and Sensory Modalities. *Frontiers in Integrative Neuroscience*, *12*. https://www.frontiersin.org/articles/10.3389/fnint.2018.00008

Schaefer, A., Kong, R., Gordon, E. M., Laumann, T. O., Zuo, X.-N., Holmes, A. J., Eickhoff, S. B., & Yeo, B. T. T. (2018). Local-global parcellation of the human cerebral cortex from intrinsic functional connectivity mri. *Cerebral Cortex*, *28*(9), 3095–3114. https://doi.org/10.1093/cercor/bhx179

Shehzad, Z., Kelly, A. M. C., Reiss, P. T., Gee, D. G., Gotimer, K., Uddin, L. Q., Lee, S. H., Margulies, D. S., Roy, A. K., Biswal, B. B., Petkova, E., Castellanos, F. X., & Milham, M. P. (2009). The resting brain: Unconstrained yet reliable. *Cerebral Cortex (New York, N.Y.: 1991)*, *19*(10), 2209–2229. https://doi.org/10.1093/cercor/bhn256

Shen, X., Finn, E. S., Scheinost, D., Rosenberg, M. D., Chun, M. M., Papademetris, X., & Constable, R. T. (2017). Using connectome-based predictive modeling to predict individual behavior from brain connectivity. *Nature Protocols*, *12*(3), 506–518. https://doi.org/10.1038/nprot.2016.178

Shen, X., Tokoglu, F., Papademetris, X., & Constable, R. T. (2013). Groupwise whole-brain parcellation from resting-state fMRI data for network node identification. *NeuroImage*, *0*, 403–415. https://doi.org/10.1016/j.neuroimage.2013.05.081

Shirer, W. R., Ryali, S., Rykhlevskaia, E., Menon, V., & Greicius, M. D. (2012). Decoding subject-driven cognitive states with whole-brain connectivity patterns. *Cerebral Cortex*, *22*(1), 158–165. https://doi.org/10.1093/cercor/bhr099

Smith, S. M. (2012). The future of FMRI connectivity. *NeuroImage*, *62*(2), 1257–1266. https://doi.org/10.1016/j.neuroimage.2012.01.022

Song, H., Finn, E. S., & Rosenberg, M. D. (2021). Neural signatures of attentional engagement during narratives and its consequences for event memory. *Proceedings of the National Academy of Sciences*, *118*(33). https://doi.org/10.1073/pnas.2021905118

Song, H., & Rosenberg, M. D. (2021). Predicting attention across time and contexts with functional brain connectivity. *Current Opinion in Behavioral Sciences*, *40*, 33–44. https://doi.org/10.1016/j.cobeha.2020.12.007

Stojanoski, B., & Cusack, R. (2014). Time to wave good-bye to phase scrambling: Creating controlled scrambled images using diffeomorphic transformations. *Journal of Vision*, *14*(12), 6. https://doi.org/10.1167/14.12.6

Stokes, M. G., Buschman, T. J., & Miller, E. K. (2017). Dynamic coding for flexible cognitive control. In *The Wiley Handbook of Cognitive Control* (pp. 221–241). John Wiley & Sons, Ltd. https://doi.org/10.1002/9781118920497.ch13

Summerfield, C., Greene, M., Wager, T., Egner, T., Hirsch, J., & Mangels, J. (2006). Neocortical connectivity during episodic memory formation. *PLOS Biology*, *4*(5), e128. https://doi.org/10.1371/journal.pbio.0040128

Tambini, A., Ketz, N., & Davachi, L. (2010). Enhanced brain correlations during rest are related to memory for recent experiences. *Neuron*, *65*(2), 280–290. https://doi.org/10.1016/j.neuron.2010.01.001

Tambini, A., Rimmele, U., Phelps, E. A., & Davachi, L. (2017). Emotional brain states carry over and enhance future memory formation. *Nature Neuroscience*, *20*(2), 271–278. https://doi.org/10.1038/nn.4468

Theyel, B. B., Llano, D. A., & Sherman, S. M. (2010). The corticothalamocortical circuit drives higher-order cortex in the mouse. *Nature Neuroscience*, *13*(1), 84–88. https://doi.org/10.1038/nn.2449

Thomaz, C. E., & Giraldi, G. A. (2010). A new ranking method for principal components analysis and its application to face image analysis. *Image and Vision Computing*, *28*(6), 902–913. https://doi.org/10.1016/j.imavis.2009.11.005

Tompary, A., Al-Aidroos, N., & Turk-Browne, N. B. (2018). Attending to what and where: Background connectivity integrates categorical and spatial attention. *Journal of Cognitive Neuroscience*, *30*(9), 1281–1297. https://doi.org/10.1162/jocn_a_01284

Tompary, A., Duncan, K., & Davachi, L. (2015). Consolidation of Associative and Item Memory Is Related to Post-Encoding Functional Connectivity between the Ventral Tegmental Area and Different Medial Temporal Lobe Subregions during an Unrelated Task. *Journal of Neuroscience*, *35*(19), 7326–7331. https://doi.org/10.1523/JNEUROSCI.4816-14.2015

Turk-Browne, N. B. (2013). Functional interactions as big data in the human brain. *Science*, *342*(6158), 580–584. https://doi.org/10.1126/science.1238409

Turk-Browne, N. B., Norman-Haignere, S. V., & McCarthy, G. (2010). Face-Specific Resting Functional Connectivity between the Fusiform Gyrus and Posterior Superior Temporal Sulcus. *Frontiers in Human Neuroscience*, *4*, 176. https://doi.org/10.3389/fnhum.2010.00176

Van Dijk, K. R. A., Hedden, T., Venkataraman, A., Evans, K. C., Lazar, S. W., & Buckner, R. L. (2010). Intrinsic functional connectivity as a tool for human connectomics: Theory, properties, and optimization. *Journal of Neurophysiology*, *103*(1), 297–321. https://doi.org/10.1152/jn.00783.2009

Verschooren, S., Schindler, S., De Raedt, R., & Pourtois, G. (2019). Switching attention from internal to external information processing: A review of the literature and empirical support of the resource sharing account. *Psychonomic Bulletin & Review*, *26*(2), 468–490. https://doi.org/10.3758/s13423-019-01568-y

Wang, Y., Cohen, J. D., Li, K., & Turk-Browne, N. B. (2015). Full correlation matrix analysis (FCMA): An unbiased method for task-related functional connectivity. *Journal of Neuroscience Methods*, *251*, 108–119. https://doi.org/10.1016/j.jneumeth.2015.05.012

Watanabe, T., Kimura, H. M., Hirose, S., Wada, H., Imai, Y., Machida, T., Shirouzu, I., Miyashita, Y., & Konishi, S. (2012). Functional dissociation between anterior and posterior temporal cortical regions during retrieval of remote memory. *The Journal of Neuroscience: The Official Journal of the Society for Neuroscience*, *32*(28), 9659–9670. https://doi.org/10.1523/JNEUROSCI.5553-11.2012

Weel, M. J. D. der, Griffin, A. L., Ito, H. T., Shapiro, M. L., Witter, M. P., Vertes, R. P., & Allen, T. A. (2019). The nucleus reuniens of the thalamus sits at the nexus of a hippocampus and medial prefrontal cortex circuit enabling memory and behavior. *Learning & Memory*, *26*(7), 191–205. https://doi.org/10.1101/lm.048389.118

Wheeler, M. E., Petersen, S. E., & Buckner, R. L. (2000). Memory's echo: Vivid remembering reactivates sensory-specific cortex. *Proceedings of the National Academy of Sciences*, *97*(20), 11125–11129. https://doi.org/10.1073/pnas.97.20.11125

Woolrich, M. W., Ripley, B. D., Brady, M., & Smith, S. M. (2001). Temporal autocorrelation in univariate linear modeling of fmri data. *NeuroImage*, *14*(6), 1370–1386. https://doi.org/10.1006/nimg.2001.0931

Yeo, B. T. T., Krienen, F. M., Sepulcre, J., Sabuncu, M. R., Lashkari, D., Hollinshead, M., Roffman, J. L., Smoller, J. W., Zöllei, L., Polimeni, J. R., Fischl, B., Liu, H., & Buckner, R. L. (2011). The organization of the human cerebral cortex estimated by intrinsic functional connectivity. *Journal of Neurophysiology*, *106*(3), 1125–1165. https://doi.org/10.1152/jn.00338.2011

Yeshurun, Y., Nguyen, M., & Hasson, U. (2021). The default mode network: Where the idiosyncratic self meets the shared social world. *Nature Reviews Neuroscience*, *22*(3), Article 3. https://doi.org/10.1038/s41583-020-00420-w

Zhao, Y., Chanales, A. J. H., & Kuhl, B. A. (2021). Adaptive memory distortions are predicted by feature representations in parietal cortex. *The Journal of Neuroscience*, *41*(13), 3014–3024. https://doi.org/10.1523/JNEUROSCI.2875-20.2021